3RD 3D NANOMANUFACTURING WORKSHOP

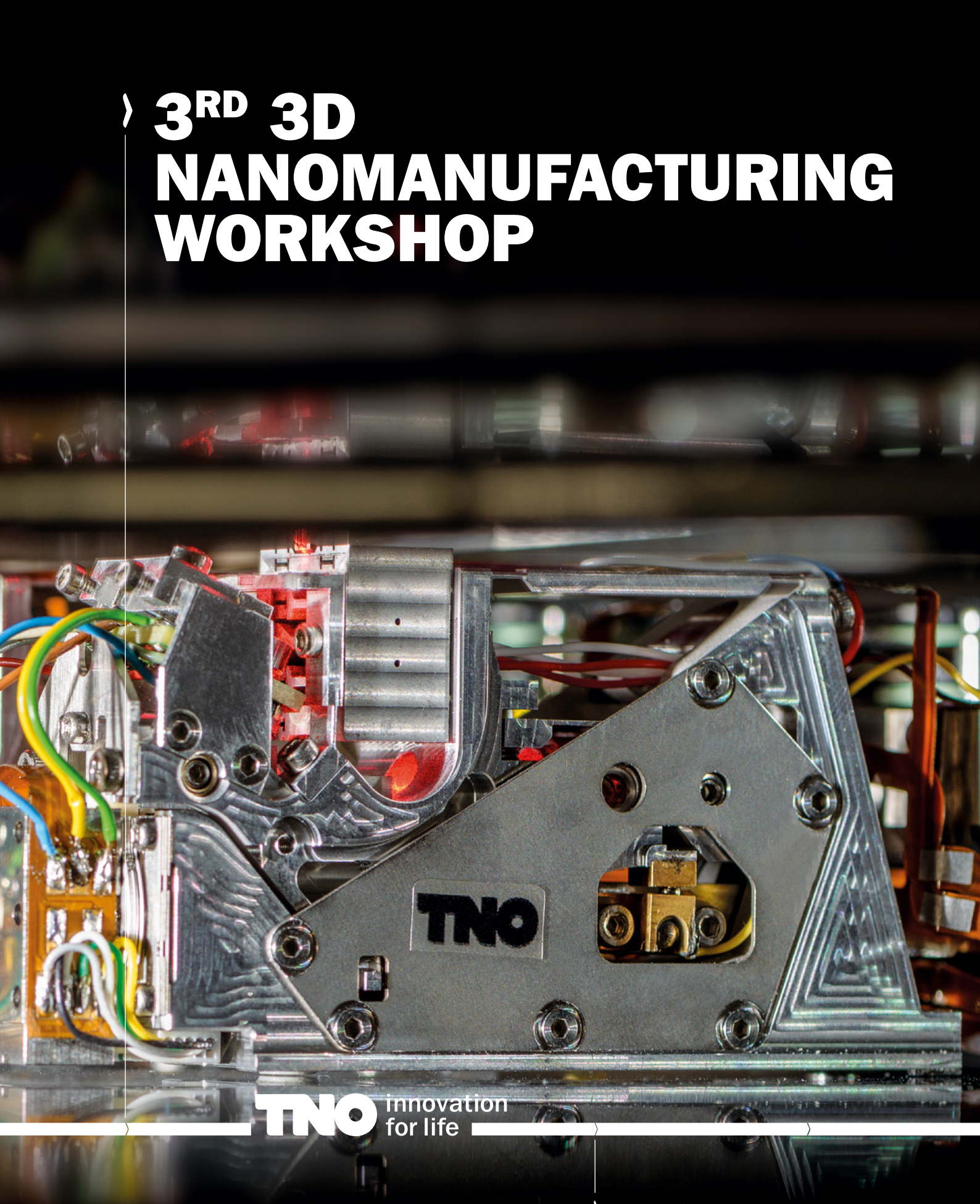

TNO innovation for life

6 NOVEMBER 2017

“THE EFFECT OF CONCEPT-DRIVEN REVOLUTION IS TO EXPLAIN OLD THINGS IN NEW WAYS.

THE EFFECT OF TOOL-DRIVEN REVOLUTION IS TO DISCOVER NEW THINGS THAT HAVE TO BE EXPLAINED.”

Freeman Dyson

EVENT PROCEEDINGS

DISSEMINATION EVENT

6 NOVEMBER 2017

EARLY RESEARCH PROGRAM – 3D NANOMANUFACTURING –

PREFACE

By end of 2017 there will be more than 8.4 billion connected devices (Gartner 2017). This means for the first time, Internet of Things (IoT) devices will outnumber the world's population. In 2020, the number of connected devices will increase to more than 20 billion. This means nearly every devices we own or can imagine will be connected to the Internet. The range is from our mobile phones, wearables, home appliances to even our cities. This full integration of data can have an unprecedented impact in our society by better management of water, energy, transportation and safety, and reaching fully sustainable cities.

Growth in IoT scales up the demands for more powerful and energy efficient nanodevices. To enable the power and efficiency demand, 1) the device dimensions are shrinking to atomic dimensions and 2) 3D nanoarchitectures have been introduced to achieve new functionalities and to make optimum use of the available space. However, the technologies currently used for production and quality control approach physical boundaries and will no longer be technologically or economically feasible. As a result of both challenges breakthroughs in manufacturing and metrology methods for (3D) nanoarchitectures are required.

TNO's early research program (ERP) 3D Nanomanufacturing, in close collaboration with its industrial and academic partners have established an innovation ecosystem, to bring solutions for nanomanufacturing and nanometrology challenges. Thanks to our industrial partners, the program has a clear long-term focus on real industrial challenges. The solutions are being developed in close collaborations between our academic partners for low Technical Readiness Levels (TRL) and TNO for developing the technology to an acceptable level to be taken over by industry; in short tackling the very high technical risks.

Similar to last three years, again this year we organize the Nanomanufacturing Dissemination Workshop. One of the unique and valuable dimensions to this dissemination workshop is the way it brings industrial and academic world together. The workshop disseminates the technical developments which were achieved every year. Our internationally renowned speakers will present the latest achievements in the field and describe the upcoming challenges. Following that, several oral contributions will present the recent developments in this program. Moreover, the detail of the developments will be discussed and presented by poster presentations.

This proceeding includes the Keynote and invited talks, oral contributions of the program and more than 50 poster presentations. The reader will discover that both industry challenges and possible solutions are being presented in this proceeding. Finally, we would like to express our deep appreciation to our invited speakers, Dr. Urs Duerig, Prof. Willem Vos, Prof. Paul Koenraad, Dr. Stefan Witte and Dr. Jason Benkoski.

On behalf of Organizing committee

Hamed Sadeghian
Chair of the workshop

3RD ERP 3D NANOMANUFACTURING DISSEMINATION WORKSHOP

10:30 - 11:00	Registration
11:00 - 11:15	Welcome and opening by Paul de Krom, CEO Board of Directors, TNO
11:15 - 11:45	Keynote speaker: Urs Duerig, Research Fellow, IBM Research *'Closed loop 3-D nano-fabrication using thermal probes'*
Session I: 3D Nanomanufacturing Chair: Arnold Stokking, Managing Director Industry, TNO	
11:45 - 12:15	Invited speaker: Willem Vos, Professor, University of Twente *'In 3 steps to 3d": Fabrication, nondestructive imaging, and photonic functionality of 3D silicon nanostructures'*
12:15 - 12:30	Hamed Sadeghian, Principal Scientist, TNO *'Early Research Program 3D Nanomanufacturing'*
12:30 - 12:45	Arjen Boersma, Senior Scientist, TNO *'High throughput STED nanolithography'*
12:45 - 13:00	Invited speaker: Jason Benkoski, Principal Scientist, The Johns Hopkins University *'Microfluidic 3D Printing of Hierarchically Structured Nanomaterials'*
13:00 - 14:00	Lunch and poster session
14:00 - 14:20	NOMI Innovation Program Collaboration signing ceremony
Session II: Nanotomography Chair: Hamed Sadeghian, Principal Scientist, TNO	
14:20 - 14:50	Invited speaker: Paul Koenraad, Professor, Eindhoven University of Technology *'Atom Probe Tomography: Element specific 3D microscopy at the atomic level'*
14:50 - 15:05	Erwin van Zwet, Senior Scientist, TNO *'Photo-Thermo-Acoustic nanoimaging for metrology applications'*
15:05 - 15:20	Maarten van Es, Scientist, TNO *'Nanotomography with scanning subsurface ultrasonic resonance force microscopy'*
15:20 - 16:15	Break and poster session
Session III: Nanometrology Chair: Rogier Verberk, Director Semiconductor equipment, TNO	
16:15 - 16:45	Invited speaker: Stefan Witte, Professor, ARCNL *'Metrology through optically opaque media: from extreme ultraviolet to pump-probe methods'*
16:45 - 17:00	Wouter Koek, Senior Scientist, TNO *'Ptychography for nanometrology applications'*
17:00 - 17:15	Rodolf Herfst, Scientist, TNO *'High bandwidth, picometer resolution positioning stage for metrology applications'*
17:15 - 17:30	Teun van den Dool, Senior Scientist, TNO *'Miniaturized, fast 2D parallel nanopositioning stages for metrology applications'*
17:30 - 17:40	Best Poster Award
17:40 - 17:45	Closing
17:45 - 18:30	Meet and greet, including drinks and snacks

ORGANIZING COMMITTEE


Hamed Sadeghian


Nicole Nulkes - De Groot


Kitty van der Welle


Marco van der Lans


Kim Dielwart


Rik Kruidhof

CONTENTS

ABSTRACTS

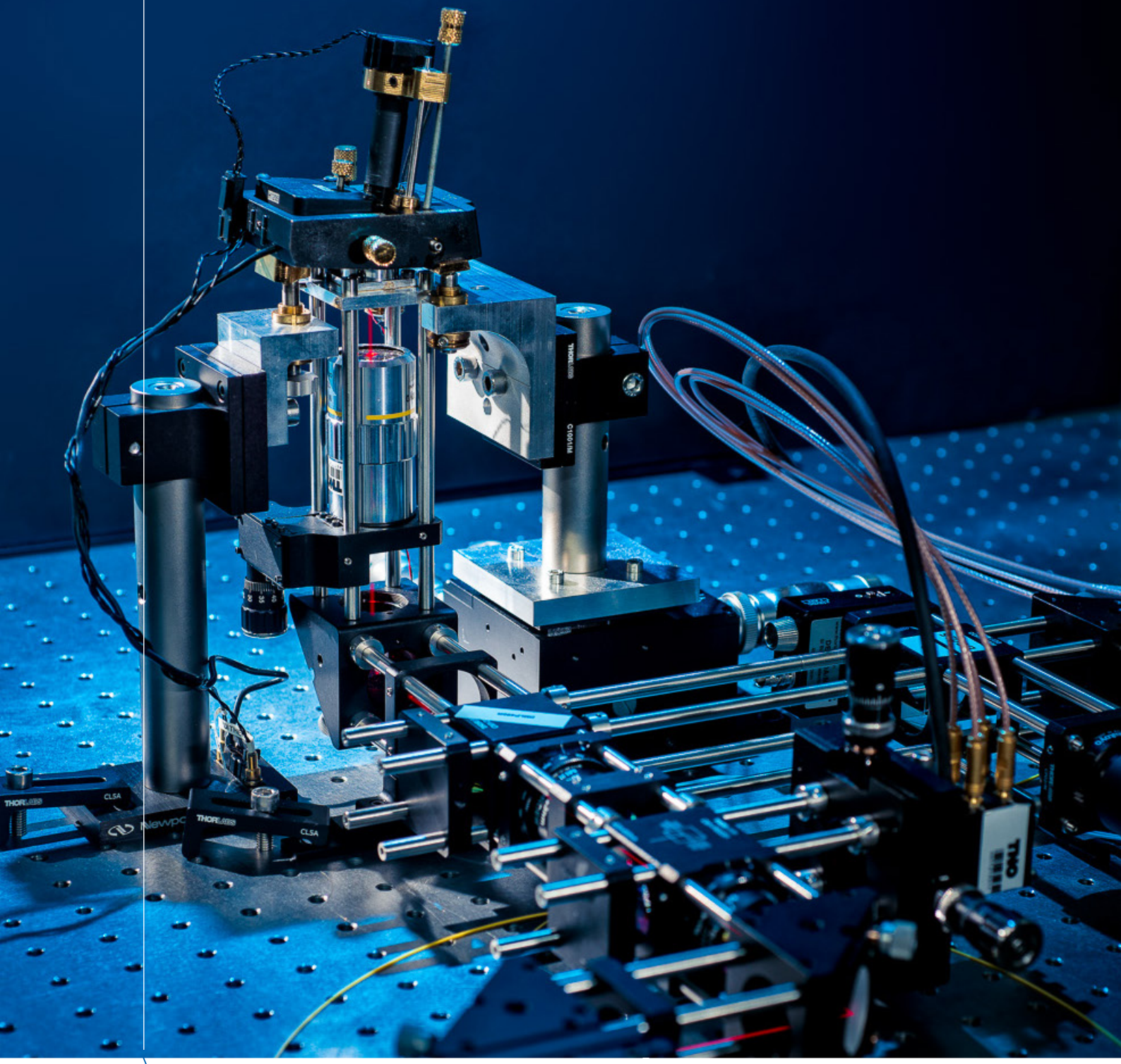

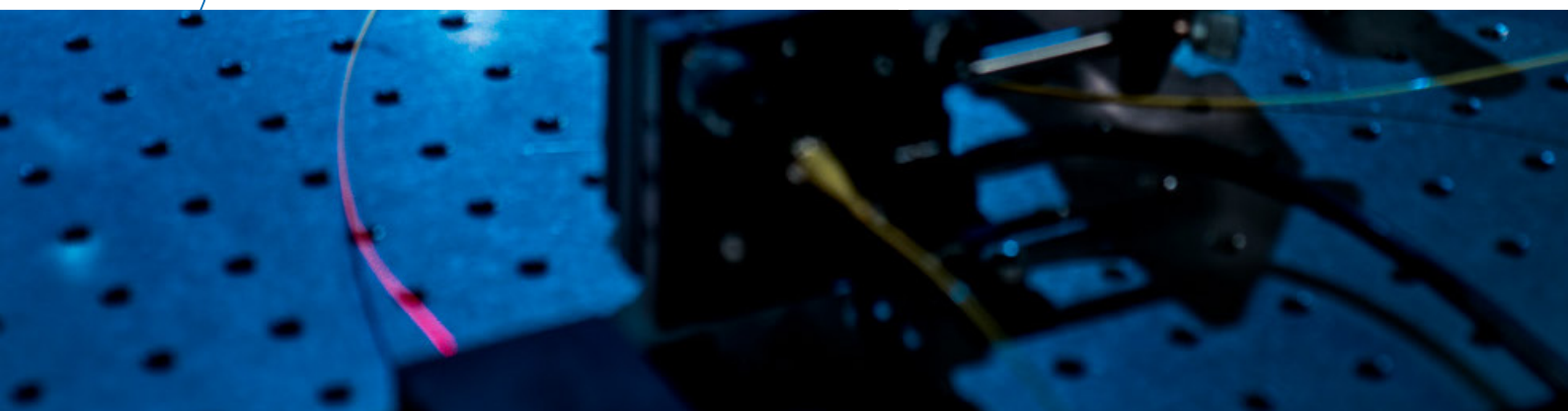

KEYNOTE SPEAKER: URS DUERIG, RESEARCH FELLOW, IBM RESEARCH – ZURICH, SWITZERLAND; NOW AT SWISSLITHO AG, ZURICH, SWITZERLAND

CLOSED LOOP 3D NANO-FABRICATION USING THERMAL PROBES

Thermal scanning probe lithography (tSPL) emerged as an off-spring from IBM's Millipede data storage project which pioneered the highly parallel operation of cantilever arrays to emboss and read-back digital data in the form of nm size indents in a polymer media. In tSPL we also use heated atomic force microscope (AFM) tips but here we locally evaporate a thermally sensitive resist to create lithographic patterns. By this process we are able to fabricate precise 3D patterns and high resolution structures without the use of charged particles, such as electrons, which have been implicated in substrate damage. Moreover, AFM imaging is exploited for in-situ inspection of the substrate surface before patterning and of the lithographic structures written into the substrate. This capability significantly expands the scope of direct write mask-less lithography beyond the common state of the art in two ways. First, it allows to precisely align the lithographic pattern with pre-existing features such as nano-wires and even single layer graphene or MoS2 flakes. Second, it allows to fabricate 3-D structures with 1 nm topographic precision using on the fly feedback control of the patterning process.

An overview of the most exciting latest developments will be presented. Starting with high resolution 2-D lithography, sub 10 nm line features written at a half-pitch of 14 nm have been transferred into silicon using ultra-thin lithographic layers combined with a SiO2 hard-mask technology. 3-D patterning is typically not on the radar in the community. Yet, it allows to expand the engineering boundaries, in particular for optical applications to the nm scale. As an example, we fabricated ultra-precise Gaussian optical resonator arrays which confine the light in micrometer size spots on a Bragg mirror cavity. The precision offered by the fabrication process is required to achieve predictive power of model calculations, in particular for the inter-cavity coupling, when

compared with actual device characteristics. Lastly, we demonstrate how the enhanced overlay capabilities of tSPL can be used for the fabrication of nano-wire FETs and for the controlled fabrication of contact and gate structures on single sheets of VdW materials. By avoiding irradiation with high-energy electrons, which is typically the case in electron beam lithography, charging of insulating oxide coatings or beam induced damage of delicate monolayer films can be firmly excluded.

INVITED SPEAKER: WILLEM VOS,
PROFESSOR, UNIVERSITY OF TWENTE

"IN 3 STEPS TO 3D": FABRICATION, NON-DESTRUCTIVE IMAGING, AND PHOTONIC FUNCTIONALITY OF 3D SILICON NANOSTRUCTURES

The realization of three-dimensional (3D) nanophotonic metamaterials requires technologies beyond common planar processing. Hence, we present 3 crucial steps to realize functional 3D nanostructures: fabrication, non-destructive imaging of the 3D structure, and evaluation of nanophotonic functionality. We chose to focus on photonic band gap crystals made from silicon with a 3D diamond-like structure (see Figure 1), as these have broad photonic band gaps that are robust to unavoidable disorder [1]. Moreover, this crystal structure is functionalized by inserting intentional point defects that act as 3D resonant cavities [2].

We present a CMOS-compatible method to pattern two etch masks in one step on two perpendicular faces of a wafer, aligned within 5 nm [3]. At this time, we are extending this methodology to the wafer-scale in collaboration with ASML and TUE (other partners welcome!) We etch nanopores using deep reactive ion etching where we systematically varies all control parameters. This optimization has yielded a process to achieve pores with an ultra-high depth-to-width aspect ratio up to 30. Interestingly, the in-situ characterization of 3D nanostructures still remains a major outstanding challenge. Since electron microscopy only views the external surface of a structure, we have initiated a non-destructive X-ray holotomography study to determine the internal structure of a complete

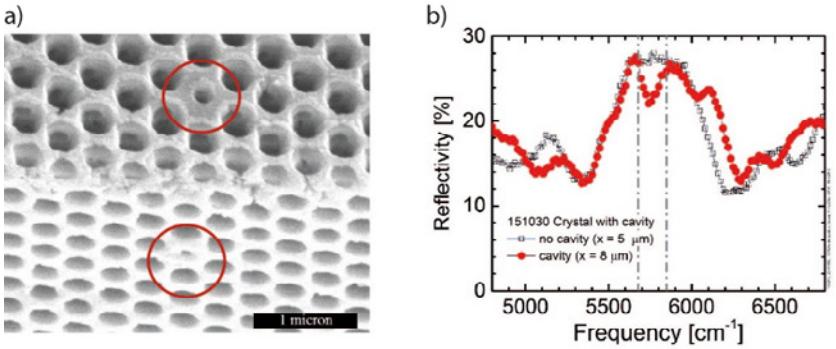

Figure 1. a) Inverse woodpile photonic crystal on silicon with a point defect. Red circles indicate intentionally smaller pores that create a point defect inside the structure. b) Broadband reflectivity measured on 3D photonic crystal with cavity (red) and without cavity (black). A resonance appears at 5700 cm-1 corresponding to a wavelength of 1750 nm in the near infrared.

3D crystal. X-ray tomography data appear crucial to correctly interpret photonic gap formation that is inferred from optical micro-reflectivity.

Authors: Willem L. Vos[1], Diana A. Grishina[1], Cornelis A.M. Harteveld[1], Alexandra Pacureanu[2], Ad Lagendijk[1], and Peter Cloetens[2]

1 Complex Photonic Systems (COPS), MESA+ Institute for Nanotechnology, University of Twente, P.O. Box 217, 7500 AE Enschede, The Netherlands

2 European Synchrotron Radiation Facility (ESRF), B.P. 220, F-38043 Grenoble, France

[1] K. M. Ho, C. T. Chan, C. M. Soukoulis, R. Biswas, and M. Sigalas, Solid State Commun. 89, 413 (1994).

[2] L. A. Woldering, A. P. Mosk, and W. L. Vos, Phys. Rev. B 90, 115140 (2014)

[3] D.A. Grishina, C.A.M. Harteveld, L.A. Woldering & W.L. Vos, Nanotechnology 26, 505302 (2015)

HAMED SADEGHIAN, PRINCIPAL SCIENTIST, TNO

EARLY RESEARCH PROGRAM 3D NANOMANUFACTURING

The Dutch semiconductor industry is the European leader. In the race for more functionality and lower power consumption, the key lies in miniaturizing the details on a chip and better utilization of the third dimension. To be able to produce these nanoarchitectures with precision, reliability and at high speed, new manufacturing and inspection techniques are required. The main use case in this program centers on this. The research is aligned with the goals of the Topsector HTSM roadmaps: Semiconductor Equipment, Advanced Instrumentations, Nanotechnology. Cooperation is being developed with a large number of universities and knowledge organizations and companies. Apart from the main focus, other applications are also under consideration: photovoltaic components, sensors, instruments for healthcare (e.g. organ on chip) and security.

The program is setup based on the following vision of the future:

- We see a future where humanity will solve many of future's challenges in data, energy and life sciences by a continuous miniaturization in device fabrication down to an atomic scale
- The NOMI-ecosystem develops the technologies that enable exploration and exploitation of the atom-scale world level leading to the real-world applications
- The NOMI-ecosystem research to create the instruments to image, measure and fabricate devices at the level of individual atoms at an humanly acceptable and economically attractive level

In this talk, I will present the technology research lines and the target use cases. The developments in the research projects and the achieved results so far will be discussed.

ARJEN BOERSMA, SENIOR SCIENTIST, TNO

HIGH THROUGHPUT STIMULATED EMISSION DEPLETION NANO-LITHOGRAPHY (STED)

STED is generally recognized as a very promising tool to manufacture 3D sub-micron features using a maskless lithography step. However, STED is not widely used in Industry (or even Academia), because of its relative slow manufacturing speed. A major reason for this slow speed is the mismatch between the physical processes (light absorption and stimulated emission rate) and the chemistry of the photo initiators. We propose a route towards fast STED in which we will replace the current photo initiators (developed for single photon lithography) by the system of two initiators. One dye will be responsible for the light management, the co-initiator will initiate the polymerization reaction that will generate the final features. Optimization of this mixture with respect to the time constants of the initiation and polymerization process, will lead to a significant increase in speed, and may approach the required writing speed of 1 m/s. The corresponding feature size and resolution depends on both the hardware (laser, stage, etc.), and the photo initiator chemistry, and may reach 10 and 100 nm respectively. An interesting first use case is the mask less manufacturing of 2D structures for feature sizes between e-beam and UV lithography.

INVITED SPEAKER: JASON BENKOSKI, PRINCIPAL SCIENTIST, THE JOHNS HOPKINS UNIVERSITY

MICROFLUIDIC 3-D PRINTING OF HIERARCHICALLY STRUCTURED NANOMATERIALS

We present an enhanced 3-D printing process that can reproduce the complex hierarchical structure of biological materials. The key modification is a microfluidic printer head. It contains a network of microscopic channels that processes fluids in the laminar flow regime, where shear, temperature, mass transfer, and concentration profiles can be precisely controlled. This control delivers phase morphologies and composition profiles that are not accessible through bulk shear or annealing. The self-assembly of nanoparticles within the polymer precursor defines the internal structure from 100 µm down to several nm. The translation of the 3-D printer head then defines the hierarchical structure at larger length scales. We present two examples of this capability. The first is a hierarchically structured nanocomposite consisting of alumina nanowhiskers in a chitin matrix. The helicoidal orientation of the alumina nanowhiskers is modeled after mineralized crustacean shells and bone. The second system is a hyaluronate hydrogel loaded with collagen nanofibrils. It, too, possesses helicoidal alignment of the nanofibrils with pseudo-vasculature at larger length scales. With the inclusion of induced pluripotent stem cells, the biomimetic scaffolding will be used to culture heart muscle surrogates for the study of hypertrophic cardiomyopathy.

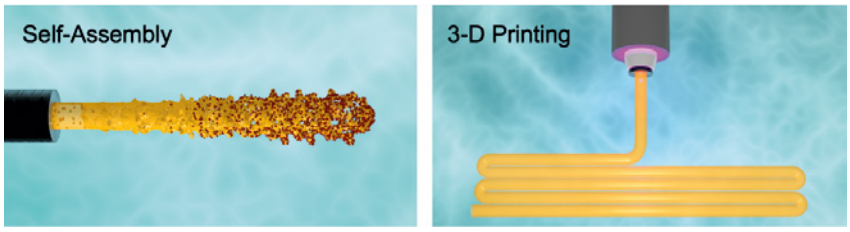

INVITED SPREAKER: PAUL KOENRAAD, PROFESSOR, EINDHOVEN UNIVERSITY OF TECHNOLOGY

ATOM PROBE TOMOGRAPHY: ELEMENT SPECIFIC 3D MICROSCOPY AT THE ATOMIC LEVEL

Present day material science depends on the construction of nanostructured materials in which atomic scale details are of key importance. It is thus essential to have microscopy techniques that allow such details to be assessed in 3D at the atomic scale. In the presentation I will introduce the Atom Probe Tomography technique that is based on laser induced field emission in combination with a time-of-flight analysis. By this it can create atomically resolved, element specific, 3D maps of the composition of nanostructured materials. Due to recent advances this technique can now be applied to metals, insulators and semiconductors and their hybrid structures. A few years ago in Eindhoven we have set up a National Atom Probe Facility to facilitate material analysis at the ultimate atomic level. I will present several examples of recent results that we have obtained by Atom Probe Tomography on a number of hybrid nanostructured materials to show the capability of the technique to answer detailed questions on the 3D elemental distribution in novel materials at the atomic scale.

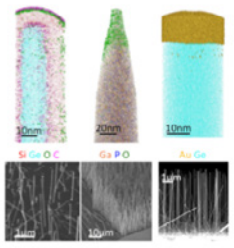

Fig. 1 Examples of Atom Probe Tomography performed on semiconductor nanowires

ERWIN VAN ZWET, SENIOR SCIENTIST, TNO

PHOTO THERMO ACOUSTIC NANOIMAGING

In the semiconductor industry there is the ever remaining drive to integrate more functionality within the same footprint. This has resulted in processes where structures are buried under optically opaque layers, while there is still the need to perform metrology, inspection and alignment on these structures. Photo Thermo Acoustic Imaging (PTAI) is a technology that enables, non-contact, depth resolved measurements at buried structures, such as alignment markers.

TNO has designed and built an optical pump-probe setup based on a Sagnac interferometer, with a shot noise limited measurement sensitivity at the picometer level. The design considerations of the Sagnac interferometer will be explained, and the first measurement results obtained with the setup will be presented.

MAARTEN VAN ES, SCIENTIST, TNO

NANOTOMOGRAPHY WITH SCANNING SUBSURFACE ULTRASONIC RESONANCE FORCE MICROSCOPY

Nondestructive imaging of buried patterns is becoming a challenge at upcoming process nodes in semiconductor industry due to ever decreasing feature sizes and the use of optically opaque layers. Such imaging is needed at various steps in the production process such as alignment and overlay as well as CD metrology and defect detection. Within the ERP 3D Nanomanufacturing we have developed Scanning Subsurface Ultrasonic Resonance Force Microscopy (SSURFM), a technique which combines the nm resolution of Atomic Force Microscopy with high frequency ultrasound for sensitive detection of buried features through their visco-elastic response to the applied sound. We will discuss how we optimized this technique with respect to existing methods presented in scientific literature such that it is sensitive enough to be used with relevant material stacks. We will also discuss various enhancements we are developing for more robust, quantitative and practical use, including various ways to excite the ultrasound using the sensing cantilever and careful characterization of the response as a function of feature dimensions. We will do so with examples of measurements on representative samples such as might be used for e.g. overlay or metrology applications.

INVITED SPEAKER: STEFAN WITTE, PROFESSOR, ARCNL AND VU UNIVERSITY AMSTERDAM

METROLOGY THROUGH OPTICALLY OPAQUE MEDIA: FROM EXTREME ULTRAVIOLET TO PUMP-PROBE METHODS

Besides being essential for imaging, light is an important tool for nanometrology as it allows fast, non-invasive and non-contact detection with sensitivity to sub-micron structures. When target structures have known shapes, nanometer-level position determination can be achieved using visible light. However, as lithographic structures become three-dimensional, an increasingly important requirement for metrology is the ability to detect features below layers of optically opaque materials such as metals.

At ARCNL we work on different metrology techniques that have the ability to 'see' through materials that are optically completely opaque. One such method is the use of extreme-ultraviolet and soft-X-ray radiation, which enables the detection of much smaller structures, but also has the ability to penetrate through many optically opaque media. Another technique is based on the use of optically induced ultrasound pulses. By irradiating a metal layer with a femtosecond laser pulse, an ultrasound pulse can be launched into the layer and reflect from buried interfaces. The returning ultrasound echo can also be detected by optical means.

I will discuss the principles and development of these methods, show first results on feature detection below metal layers, and discuss the possibilities for metrology applications based on these novel approaches.

WOUTER KOEK, SENIOR SCIENTIST, TNO

PTYCHOGRAPHY FOR NANOMETROLOGY APPLICATIONS

Optical (imaging) methods are widely used to inspect and characterize samples for a broad variety of applications. In many applications there is an on-going need to resolve ever smaller features, which requires that either the wavelength is decreased and/or the numerical aperture is increased.

Due to its short wavelength, soft x-ray radiation is considered as a promising illumination for various nanometrology applications. Because high numerical aperture optics are not practically realizable for this wavelength range, there is a great interest in so-called lens less imaging techniques, of which ptychography is considered as one of the most promising measurement concepts.

In this study we have examined the feasibility of using ptychography for nanometrology applications. We have developed a simulation environment that allows us to assess the performance of (soft xray) ptychography with respect to important metrics such as throughput, measurement accuracy and spatial resolution. In this talk we will present our findings relating to throughput, and discuss how this impacts real-world applications.

RODOLF HERFST, SCIENTIST, TNO

HIGH BANDWIDTH, PICOMETER RESOLUTION POSITIONING STAGE FOR METROLOGY APPLICATIONS

High resolution and high throughput imaging are typically mutually exclusive. While there is a wide range of techniques to image features beyond the diffraction limit of light, they all have their own benefits and drawbacks, and are often very slow compared to optical systems. As such, extending the performance of optical microscopes remains desirable. At TNO we have developed the META instrument: a platform for precise and high speed position of high resolution optical elements such as nano-antennas, super oscillatory lenses and hyper lenses. A key component in this system is a high speed MEMS nanopositioning stage which enables sub-nm position of a metamaterials optical lens with very high bandwidth. We present a design and process for this MEMS device as well as laser vibrometer measurements that show its performance. A first eigenfrequency of 500±25 kHz was observed. Together with the relatively low (approximately 2-2.5) quality factor a high positioning bandwidth is possible with this device, enabling further development of high throughput high resolution

TEUN VAN DEN DOOL, SENIOR SCIENTIST, TNO

MINIATURIZED, FAST 2D PARALLEL NANOPOSITIONING STAGES FOR METROLOGY APPLICATIONS

Some metrology methods have very nice performance (for instance in terms of resolution), but are slow. An example is AFM (Atomic Force Microcopy). The resulting low throughput prevents wide-spread application in semicon fabs. One way to increase throughput is to operate many metrology devices in parallel. TNO's parallel arm AFM inspection system is an example of such a solution. But the arms in that system are limiting flexible application; the positions of the AFM systems is restricted to a certain part of the surface to be inspected.

As a next step in parallelization, TNO is developing more flexible positioning systems. One of them consists of independent, free flying carriers based on magnetic levitation. A first version with a carrier size of 50x50mm is currently being implemented. The target size of future systems is below 10x10mm. This first system will have a coarse metrology system with a resolution below 1 micron. The target resolution of future versions of the system is below 1 nm.

POSTERS

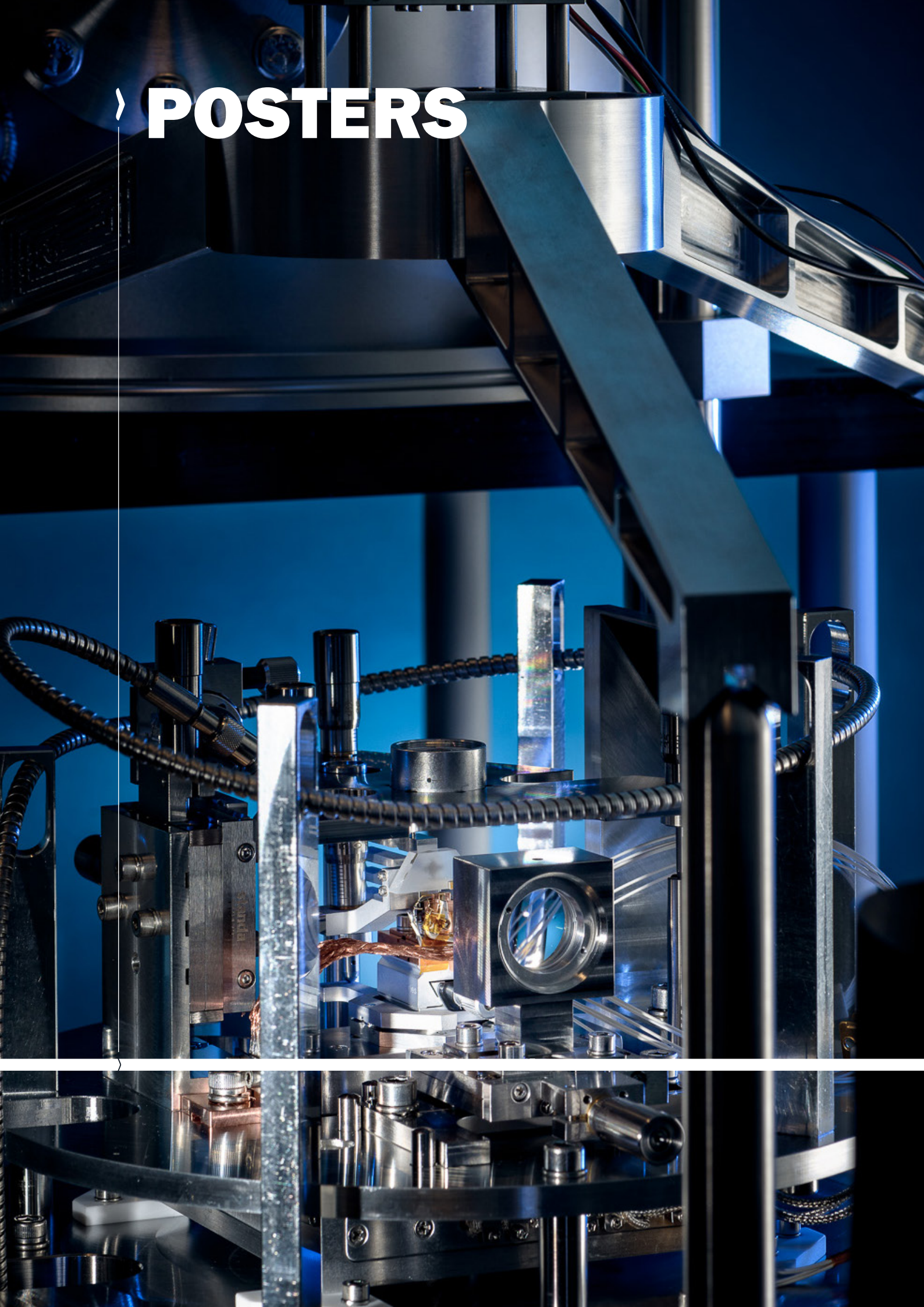

CONTENTS

This project has received funding from the Electronic Component Systems for European Leadership Joint Undertaking under grant agreement No 621280. This Joint Undertaking receives support from the European Union's Horizon 2020 research and innovation programme and Netherlands, France, Belgium, Germany, Czech Republic, Austria, Hungary, Israel

Fast and flexible 3D scanning probe nano-patterning and lithography

Klára Maturová, Benjamin Biemond, Violeta Navarro, Sasan Keyvani, Mehmet Selman Tamer, Marco van der Lans, Hamed Sadeghian

Department of Optomechatronics, Nomi group

TNO innovation for life

- nanopatterning using commercial AFM setup
- maskless nanopatterning
- combined imaging and patterning tool

INTRODUCTION

To sustain the increasing miniaturization of semicon devices, novel patterning and metrology techniques are required that can pattern and measure devices with nanometer precision. The Nomi group at TNO Optomechatronics develops those techniques.
In this project, TNO has invented two nano-patterning techniques that employ Atomic Force Microscope setups and use vibrating cantilevers to image at nanoscale and manipulate the sample using the same probe. These techniques are

- versatile and don't need mask fabrication
- cost-effective
- reliable
- nanometer-scale accurate.

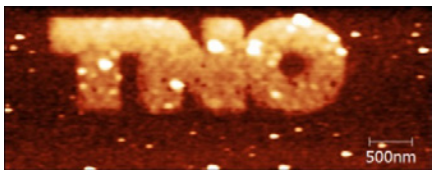

MODEL

A dynamical model is used to capture the complex forces that occur between the tip and the sample. By understanding this dynamics, two nanopatterning techniques are invented in which the AFM probe is excited at one or two frequencies.

MONO-FREQUENCY METHOD

The AFM cantilever is excited by a harmonic signal near the resonance frequency. By altering the excitation frequency and amplitude ratio between response output and free-air response, the tip-sample force can be tuned. The dynamical model allows to precompute the attained forces, shown in the colors of the next figure.

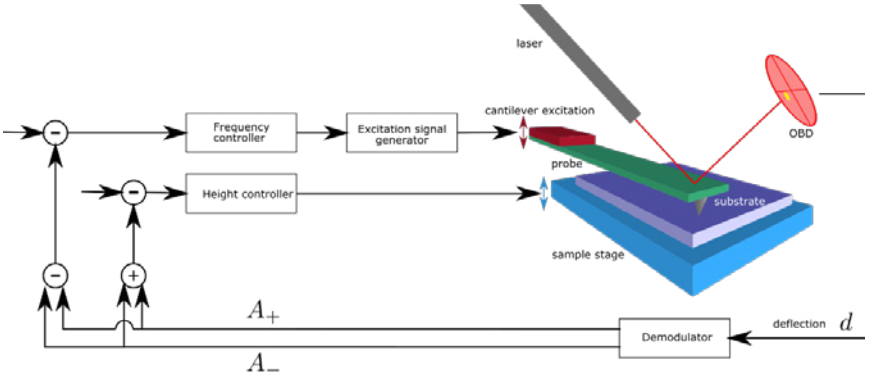

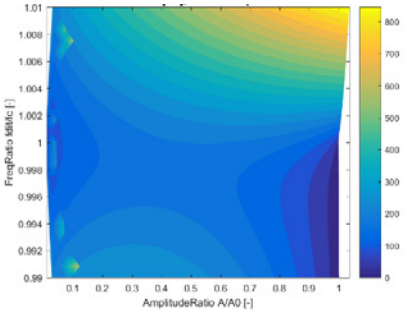

EXPERIMENTAL DEMONSTRATION

Selecting the parameters in the top left corner allowed to pattern the TNO logo shown on the left, and the circles shown below, using a Bruker Dimension FastScan and Zurich Instruments Lock-in Amplifier.

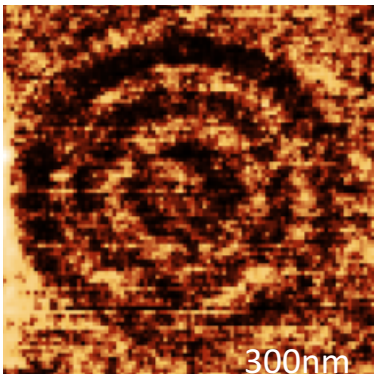

DUAL-FREQUENCY METHOD

By exciting the cantilever with two frequencies close to resonance, some robustness to resonance frequency variation is attained with the control scheme sketched above. In addition, higher contact forces are attained:

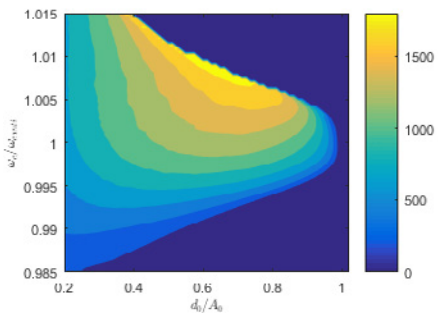

EXPERIMENTAL DEMONSTRATION

Employing this nanopatterning method on the same setup, a zigzag pattern has been generated by passing the sample once with relatively mild excitation amplitude:

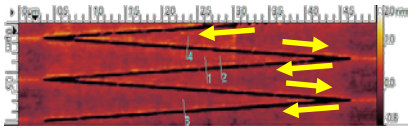

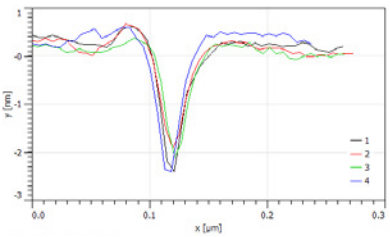

Experiments have shown patterning depths up to 40 nm.

CONCLUSION

Two techniques are invented that allow effective writing of 10-200 nm features on different materials.
By nanopatterning on EUV masks, this technique supports EUV Lithography system optimization by enabling sensitivity studies.

This research was supported by TNO's Early Research Program 3D Nanomanufacturing Instruments

High throughput STimulated Emission Depletion lithography

Arjen Boersma[1], Yunqi Wang[1], Fidel Valega MacKenzie[1], Erwin van Zwet[2], Rik Kruidhof[2], Hamed Sadeghian[2]

1 Department of Materials Solutions
2 Department of Optomechatronics

TNO innovation for life

Introduction

Stimulated Emission Depletion (STED) lithography is generally recognized as a very promising tool:

- overcoming Abbe diffraction limit
- manufacture 3D sub-micron features
- mask-less lithography
- 100 nm resolution
- 10 nm feature size features
- directly in a polymer resin.

However, STED is not widely used in Industry (or even Academia), because of its relative slow manufacturing speed. At TNO the goal of the current STED project is to combine high resolution features with high writing speeds (m/s)

Technology

STED lithography uses two laser beams:

- The excitation beam excites the photo-initiator in the resin ①
- The deactivation or depletion beam quenches the excited state ②

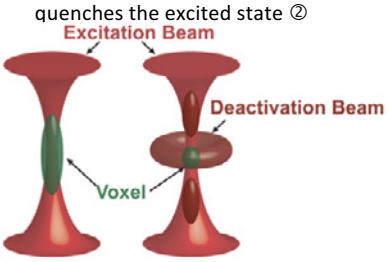

Figure 1: Excitation and depletion steps

The laser intensity of the conical excitation beam is high enough in the focal point to start polymerization (voxel) The deactivation (depletion) beam reduces the size of the voxel, by preventing the formation of radicals and subsequent polymerization. The two laser beams are combined using a microscope with high NA objective.

State-of-the-Art

The current writing speed using the STED lithography is limited to < 1 mm/s. This is due to:

- limitations in hardware
- mismatch in chemistry

For high writing speeds, intense laser light is required. The poor absorption of this light by the state-of-the-art photo-initiators leads to:

- overheating of the polymer
- overexposure of initiator
- leading to energy states that cannot be quenched

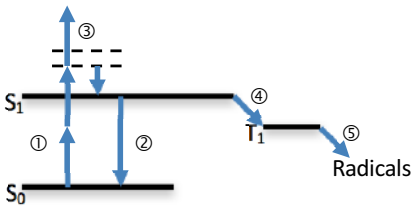

Figure 2: Energy states of a photo-initiator leading to the formation of radicals

Energy states

① two-photon capture leading to excited state and fallback to (semi-)stable state S_1.
② Stimulated emission of exited photons leads to quenching to ground state S_0.
③ Three- or four photon capture leads to over-excited states that cannot be quenched.
④ with Inter System Crossing the energy state falls back to a more stable energy state T_1
⑤ That can form a radical that will initiate polymerization.

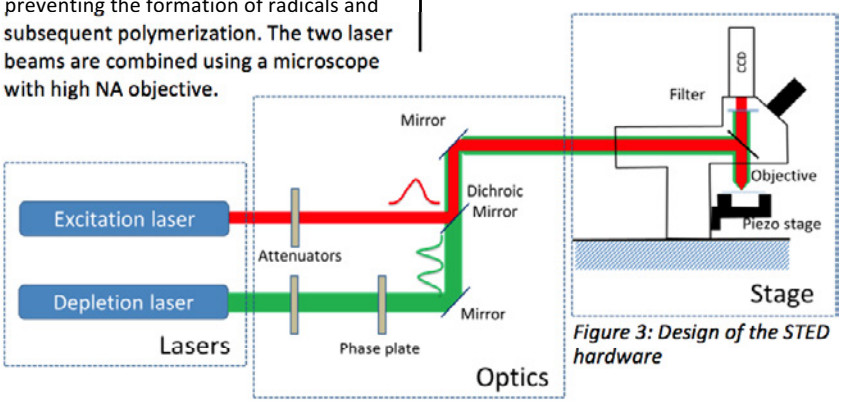

Figure 3: Design of the STED hardware

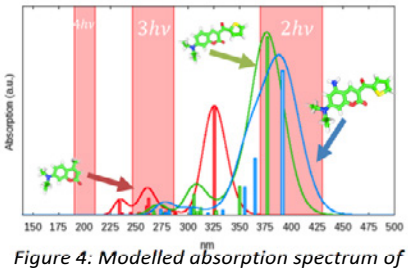

Figure 4: Modelled absorption spectrum of modified photo-initiators to reduce ③

TNO approach

The approach that decreases the risks significantly, is the use of a system of two initiators. One dye will be responsible for the light management ①,②, the co-initiator will initiate the polymerization reaction that will generate the final structures ⑤. Optimization of this mixture with respect to the time constants of the initiation and polymerization process, will lead to a significant increase in speed, and is expected to approach the required writing speed of 1 m/s.

Use cases

Several applications have been identified:

- Mask less 2D nanolithography, as a low-cost alternative for E-beam litho. The combination of a UV resin and a STED resin will improve the resolution.
- Lab tool development for High Throughput STED, optimized for the use of the new STED resins
- Flat Panel Displays using large scale flexible nanopatterning

CONCLUSIONS

STED lithography is a very promising technology for 3D nanomanufacturing. Combination of resolution and speed seems feasible.
The use of a new combination of photo-initiators separates critical functionalities, and enables to optimize both the light interaction and the radical formation.
TNO has the capabilities to develop bench-top device:

- Naninstrumentation
- Optics
- Materials

This research was supported by TNO's Early Research Program 3D Nanomanufacturing Instruments

Thermal Nanolithography: A technology compatibility study

H. Sadeghian[1], P. Paul[2], K. Maturova[1], J. Wildschut[1], S. Weber[2] , S. Bonanni[2], M. Koppen[3], R. Kruidhof[1]

1 Department of Optomechatronics, TNO, Delft
2 SwissLitho AG, Zurich
3 Department of Instrument Manufacturing, TNO, Delft

SwissLitho AG
Innovative Nanofabrication Tools

TNO innovation for life

INTRODUCTION

TNO and SwissLitho AG are developing a high-throughput, mask-less nanopatterning solution for nanostructures down to few nanometers using thermal scanning probe lithography (t-SPL).

The solution enables:

- Nanopatterning on wafers and samples
- Nanopatterning of many locations simultaneously
- 10 nm patterning resolution
- In-situ closed loop metrology of patterned features

Figure 1 – SwissLitho and TNO logos made with SwissLitho NanoFrazor.

KEY FEATURES

The key features of the combination of the high-throughput and t-SPL technologies are:

- Very short time-to-feature
- 10 nanometers half pitch
- 2 nanometer vertical resolution
- 2.5D write capability
- no vacuum required
- no charged particles – no charge injection to substrate
- no electron damage
- In-situ overlay measurement and alignment
- Standard pattern transfer processes and materials

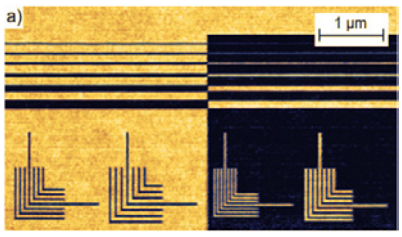

Figure 2 - SwissLitho patterned substrate

APPLICATIONS

The foreseen solution is highly flexible; various process development and scientific research applications are listed.

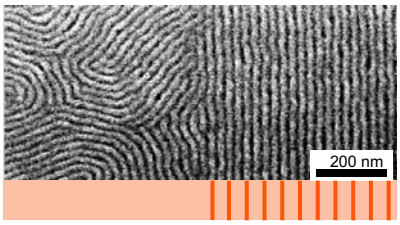

Figure 3 - Directed Self-Assembled pattern

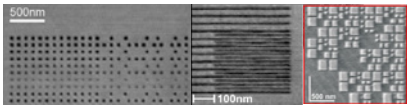

Figure 4 - Contact holes, Dense lines and Isolated features

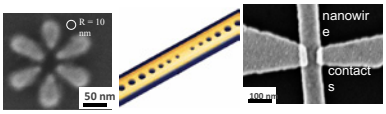

Figure 5– Plasmonic structures and contacts

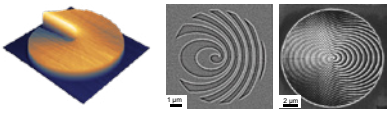

Figure 6 - 3D feature, 2D and 3D Nano optics

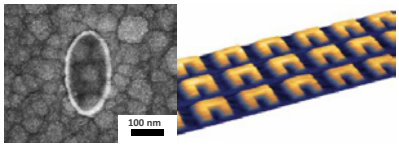

Figure 7 – Nanomagnetism (magnetic ellipse) and Metamaterials

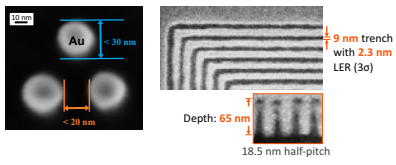

Figure 8- Plasmonic structure and High Resolution Silicon etch

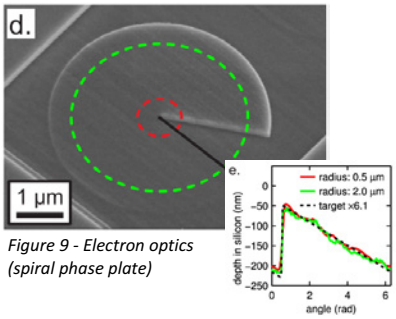

Figure 9 - Electron optics (spiral phase plate)

PROOF-OF-PRINCIPLE SETUP

To test the compatibility of the t-SPL and parallelization technologies, a test setup was built. This setup consists of the SwissLitho cantilever with control software and electronics for writing and scanning and the TNO miniaturized scan head with all the actuation. This setup has been shown to have similar performance to the SwissLitho systems.

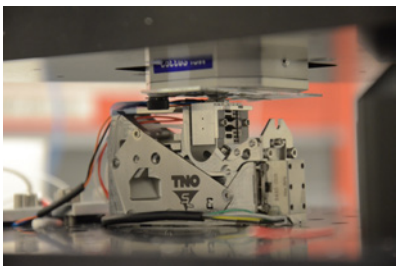

Figure 1 – TNO / SwissLitho test setup.

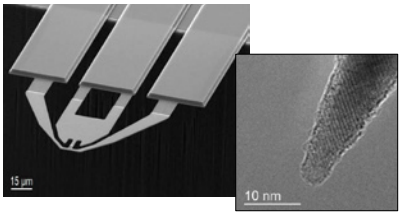

Figure 2 and 3 – SwissLitho t-SPL cantilever and Silicon tip with radius of 2 nm (TEM image).

CONCLUSION

High throughput 3D Thermal Probe Lithography is a versatile enabling technology in research.
TNO and SwissLitho have proven compatibility of their respective technologies and are now proving feasibility for industry.

Reflection Confocal Nanoscopy using Super Oscillatory Lens (SOL)

A. Nagarajan[1,2], P. Stoevelaar[1,2], F. Silvestri[1], M. Siemons[1,3], G. Gerini[1,2], S.M.B. Bäumer[1]

1 Optics department, TNO
2 Electromagnetics group, Eindhoven University of Technology
3 Department of Applied Physics, Delft University of Technology

TNO innovation for life

RATIONALE

The current trends in the semiconductor industry requires **nanoscopes** for accurate and rapid metrology. Direct imaging techniques like Scanning Electron Microscope and Atomic Force Microscopes suffers from low throughput, whereas defect detection techniques like scatterometry relay on lookup tables and are probabilistic.

SUPER OSCILLATORY LENS (SOL)

A SOL consisting of a binary amplitude mask of concentric metal rings, can focus the laser light into a sub-diffraction spot in the post-evanescent field by precisely tailoring the interference of a large number of beams diffracted from individual rings. The sub-diffraction limited central hotspot is surrounded by high-intense side bands. These side bands doesn't influence the imaging capabilities of the lens as long as the object is within the field of view.

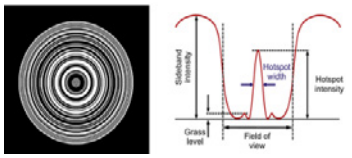

Figure 1: (Left) A 40 µm SOL consisting of 24 rings optimized for 635 nm **(Right)** Field pattern of SOL: sub-diffraction limited hotspot surrounded by high intense side bands.

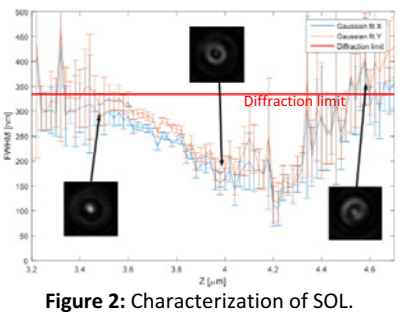

Figure 2: Characterization of SOL.

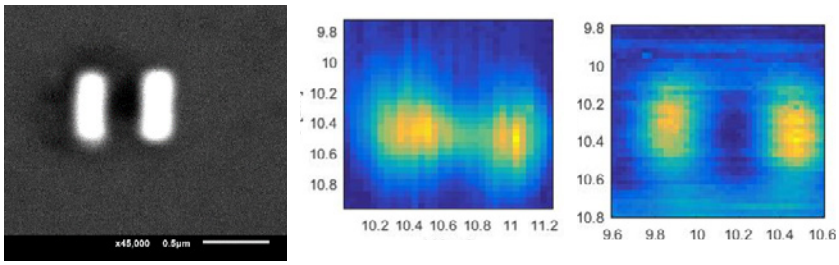

Figure 3: (**Left**) SEM image of the test structure consisting of two slits of 180 nm wide separated by 320 nm
(**Center**) Imaging using Conventional Reflection Confocal microscope
(**Right**) Imaging using SOL

EXPERIMENTAL RESULTS

A test structure consisting of two Gold slits of 180 nm wide and separated by 320 nm (See **Figure 3 (I)**) is imaged using both conventional reflection confocal system and using SOL. As seen from **Figure 3**, SOL offers an improvement in the resolution. The setup is illustrated in **Figure 4**. A 4f system is used to relay the field pattern of SOL onto the sample which is raster scanned to obtain the image.

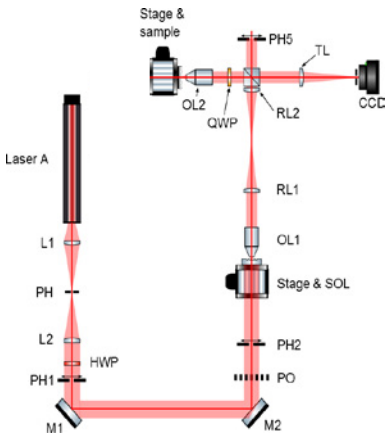

Figure 4: Schematic of the Reflection Confocal Nanoscope.

SIMULATION RESULTS

The performance of the SOL confocal microscope are compared against the ones of a conventional system by means of simulations. The coherent spread functions of the two systems are convolved with objects of different sizes to check the maximum resolution achievable.. **Figure 5** reports the results of the simulations. SOL offers improvements in resolution, but results in ghosts due to illumination from side bands.

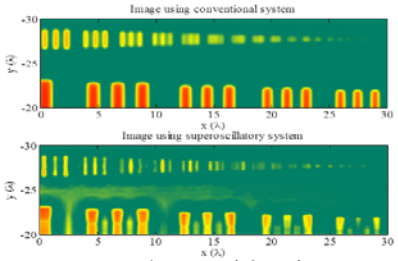

Figure 5: Simulations: (**above**) Imaging using conventional lens (**below**) Imaging using SOL

CONCLUSION

We present a novel reflection nanoscope using SOL. The effects of sidebands limits the usecase of the lens and further investigations need to be performed to both quantify and correct the influence of sidebands in imaging

This research was supported by TNO's Early Research Program 3D Nanomanufacturing Instruments

ROBUST OPTIMIZATION FOR METASURFACE MICROLENSES

F.Silvestri[1], G.Gerini[1,2], S.Bäumer[1], E.van Zwet[3]

1 Department of Optics, TNO, Delft
2 Electromagnetics Group, TU/e, Eindhoven
3 Department of Optomechatronics, TNO, Delft

TNO innovation for life

DIELECTRIC RESONATOR LENSES

Typically, state-of-the-art metasurface lens designs do not address standard optical system requirements such as:

- chromatic aberrations
- field of view
- parasitic apodization
- manufacturing tolerances

This study has taken all these requirements into account to compare the applicability of metasurface lens designs for maskless lithography applications.

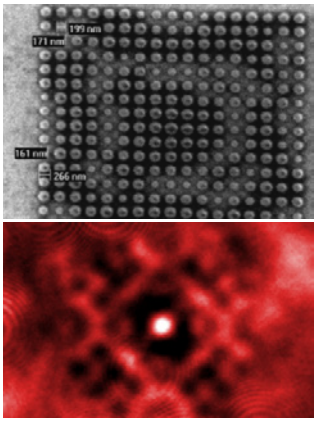

a) Dielectric resonator lens (635 nm)
b) Measurement of the light distribution at lens focal plane;
c) Unit cell for lens (405 nm).

EFFECT OF TOLERANCES ON TRANSMISSION PROPERTIES

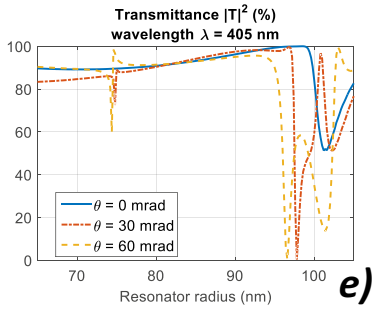

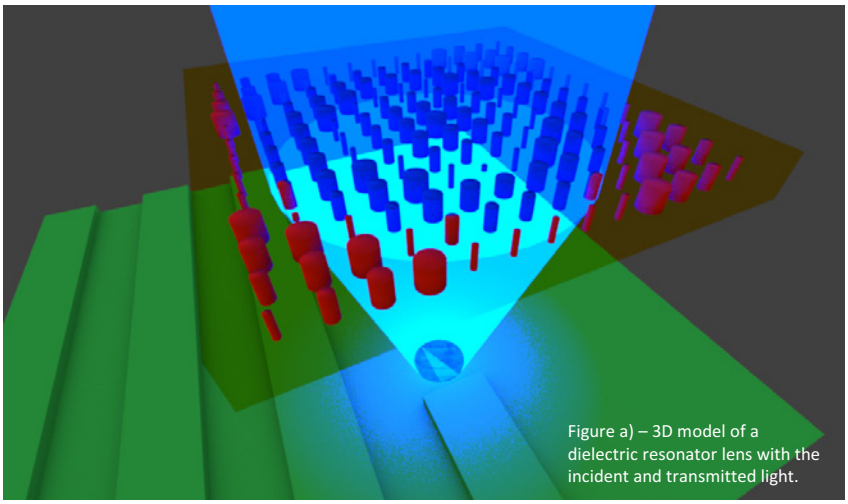

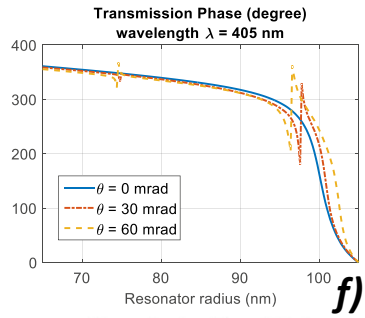

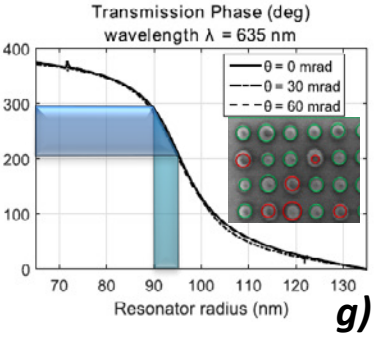

d) Transmittance and (e) phase functions for dielectric resonators with respect to radius for different wavelengths and angles of incidence;
f) Phase aberrations in the lens wavefront due to lithographic tolerances (inset);
g) Performance of the optimized lens versus a design (h) obtained through an analytical process.

ROBUST OPTIMIZATION

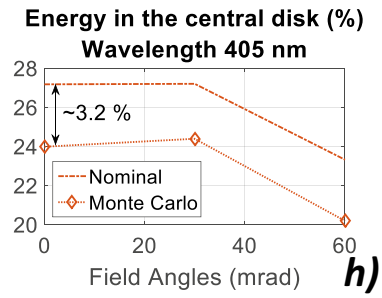

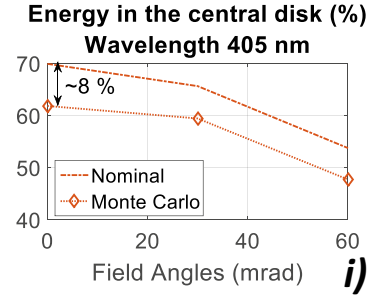

CONCLUSION

The robust optimization for metasurface lenses provides a better balancing of performance over desired FoV and bandwidth and a reduction of sensitivity towards lithographic tolerances.

This research was supported by TNO's Early Research Program 3D Nanomanufacturing Instruments

Metasurface enhanced AFM cantilever

B. Speet [1], F. Silvestri[1], G. Gerini[1,2], S. Mashaghi Tabari [3]

1 TNO – Delft; Optics Department
2 Technology University of Eindhoven; Electromagnetics Group
3 TNO – Delft; Opto-mechatronics Department

TNO innovation for life

RATIONALE

- Laser beam light not entirely intercepted by the AFM cantilever.
- The tail of the beam illuminates a portion of the surface under measurement.
- The light scattered by the surface (noise) is intercepted by the sensor, superimposing to the light directly reflected by the cantilever (signal). See Fig. 1.
- AFM accuracy reduced by signal-to-noise ratio deterioration.

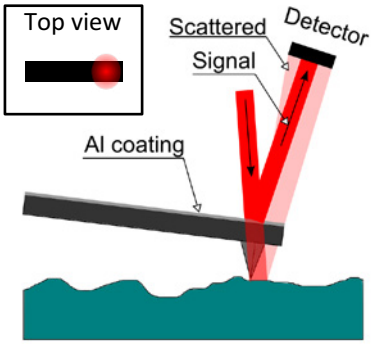

Figure 1: Schematic representation of the described problem.

PROPOSED SOLUTION

- A polarizing metasurface of non circular symmetric dielectric nanoresonators (Fig. 2) could be directly integrated on the cantilever.
- This surface rotates the impinging light to the orthogonal polarization.
- At the sensor, it is possible to discriminate the desired light reflected from the cantilever from the one due to the surface scattering.
- Fig. 3 shows the proposed solution based on the metasurface combined with proper polarizers.

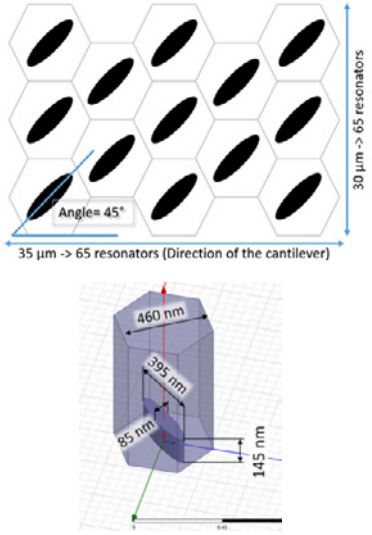

Figure 2: (top) Array of elliptical nanoresonators for polarization rotation. (bottom) Unit cell detail.

- The nanoresonators are manufactured with technologies compatible with the manufacturing of the cantilever and AFM tips.
- The final configuration includes a thin layer of low refractive index material (e.g. SiO2) between the nanoresonators and the reflecting Al layer, to prevent the excitation of Surface Plasmon Polaritons (SPP).

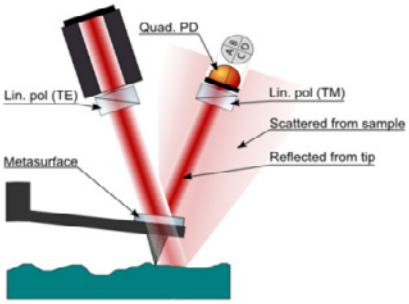

Figure 3: Modified cantilever with an integrated metasurface and relative polarization discrimination based concept.

- Three different configurations can be considered, in order to reduce the impact in terms of weight of the additional material deposited on the cantilever weight (see Fig. 4).

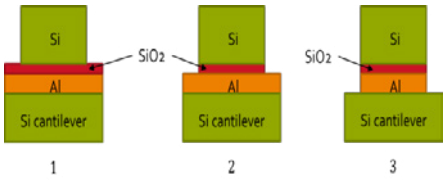

Figure 4: Different implementations of the metasurface cantilever integration.

RESULTS

- Fig. 5 shows: (a) total reflected power; (b) power associated to the polarized rotated component, normalized to the incident power.
- Configuration 2 can achieve the best optical performance.
- Configuration number 3 is less performing from the optical point of view, but offers a reduction of the cantilever weight compared to the original structure.

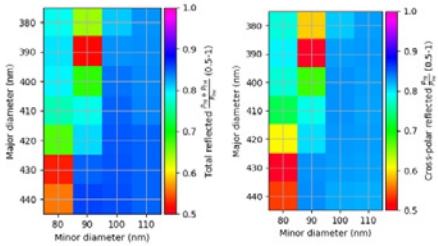

Figure 5: Total reflected power (on the left), Cross-polar power ratio (on the right); resonators' height 120 nm, configuration 2 of Fig. 4.

CONCLUSION

- A full-dielectric metasurface polarization rotator is proposed for integration on an AFM cantilever to improve the signal-to-noise ratio of the AFM system.
- The metasurface is compatible with the manufacturing technologies of the cantilever and has minimal impact on its mechanical properties.

This research has been supported by TNO's Early Research Program 3D Nanomanufacturing Instruments

OPTICAL SYSTEMS BASED ON METASURFACE ELEMENTS

J.Berzins[1,2], F.Silvestri[1], G.Gerini[1,3], F.Setzpfandt[2], T.Pertsch[2], S.Bäumer[1]

1 TNO (Stieljesweg 1, 2628CK Delft, Netherlands)
2 Friedrich-Schiller-University Jena (Albert-Einstein-Strasse 15, 07745 Jena, Germany)
3 Eindhoven University of Technology (P.O. Box 513, 5600MB Eindhoven, Netherlands)

TNO innovation for life

METASURFACES OFFER A GREAT ALTERNATIVE TO THE CONVENTIONAL OPTICS

A metasurface is a two-dimensional arrangement of nanoscale scatterers with capability to alter phase, polarization and amplitude of light. Such metasurfaces (Fig. 1) open new possibilities in optical systems with the potential to replace conventional optical components such as:

- color filters,
- polarizers,
- microlenses.

All-dielectric metasurfaces (Fig. 2), in contrary to the more known plasmonic ones, provide a reasonable solution towards a lossless optical system, while maintaining the flexibility of controlling the electric and magnetic resonances in the range of visible light.

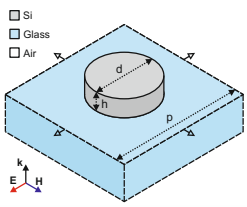

Fig. 2. Single cell of Silicon nanodisk from periodic metasurface.

COLOR FILTERS

The resonances provide a dip in the transmission, which can be tuned by the increase of the dimensions:

- height,
- diameter,
- periodicity,

or broadened depending on their ratio.

Such tunability allows the design of color filters for compact cameras. There are different options for realizing color filters. Having two filters of different colors and a full signal allows others colors to be retrieved via computational algorithms. Example of possible filter solutions are shown in Fig. 3.

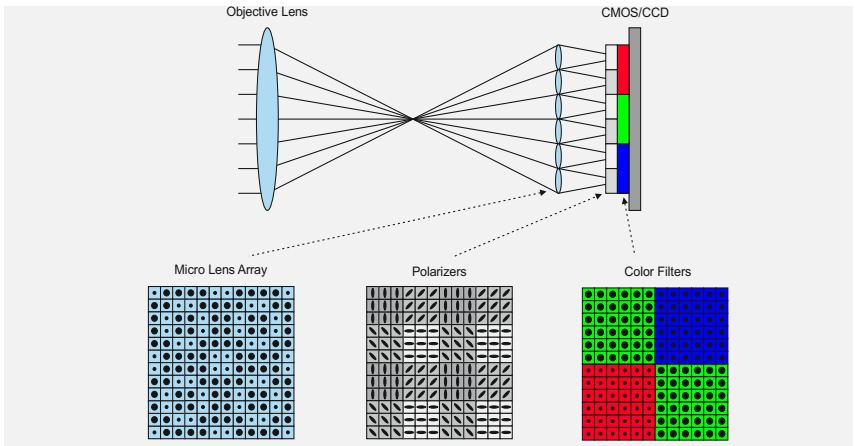

Fig. 1. Schematic representation of plenoptic camera using metasurface elements.

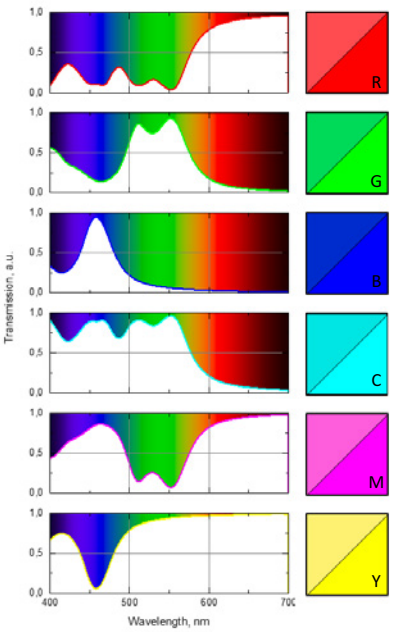

Fig. 3. Optimised RGB and CMY color functions and their representation in CIE 1931 standard, compared to ideal colors (top and bottom triangle, respectively). The size of nanodisk was varied till the best M and Y was found, other colors were derived from them.

MICROLENSES

Please refer to the presentation by F.Silvestri on “Robust Optimization for Metasurface Microlenses”.

POLARIZERS

Elongated on one axis or asymmetrical structures become polarization dependent, at particular dimensions enabling the metasurface to work as a polarizer (Fig. 4).

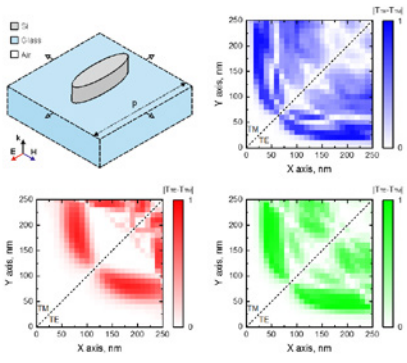

Fig. 4. Polarisation sensitive elliptical nanodisk and polarization sensitivity |TE-TM| dependance on the dimensions at RGB.

CONCLUSION

Filters, polarizers and microlenses can be successfully based on Silicon metasurface just by changing the size, shape and distribution of the nanostructures it consists of.

This research is supported by NOLOSS Project (Marie Skłodowska-Curie Innovative Training Network (MSCA-ITN-EID)) and TNO’s Early Research Program 3D Nanomanufacturing Instruments

Spectrally-Resolved Fourier-transform spectroscopy and Coherent Diffractive Imaging

Matthijs Jansen, Anne de Beurs, Kevin Liu, Kjeld Eikema and Stefan Witte

ARCNL and LaserLaB Vrije Universiteit, Amsterdam, The Netherlands

To be presented at the 3rd ERP 3D Nanomanufacturing dissemination workshop, TNO, 6 November 2017

Motivation

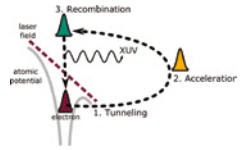

High-Harmonic Generation (HHG): Coherent extreme ultraviolet source.

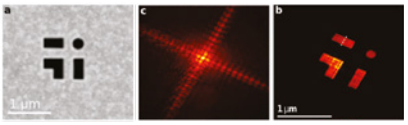

Enables monochromatic high-resolution coherent diffractive imaging. [1]

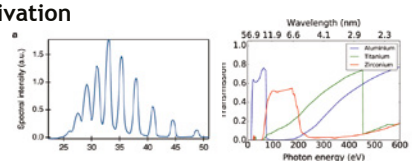

Broadband EUV sources are ideal for spectral characterization of various metals and nanostructures.

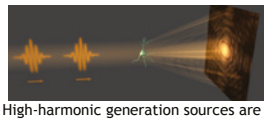

High-harmonic generation sources are uniquely suited for spatially-resolved Fourier-transform spectroscopy (FTS), enabling spectrally resolved microscopy at EUV wavelengths.

Spatially Resolved Fourier-Transform Spectroscopy using High Harmonics

- An OPCPA laser system delivers pulses of 5 mJ, with a ~25 fs pulse duration at 300 Hz repetition rate.
- A common-path interferometer splits this in two pulses of 1 mJ which are directly used for HHG.
- Spatial interferograms are recorded on the EUV CCD camera for different time delays.
- Temporal interference traces are extracted from single pixels
- A direct Fourier transform yields a spectrum for every pixel.

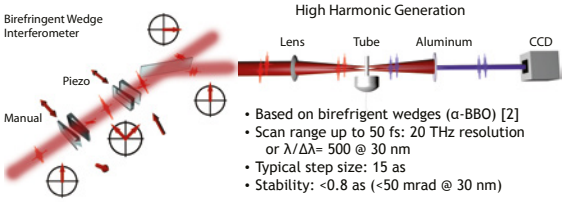

- Based on birefrigent wedges (α-BBO) [2]
- Scan range up to 50 fs: 20 THz resolution or λ/Δλ= 500 @ 30 nm
- Typical step size: 15 as
- Stability: <0.8 as (<50 mrad @ 30 nm)

- High harmonics from **Neon**
- Broad spectrum: 55 nm to 17 nm
- Short coherence length: 120 as

- High harmonics from **Argon**
- Bright: ~10^{11} photons/second
- Long pulse trains

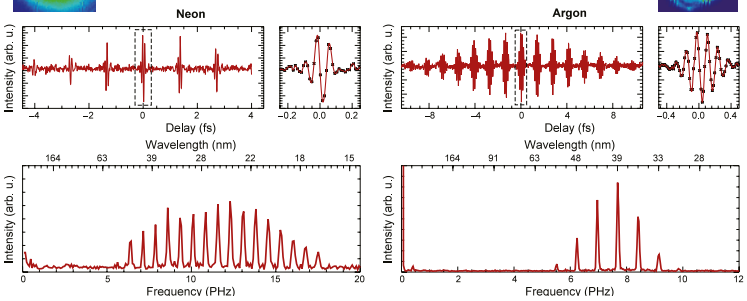

Fourier-Transform Interferometry for Coherent Diffractive Imaging

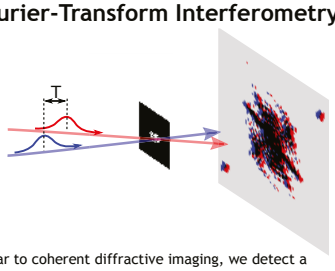

Individual diffraction patterns:

$$E_1(k) = A(k)\exp[i(\Phi(k))]$$
$$E_2(k) = A(k+\delta k)\exp[i(\Phi(k+\delta k)+\omega T)]$$

Measured intensity:

$$I(k) = |E_1(k)+E_2(k)|^2$$
$$= A(k)^2 + A(k+\delta k)^2 + A(k)A(k+\delta k)\exp[i(\Phi(k+\delta k)-\Phi(k)+\omega T)] + c.c.$$

Acquired from Fourier Transform Spectroscopy:

$$A(k)A(k+\delta k)\exp[i(\Phi(k+\delta k)-\Phi(k))]$$

- Similar to coherent diffractive imaging, we detect a farfield intensity pattern which contains information about the sample.
- Two identical, phase-locked pulses illuminate a sample at slightly different angles, resulting in two shifted, interfering diffraction patterns on the camera.
- The interference pattern resembles a distorted diffraction pattern but also includes some phase information.
- We developed an algorithm that reconstructs both the phase and intensity of the diffraction pattern for a single beam, yielding an image of the sample.

Spatially-Resolved Spectroscopy

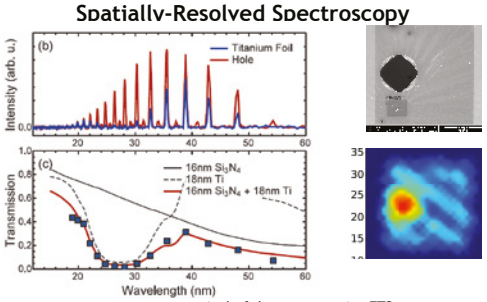

- We measure a spectrum on every pixel of the camera using FTS.
- This enables a direct spectral transmission measurement of a thin titanium film with an aperture on a silicon nitride membrane.
- The recovered absorption spectrum of the film agrees with the theoretical value and expected film thickness.

Spectrally-Resolved Coherent Diffractive Imaging

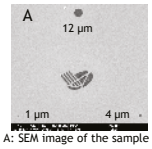

A: SEM image of the sample

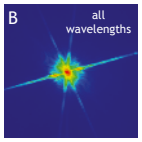

B: Broadband diffraction pattern.

- The interference of the diffaction of reference hole and main structure enables a simple image reconstruction: holography.
- We are able to retrieve high-quality diffraction patterns from the spatially-resolved Fourier-transform spectroscopy.
- For several wavelengths, a Fourier transform of the monochromatic diffraction pattern provides a good image of the sample at 4 micron resolution.
- Using our reconstruction algorithm improve the resolution to 0.7 micron. This improves the signal-to-noise of these images by two orders of magnitude.

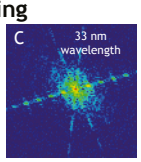

C: Diffraction pattern at 32 nm.

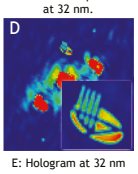

E: Hologram at 32 nm

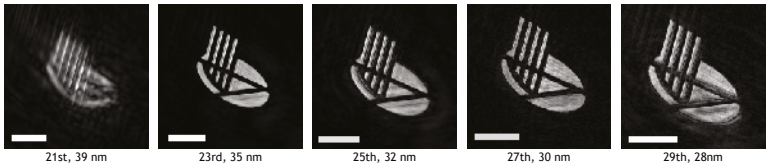

21st, 39 nm | 23rd, 35 nm | 25th, 32 nm | 27th, 30 nm | 29th, 28nm

Outlook

- To improve the resolution, we are setting up a refocusing beamline for XUV, increasing the incident flux on micron-sized samples. This will also reduce the measurement time.
- We are increasing the power of the driving laser, which should lead to higher fluxes at shorter wavelengths.
- Our first measurements used Fourier transform holography to provide an initial object guess. We are extending the approach to samples without holographic references.
- The present system is aimed at transmission microscopy, but with the proper adjustments to the imaging setup, the method extends to reflective imaging as well.

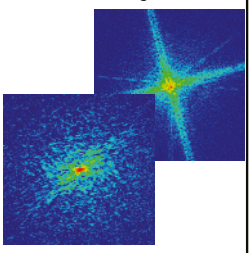

References

[1] M.D. Seaberg et al., Opt. Express 19, 22470 (2011)
[2] D. Brida et al., Opt. Lett. 37, 3027 (2012)
All spatially resolved spectroscopy results presented here have been published in:
[3] G. S. M. Jansen et al., Optica 3, 1122 (2016)

ARCNL

ADVANCED RESEARCH CENTER FOR NANOLITHOGRAPHY

Detecting gratings below opaque layers using laser induced ultrasonics

Stephen Edward[1], Alessandro Antoncecchi[2], Hao Zhang[2], Kjeld Eikema[2], Stefan Witte[2] & Paul Planken[1]

[1]EUV targets, ARCNL & University of Amsterdam

[2]EUV generation and Imaging ,ARCNL & Vrije Universiteit Amsterdam

Motivation

Detection and localization of (non-)periodic structures below an optically opaque layer for sub surface metrology applications

Approach

Laser induced ultrasonics- excitation of ultrasound waves in the opaque layer, which can travel through the layer and probe the underlying structure

Detection- Modulation of the surface reflectivity by the returning ultrasound wave (either in total reflectivity or through the appearance of a spatial structure)

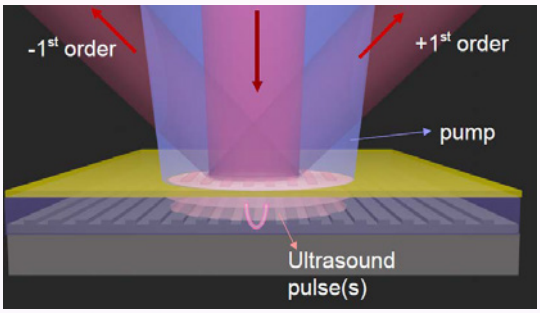

Transient grating

Generate and detect a spatially periodic sound wave that stays intact as it propagates and reflects off interfaces.

- Flat , single layer gold
- Spatially periodic illumination
- Pump- 400nm, 10μJ, 30fs
- Probe- 800nm, 2μJ, 30fs

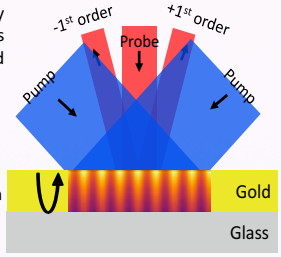

Experimental Setup

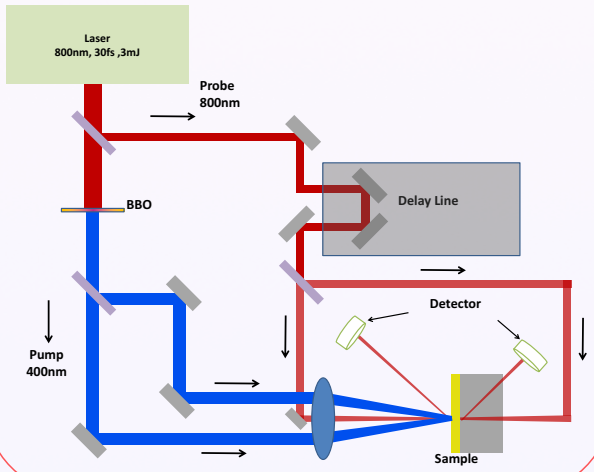

Acoustic Echo

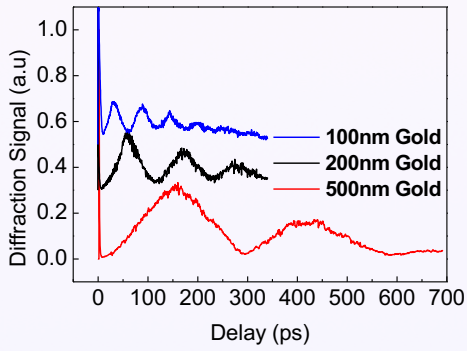

Acoustic Echo from hidden grating

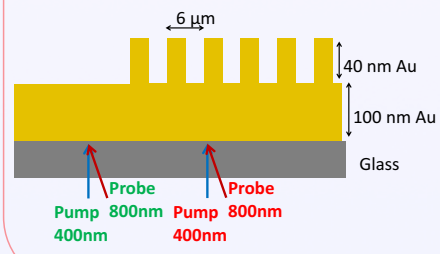

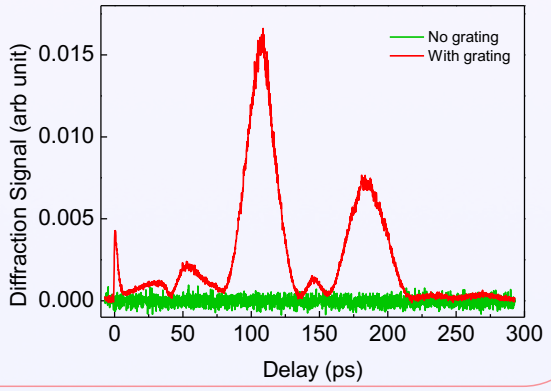

Future Work

- Detecting gratings etched on silicon wafer
- Detecting grating buried under multiple layer of different metals
- Detecting and locatizing buried ASML alignment grating on real customer wafers
- Imaging non periodic structures buried under metals.

ASML NWO Universiteit van Amsterdam VU Vrije Universiteit Amsterdam Provincie Noord-Holland Gemeente Amsterdam

Nano-antenna Array Microscope

F. Bernal Arango [1,2], F. Silvestri[1] , G. Gerini[1,3]

1 TNO – Delft; Optics Department
2 Currently with Delft University of Technology
3 Technology University of Eindhoven; Electromagnetics Group

TNO innovation for life

NANO ANTENNA ARRAY MICROSCOPE

- Proposed or existing optical high-resolution near-field sensors:
  - near field scanning optical microscopy (NSOM);
  - solid immersion lenses (SIL) ;
  - negative refractive index or hyperbolic metamaterial lenses.
- Novel concept: plasmonic nano-antenna array microscope (Fig.1-2).
  - An array of nano-antennas is placed very close to the object of interest (< 30 nm).
  - The near field of the illuminated object couples with the nano-antenna array.
  - The high spatial frequency content is encoded into the nano-antenna array far-field radiation.

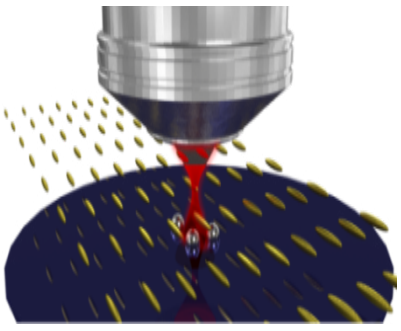

Figure 1: Artistic impression of the nano-antenna array microscope.

- The array is scanned over the object to be imaged.
- For each position, the patterns of the array scattered field are recorded.
- By processing these patterns, it is possible to reconstruct the object's image.

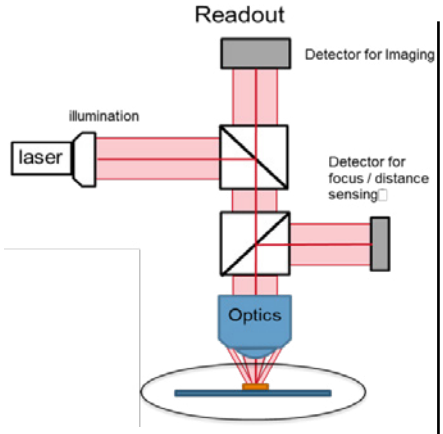

Figure 2: Nano-antenna array microscope optical system.

PROs and CONs

Pros:
- Ease of manufacturability (with respect to metamaterial based sensors);
- Ease of integration in a miniaturized scanning head for parallelization (with respect to SIL);
- Imaging well beyond the diffraction limit (< λ/20).

Cons:
- Throughput

THEORETICAL RESULTS

- 9x9 array of gold nano-dipoles at 20 nm from the object; inter-element distance: 150 nm.
- Wavelength of operation: λ= 800 nm.
-
- Object: 3 point source particles in a rotated L configuration (30x40 nm).
- Near field model based on point dipole representation.
- Near field coupled with conventional confocal microscope model.
- Simple reconstruction model: differences between diagonal and anti-diagonal quadrants in Fourier image plane.

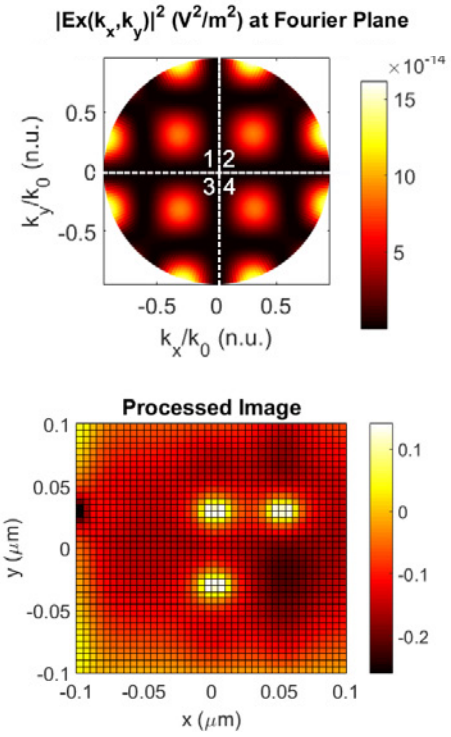

Figure 3: Fourier image plane (top) with highlights on the four quadrants used for the post-processing algorithm; final processed image showing the three particles placed at distances below the diffraction limit.

CONCLUSION

- **A near-field microscope concept based on an array of plasmonic nano-antennas has been studied.**
- **A resolution well beyond the diffraction limit has been demonstrated theoretically: particles separated by 30-40 nm could be resolved using 800 nm light.**

This research has been supported by TNO's Early Research Program 3D Nanomanufacturing Instruments

Ptychography for nanometrology applications: *Throughput analysis*

Wouter Koek[1], Bastiaan Florijn[1], Davy van Megen[1], Stefan Bäumer[1], Rik Kruidhof[2]

1 Department of Optics, TNO, Delft
2 Department of Optomechatronics , TNO, Delft

TNO innovation for life

We have analyzed the performance of (soft xray) ptychography[1] with respect to *throughput*, *measurement accuracy* and *spatial resolution*. The results for throughput are presented here.

We have simulated soft xray ptychographic measurements and performed the subsequent numerical reconstruction. The presented simulations assume a wavelength of 13 nm, a spot size of 500 nm (D4σ), a detector with 400x400 pixels (at a numerical aperture of 0.8), and the sample as shown in Figure 1.

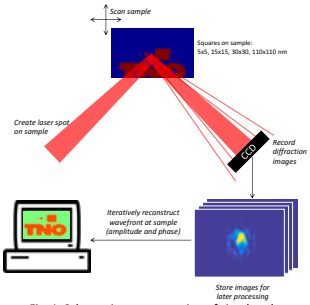

Fig. 1. Schematic representation of simulated experiment and subsequent numerical recontruction.

PHOTON-LIMITED PERFORMANCE

Figure 2 shows the logarithm of the recorded energy fraction that is captured by a single pixel. Clearly, pixels at the detector's edge (corresponding to high spatial frequencies) receive many orders of magnitude less photons than those in the center. High spatial frequencies (needed to resolve smaller details) will thus suffer more from photon shot noise.

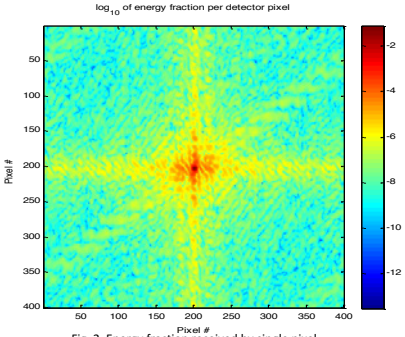

Fig. 2. Energy fraction received by single pixel. Note the logarithmic scale.

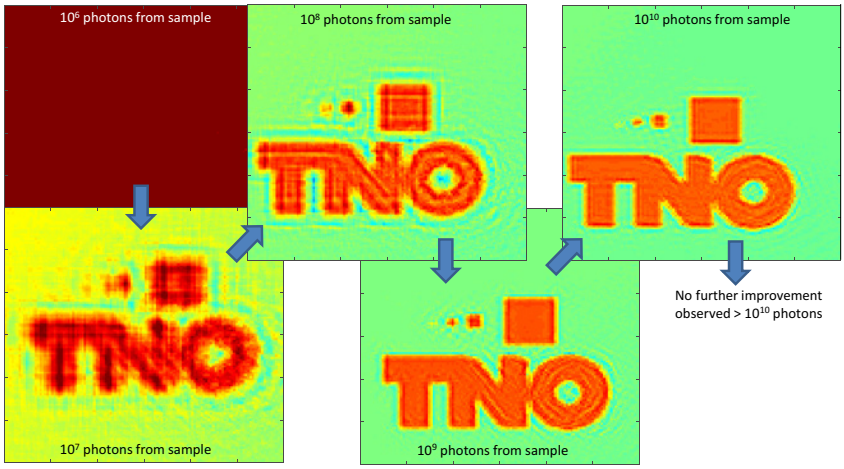

Fig. 3. Reconstructed sample reflectivity. Each reconstruction is based on a set of 121 diffraction images, where each diffraction image contains the specified number of photons.

Consequently, the amount of detail in the reconstructed image depends on the amount of photons that are scattered towards the detector. Figure 3 shows that each diffraction image should contain 10^9-10^{10} photons in order obtain optimal performance of the simulated system. Although this outcome is system- and sample specific, it is in good agreement with recent ptychographic experiments.[2,3]

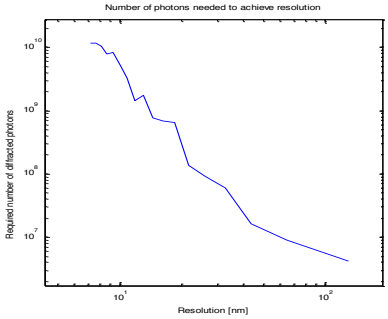

Fig. 4. Required number of photons coming from the sample in order to achieve a certain spatial resolution.

In order to avoid photon shot noise-limited performance, each detector pixel should capture at least 5 photons.[4] Because each detector pixel is associated with a particular spatial frequency, the diffraction image of Figure 2 can be used to construct the resolution-vs-dose chart of Figure 4. There is good qualitative agreement with this chart and the images in Figure 3; coarse features appear at ~10^7 photons, ~10^9 photons are needed for fine details and steep edges, and no further improvement is observed > 10^{10} photons.

THROUGHPUT

Data redundancy is inherent to ptychography, meaning that each location on the sample is illuminated multiple times. In our simulation (at least) 25 different diffraction images needed to be recorded to reconstruct an area of 1 μm^2. Current commercially available coherent soft xray sources produce ~10^{10} photons per second (at 13 nm).[5]
When assuming a sample reflectivity of 4.5e-4 (SiO_2 at 45°), and requiring 10^9 recorded photons per image, the speed at which the surface of a typical semi-conductor sample can be measured is limited to ~1.5 hours per μm^2. Due to their much higher reflectivity EUV masks can be measured considerably faster. Note that for full 3D reconstructions the expected speed is even one to two orders of magnitude slower.[6]

CONCLUSION

To enable high-throughput wafer-based soft xray ptychography more source power is needed. Alternatively, a new type of ptychography, e.g. using a-priori knowledge to enhance throughput, needs to be developed.

References
1) Ultramicroscopy 109, p 1256-1262 (2009)
2) Optics Letters 41, p5170-5173 (2016)
3) Nature Photonics 11, p259-263 (2017)
4) J. Phys. Condens. Matter 28 (2016)
5) KM-Labs XUUS 4 (kmlabs.com)
6) Nature 543, p402-406 (2017)

This research was supported by TNO's Early Research Program 3D Nanomanufacturing Instruments

Electromagnetic Modelling Tool for X-ray Ptychography Simulation Frameworks

L. Pjotr Stoevelaar[1,2], Giampiero Gerini[1,2]

1 Optics, Technical Sciences, TNO
2 Department of Electrical Engineering, Eindhoven University of Technology

TNO innovation for life

INTRODUCTION

- Miniaturization trends of the semiconductor industry require higher resolution imaging techniques.
- More conventional techniques like Critical Dimension Scanning Electron Microscopes (CD-SEM) and Optical (scattering) Critical Dimension tools (OCD) are reaching their limits.
- Promising new technologies are based on X-ray.
- Due to the very poor focusing power that can be achieved at these wavelengths, lens less imaging techniques, such as X-ray ptychography are highly preferable.

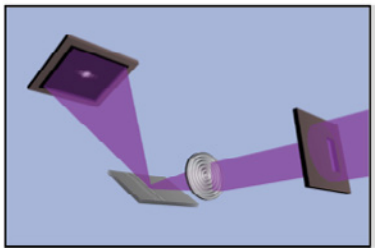

Fig. 1 A X-ray ptychography setup: a illumination beam is scanned over the object and the scattered fields are recorded onto the detector .

PTYCHOGRAPHY

- In a ptychography setup a robust data set is made by scanning a beam over tan object and recording the scattered field.
- A reconstruction algorithm is then used to compute the image of the object.
- These data sets are normally obtained experimentally.

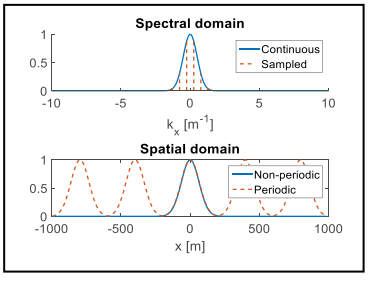

Fig. 2 Illustration of the sampling process of the illumination beam

PROBLEM

- Experimental ptychography setups are complex and expensive.
- More convenient is an accurate and quick modeling tool.
- Modeling the complete domain with a Finite Element Method is almost impossible, due to large the large illuminated area and the very small features of the object.
- By decomposing the beam in a spectrum of plane waves, the simulation domain no longer determined by beam width.
- Analytic decomposition of the background field in a incoming, reflected and transmitted part is now possible.

ILLUMINATION BEAM SAMPLING

- By sampling the illumination beam in the spectral domain, a periodic beam is obtained in the spatial domain.
- Sufficient sampling prevents replicas from entering the scanning area.
- For a Gaussian beam the necessary number of plane waves is given by:
- $N = \left\lceil \frac{2B_s B_k}{\pi} \right\rceil$, where B_k is the spectral bandwidth and B_s is the spatial bandwidth.
- The spectral bandwidth is given by: $B_k = \frac{2}{w_0}$, with w_0 the minimum waist size of the beam.
- The spatial bandwidth is given by: $B_s = 2w_0 + \Delta r_{max}$, with Δr_{max} the distance between the central scan position and the most outer scan position.

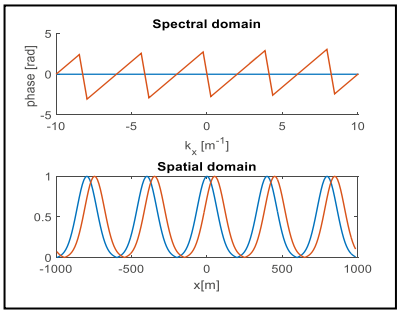

Fig.3 Illustration of the Fourier transform shift property

BEAM SCANNING

- The effected of beam scanning can be computed without recomputing the near-field when using the plane wave decomposition.
- The Fourier transform shift property: a shift in space ←→ a linear phase shift in the spectral domain.
- Summing all plane waves with the correct phase results into a shifted beam.
- The Fourier transform shift property is shown in Fig. 3.

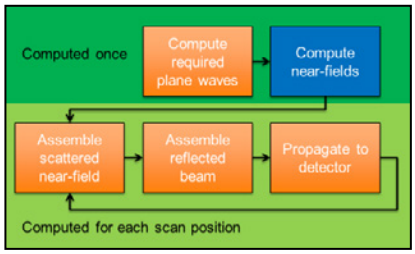

Fig. 4 Flow computation steps in simulation tool

SIMULATION TOOL STRUCTURE

- Total field at detector is given by the reflected field and the scattered field.
- Both fields are computed in near-field.
- Then both fields are summed and propagated.
- The flow diagram of the of the simulation tool is shown in Figure 4 : first the program computes the plane waves required for the near-field simulation, then solves the scattering problem for all these plane waves. Finally, for each scan position the scattered field and reflected beam are assembled and propagated to the detector.

CONCLUSION

- Effective and accurate method for generating x-ray scattering datasets.
- No need for an expensive and complex measurements set-up in ptychography algorithm development.

This research was supported by TNO's Early Research Program 3D Nanomanufacturing Instruments

Sub-wavelength metrology for Advanced Defect Classification

P. van der Walle[1], E. Kramer[1, 2], J.C.J. van der Donck[1], W. Mulckhuyse[1], L. Nijsten[1], F. Bernal Arango[1,2], A. de Jong[1], E. van Zeijl [1], H.E.T Spruit[1], H. van den Berg[1], G. Nanda [3], A. van Langen-Suurling [3], P.F.A. Alkemade [3], S. Pereira [2] and D.J. Maas[1]

1 Department of Nano-Instrumentation, TNO, Delft
2 Department of Imaging Physics, Delft University of Technology, Delft
3 Kavli Institute of Nanoscience, Delft University of Technology, Delft

TNO innovation for life

Particle defects are one of the main contributors to yield loss in semi-conductor manufacturing. Therefore these have to be minimized and, when they do occur, to be characterized in order to determine their origin.

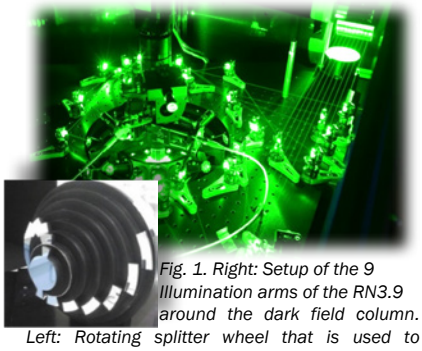

Fig. 1. Right: Setup of the 9 illumination arms of the RN3.9 around the dark field column. Left: Rotating splitter wheel that is used to illuminate from the 9 different azimuth angles.

TNO has developed the Rapid Nano particle inspection system capable of detecting 42 nm LSE particles. This sensitivity is achieved by illuminating the sample from multiple angles. In particle detection mode the signal from all these angles is added. Here, we analyze the signals from individual arms to derive the shape and size of sub-wavelength defects. Via this analysis we are able to classify and select defects for further analysis on much slower metrology tools.

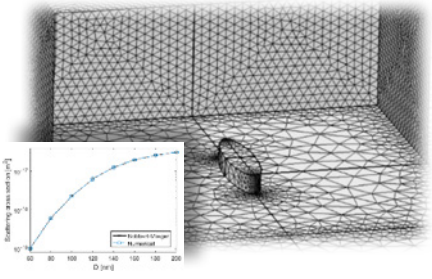

Fig. 2. Geometry and mesh used in the numerical model in COMSOL are shown (top), Match between simulated scattering cross section and the Bobbert-Vlieger model shows the validity of the simulation (bottom)

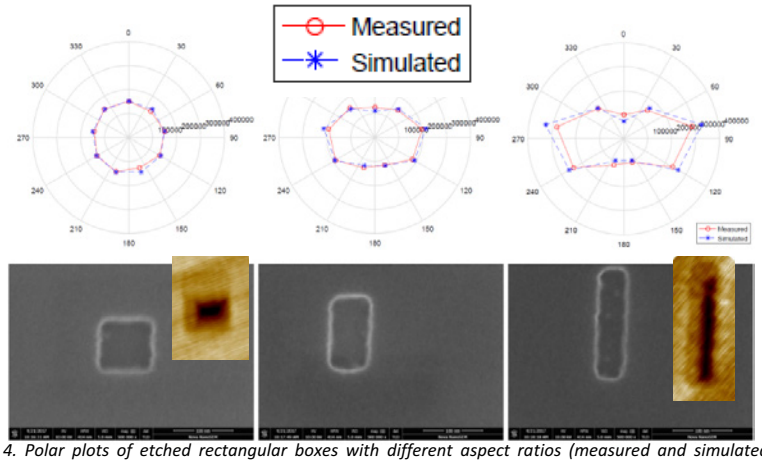

Fig. 4. Polar plots of etched rectangular boxes with different aspect ratios (measured and simulated) with corresponding SEM and AFM images (1:1 top, 1:2 center, 1:5 bottom).

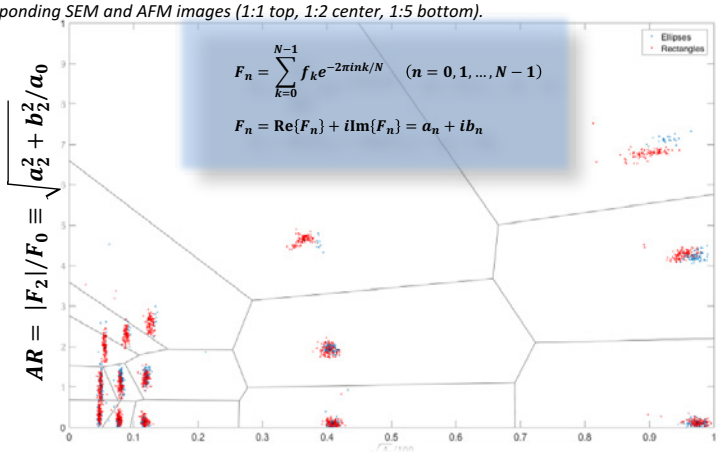

Fig 5. The polar plots of scattering versus illumination angle can be decomposed into Fourier coefficients by taken the transform over this angle. To first order the 0th order is proportional to the defect size, while the 2nd order is proportional to the aspect-ratio. Clusters of different defect types are revealed in a scatter plot of these coefficients.

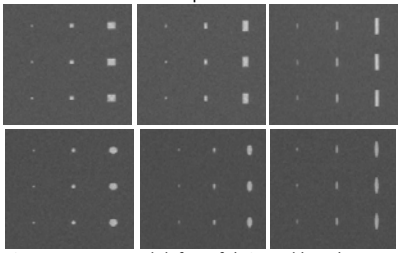

Fig. 3. Programmed defects fabricated by e-beam lithography (gold on silicon).

This project has received funding from the Electronic Component Systems for European Leadership Joint Undertaking under grant agreement No 621280. This Joint Undertaking receives support from the European Union's Horizon 2020 research and innovation programme and Netherlands, France, Belgium, Germany, Czech Republic, Austria, Hungary, Israel.

CONCLUSION

We investigated whether it is possible to extract additional information on defects by analyzing the scattering of the 9 illumination angles of the Rapid Nano separately. This investigation was done by modeling of scattering of arbitrarily shaped defects (Fig. 2) and experiments on fabricated programmed defects (Fig. 3) Figure 4 shows results on a few selected defects. The modeling and experimental results are in agreement.

By decomposing the polar plots into their Fourier components the statistical distribution of different defect types can be revealed (Fig. 5). When this distribution is known a more informed choice can be made on where to perform additional expensive defect review measurements.

Differential binary-phase interferometric particle detection

W. Koek[1], E. van Zwet[2], H. Sadeghian[2]

1 Department of Optics
2 Department of Optomechatronics

TNO innovation for life

INTRODUCTION

One of the main challenges in detecting a particle on a nano-rough surface is to differentiate the particle from a speckle background. By creating a 'special' type of speckle, the particle light can be interferometrically amplified without amplifying the speckle.

All images and figures are based on physical wave front propagation simulations.

CONCEPTUAL LAYOUT

The conceptual layout, shown in figure 1, shows the annular aperture and the phase/amplitude mask that are required to generate the 'binary phase' speckle. Two images enable difference detection.

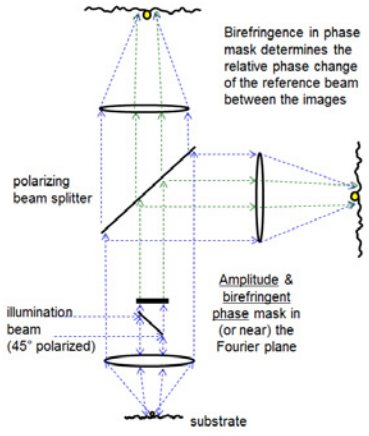

Figure 1 – Conceptual layout.

BINARY PHASE SPECKLE

Figures 2 and 3 serve to explain and demonstrate the formation of binary phase speckle.

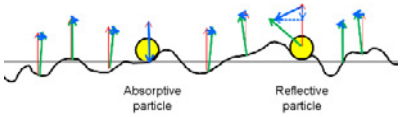

Figure 2 – Perturbation phasors (blue) due to absorptive/reflective particles and nano-rough background

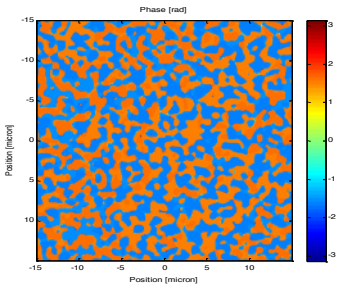

Figure 3 – Phase distribution in image.

IMAGES OF 15NM PARTICLE

Below a 15 nm particle on 0.15 nm rms surface roughness is imaged using different techniques.

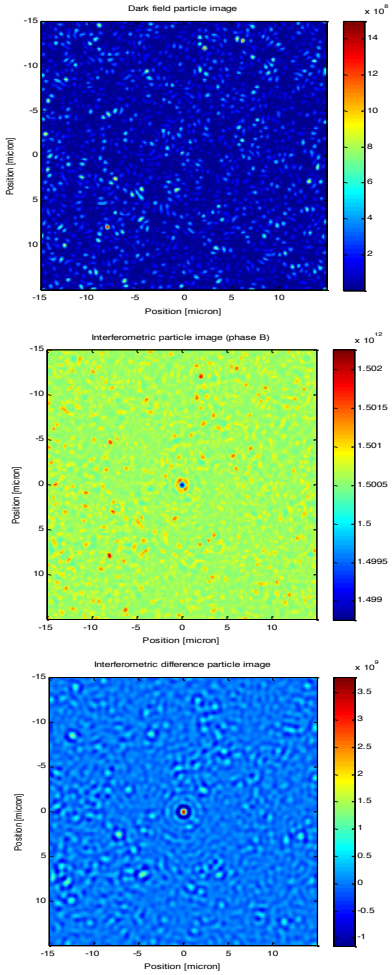

Figure 4 – Images of 15nm particle (interferometric images 1000x ref. ratio).

IMPROVED DETECTION LIMIT

When applying an identical signal-to-noise (peak-to-sigma) requirement, with the proposed method the particle detection limit can be improved from 22.5 nm to 15.5 nm (reflective particle on a surface with 0.15 nm rms roughness).

However, because in the difference image the particle has a distinct 'fingerprint' the detection limit may be reduced even further.

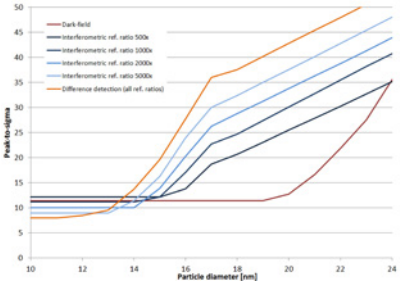

Figure 5 – Peak-to-sigma as a function of particle diameter for various detection methods.

ABBERATIONS

It is crucial that there is minimal interference between the background speckle and the reference beam. This results in very demanding (~unrealizable) requirements on the optics.

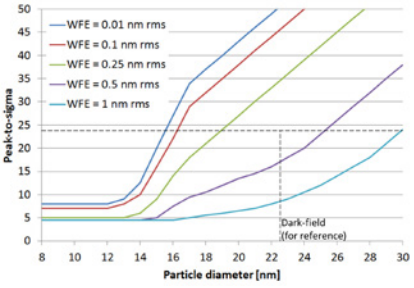

Figure 6 – Peak-to-sigma as a function of particle diameter for various levels wavefront error (WFE).

CONCLUSION

It is shown that nano particle detection can be improved with the proposed method. However, this would require optical elements with extremely small aberrations, making this a highly impractical solution.

This research was supported by TNO's Early Research Program 3D Nanomanufacturing Instruments

Spectrometer on chip

Peter Harmsma[1], Anna Tchebotareva[1], Stefan Bäumer[1]

1 Optics Department, TNO, Delft
peter.harmsma@tno.nl

TNO innovation for life

Introduction

There is a need for miniaturized devices which can establish the chemical composition of a sample in a reliable way. TNO is exploring technologies to miniaturize spectral analysis systems for this purpose. A promising route is the use of on-chip optics, fabricated using manufacturing technologies known from the semiconductor industry.

Application domains

In many applications, it is crucial to know the molecular constituents of a sample. For example, an alarm needs to be triggered in case air or soil water contains toxic compounds. Real-time knowledge of process gas concentrations helps optimizing production processes. Many relevant usages can be envisioned:

- Food: quality, ripeness, over due.
- Agriculture: crop condition, moisture, pesticides.
- Manufacturing: process optimization.
- Healthcare: breath analysis, identification of tumors vs. healthy tissue.
- Automotive: engine performance, lubricants.
- Raw materials: identification, concentration.
- Pollution: air / water monitoring.

Spectroscopy provides the highest selectivity in molecular identification, since each molecule has distinct spectral properties: absorption, reflection, luminescence, Raman spectrum, etc.

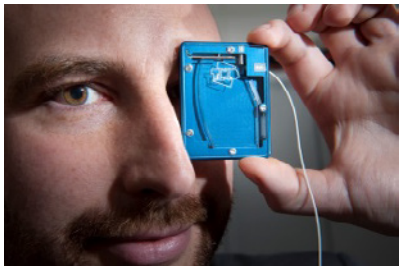

Mini-spectrometer (TNO): can it be smaller while superior performance is maintained?

Challenge 1: wavelength

Molecular spectral fingerprints are most pronounced at wavelengths between 3 and 10 μm. Common waveguide-based devices operate from 0.4 – 1.6 μm. Long-wavelength sources are still expensive. Recent initiatives such as the MIRPHAB pilot line are expected to close the gap.

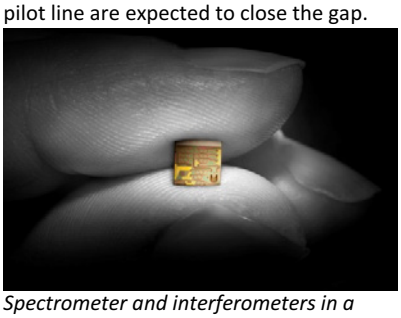

Spectrometer and interferometers in a read-out unit for FBG gratings (TNO)

Challenge 2: etendue

The small cross section and numerical aperture of a waveguide hamper efficient collection of ambient light. Improvement is expected from advanced circuit designs, and from massive parallelization enabled by chip manufacturing technology.

Etendue enhancement using many inputs (Yang, Opt. Let. 2017, 2675)

Challenge 3: light-matter interaction

In evanescent sensing based devices, sensing occurs in a few 100 nm near the sensor surface. Changes in surface properties over time should not affect the sensor accuracy and sensitivity.

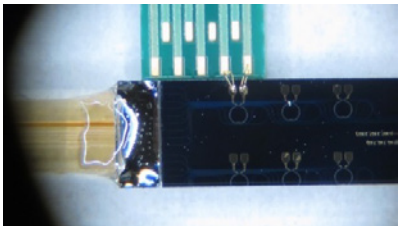

On-chip calibration unit for spectrometers on-board of satellites (TNO/LioniX/Airbus)

TNO track record

TNO has a long track record in spectrometry, in particular for space applications, and a large expertise in on-chip optical wavelength filters. For example, we have realized a spectrometric on-chip read-out unit for Fiber Bragg Gratings, and a ring-resonator based device for in-orbit calibration of spectrometers on board of a satellite.

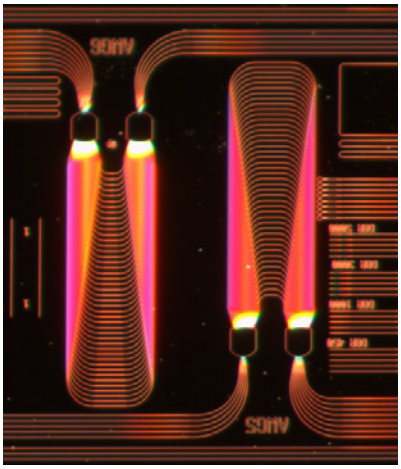

Arrayed-waveguides are often applied for spectral processing (TNO)

Fit for TNO

Miniaturized spectrometers are the cross-link between our knowledge in geometric optics spectrometers and on-chip optics. Our intentions match well with our activities in metrology and sensing. We have the relevant knowledge, not only on optics but also on chemistry, materials and contamination. We are well connected with the Dutch industry, in particular SMEs, and are well embedded in the Dutch and European photonics community.

CONCLUSION

We are in the process of mapping technologies and market needs in the field of miniaturized spectroscopy. Realization of a demonstrator device is envisioned in the near future.

This research was supported by TNO's Early Research Program 3D Nanomanufacturing Instruments

Resolution Enhancement with Solid Immersion Lens

Man Xu[1,2], Pjotr Stoevelaar[1,3], Giampiero Gerini[1,3], Stefan Bäumer[1]

1 Optics, Technical Sciences, TNO
2 Imaging Physics, Delft University of Technology
3 Department of Electrical Engineering, Eindhoven University of Technology

TNO innovation for life

Introduction

Enabling superresolution optical microscopy with large throughput.

Solid immersion lens (SIL) can improve the resolution of an optical microscopy system by a factor of n (the refractive index of the SIL). Meantime the imaging system maintains a large light throughput as compared to a near field scanning microscope. The non-contact optical approach also avoids introducing contamination to the sample.

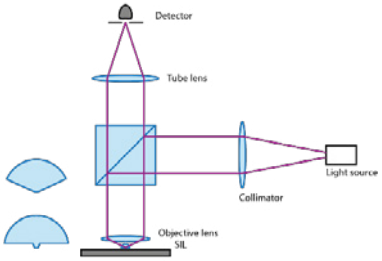

Fig. 1 Schematic drawing of a SIL microscope system.

Focal field of a high NA system

The representation of light field in the focal region of a high NA system is well-known in the form of Debye-Wolf integral [1,2]. In this paper, Novotny and Hecht's formalism [3] is used for calculation. Assuming a monochromic x-polarized plane wave with λ = 193 nm is focused by an objective with NA_{air} = 0.745. The focal fields in air and in a high index medium (n = 2) are plotted below in Fig. 2.

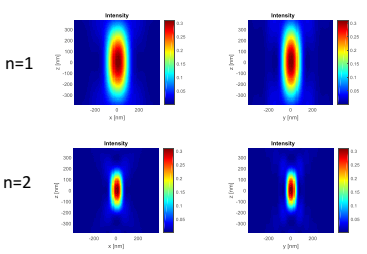

Fig. 2 Focal field of high NA object in air and high index medium with n=2.

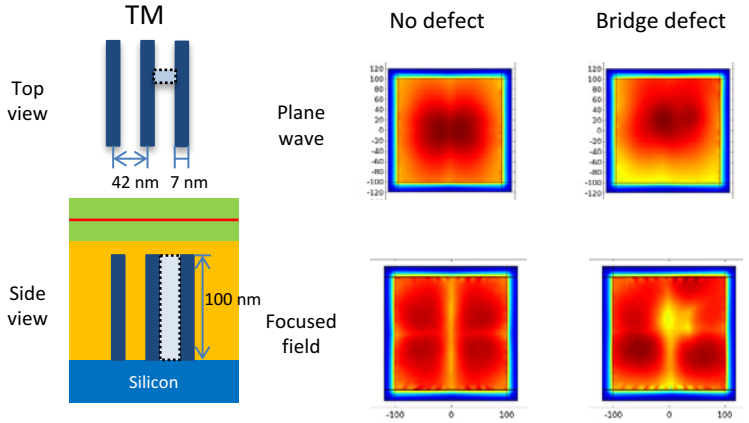

Fig. 4 Scattering by a simple structure. Plotted colormap: top row – scattered field of a plan wave incidence with TM polarization ; bottom row – scattered field of a tight focus.

The spot size is clearly reduced in a high index medium. Using a SIL, the $FWHM_x$ at the focus is reduced from 153 nm in air to 77 nm. The focus spot is elongated in the x-direction, with $FWHM_x/FWHM_y$ = 1.2.

To study the interaction between the reduced spot with nano-structures, simulations based on finite element method (Comsol®) are performed.

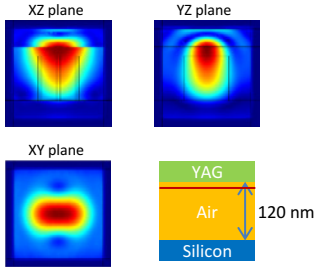

Fig. 3 Focal field of a high NA system in a multi-layer stack. The field amplitude is shown.

First, a background field calculation based on multilayer construction is needed. As seen in Fig. 3, the focus point is at the bottom of the SIL(YAG). The field below the SIL contains two parts: the propagating waves and the evanescent waves. When the distance between SIL and the structure is small (<50 nm), the evanescent waves can tunnel through and carry information of finer detail therefore enhance the resolution.

Diffraction with SIL

A simple structure consisting of 3 lines is placed 20 nm below the SIL within the focal region (illustrated in Fig. 4). The scattered field is calculated with Comsol®. Introducing a defect (bridge bar) leads to drastic change in the scattered field. Field in Fig. 3 is used as background field to calculate the scattering of the tight focus.

SIL imaging system at 193 nm

A further push for high resolution is to use shorter wavelength. Wavelength of 193 nm is of the limit for an 'optical' system. At 193 nm, YAG is the most promising material choice for SIL. It is a high index material with low birefringence. Due to the high dispersion of fused silica at 193 nm, a reflection objective lens is preferred.

References

1. E. Wolf, *Proc. Roy. Soc.* A **253**, 349 (1959).
2. B. Richards and E. Wolf, *Proc. Roy. Soc.* A **253**, 358 (1959).
3. L. Novotny and B. Hecht, *Principles of Nano-Optics*, 2nd Ed. Cambridge University Press, (2012).

CONCLUSION

- Theoretical models are applied to study SIL for its enhancement factor for an imaging system.
- The framework can be further developed for defect/particle detection analysis.

This research was supported by TNO's Early Research Program 3D Nanomanufacturing Instruments

Quantifying resolution in subsurface probe microscopy

D. Piras[1], R.M.T. Thijssen[1], M.H. van Es[1], P. van Neer[2], H. Sadeghian[1]

[1]Department of Optomechatronics
[2]Department Of Acoustics and Sonar

TNO innovation for life

INTRODUCTION

Assess resolution dependency on:

- excitation method
- applied force
- tip radius

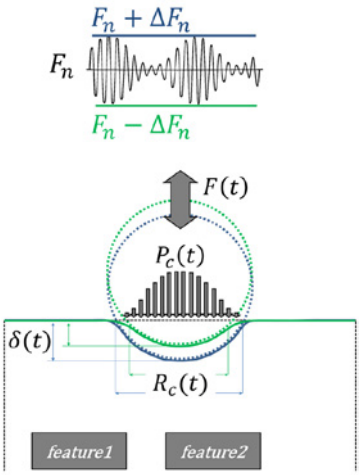

Fig. 1: Excitation scheme

METHODS

- For dynamic analysis, FEM contact is not feasible
- FEM modelling of tip sample interaction with Hertzian model
  - ➢ tip replaced by contact pressure
- Time varying top excitation MHz range
- Tip and sample in contact
- Indentation $\delta(t)$ of tip used to estimate the contact stiffness K
- imaging of two identical subsurface features
- While exciting the tip, the features are scanned

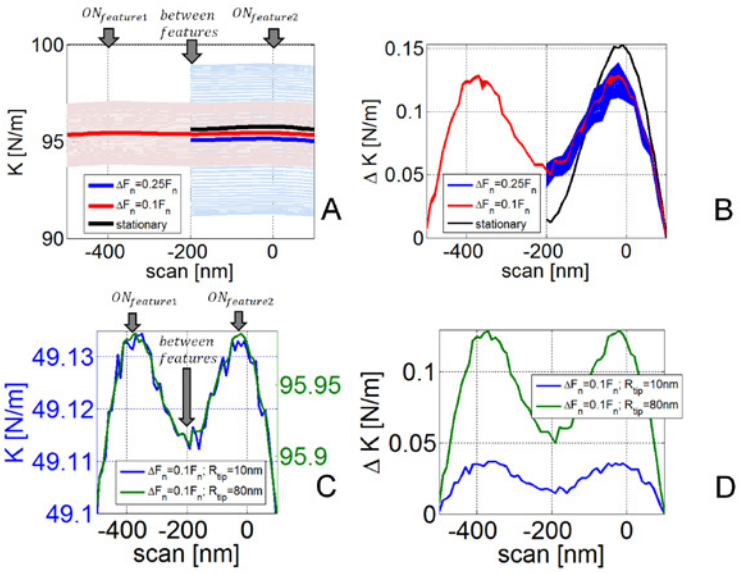

Fig. 2: Effect of excitation amplitude (A,B), Effect of tip size (C,D)

RESULTS

Measurements with a large (blunt Fig. 3A), and small (sharp Fig. 3B) tip also show Subsurface profiling is independent of the tip size (Fig. 3C)

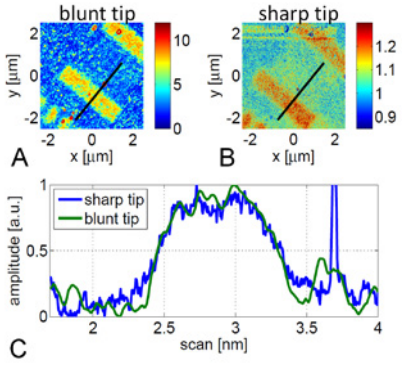

Fig. 3 Subsurface measurements with blunt (A) and sharp tip (B) and comparison of the normalized cross-section (C)

RESULTS

Dynamic excitation quite different from stationary case:

- mean contact stiffness dependent on applied load oscillation (Fig. 2A)
- compared to static, the dynamic load is less sensitive to subsurface feature (Fig. 2B)

Tip size:

- Affects nominal K value (Fig. 2C), but profile $ON\_feature1/between/ON\_feature2$ is similar
- Larger tip is more sensitive (Fig. 2D)

CONCLUSION

- In dynamic case when the steady state is not reached at each excitation time, the ability to resolve two objects is lowered.
- Subsurface resolution does not depend on the tip size: rather depends on the choice of the correct cantilever, and on the noise level

This research was supported by TNO's Early Research Program 3D Nanomanufacturing Instruments

Electrostatically actuated probes for Scanning Subsurface Ultrasonic Resonance Frequency Microscopy

Maarten. H. van Es[1], Martijn van Riel[1], Tom Duivenvoorde[1], Hamed Sadeghian[1]
[1] NOMI, Optomechatronics, TNO, Stieltjesweg 1, 2628CK, Delft, The Netherlands

TNO innovation for life

INTRODUCTION

Scanning Subsurface Ultrasonic Force Microscopy (SSURFM) relies on high frequency ultrasound in combination with Atomic Force Microscopy to detect viscoelastic properties of buried materials with high spatial resolution. The key ingredient is a very high frequency ultrasound wave which is amplitude modulated at the sensing cantilevers resonance frequency.

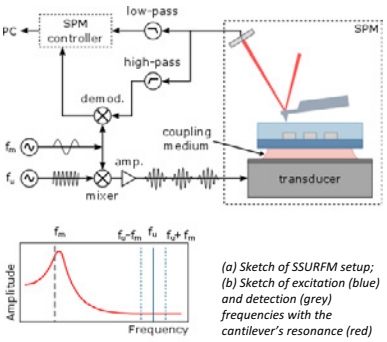

(a) Sketch of SSURFM setup; (b) Sketch of excitation (blue) and detection (grey) frequencies with the cantilever's resonance (red)

CLEAN EXCITATION

Ultrasound transducers can not always be used (e.g. industrial waferstages) so excitation on the top side is needed. Also, piezo excitation suffers from unwanted reflections and resonances. Robust and quantitative SSURFM methods need a clean driving signal.
SmartTip's electrostatic membrane probes provide those advantages.

- Actuation at the location of interest: the tip
- First contact resonance of driving structure >15MHz (est.)
- Amplitude >10nm

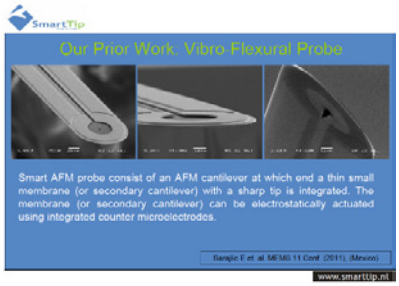

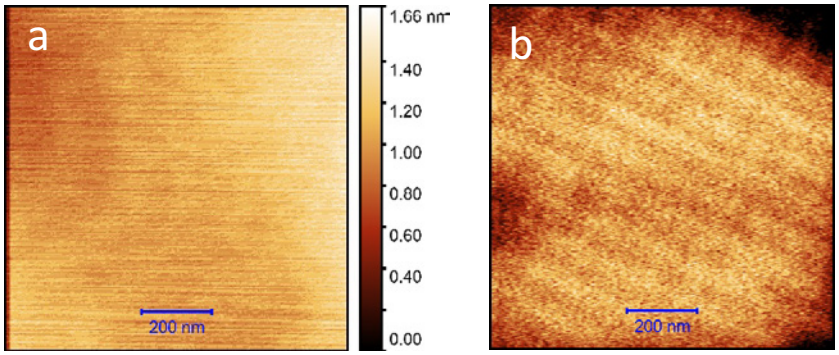

(a) Topography and (b) frequency shift image of dense gold lines in SiN measured with a SmartTip electrostatic membrane cantilever. Schematic cross section of this sample is shown in (c). Pitch of the gold lines is 100nm. Cantilever stiffness 4N/m (est.); f_o=20MHz; fm=600kHz (1st contact resonance). Thanks to the QuTech consortium for providing these samples

CUSTOM DEVELOPED TIPHOLDER

We developed a custom tipholder to be able to use the on-chip contacts for actuation while staying compatible with Park's tip holder design. Challenges:
· Small contact pads
· Strict dimensional and angular requirements

Realized design of Park AFM compatible tip holder with contact pins for electrostatically actuated membrane probes.

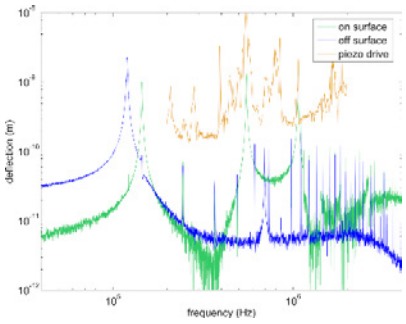

Comparison of electrosttic actuation (on and off surface) with piezo driven actuation. Note that this AFM system has many digital noise peaks at regular frequency intervals. The drive spectrum is actually very smooth.

DISCUSSION

Electrostatically actuated probes enable SSURFM from the top side with very little added complexity to the AFM system. This is a great benefit for miniaturization to integrate into e.g. parallel AFM systems. They also enable quantitative analysis due to their clean drive spectrum. Specifically Frequency Modulation-SSURFM (FM-SSURFM) is possible due to the cleanliness of this drive method (see poster "Frequency Modulation Subsurface Ultrasonic Force Microscopy").

CONCLUSION

Electrostatically actuated membrane probe tips are used for SSURFM imaging of buried features

- Top side actuation;
- Enables FM-SSURFM tracking due to its clean drive spectrum;
- Robust and easy to set up compared to piezo excitation;
- simple, small and light to integrate into (miniaturized) AFM systems.

This project has received funding from the Electronic Component Systems for European Leadership Joint Undertaking under grant agreement No 737479. This Joint Undertaking receives support from the European Union's Horizon 2020 research and innovation programme and Netherlands, France, Belgium, Germany, Czech Republic, Austria, Hungary, Israel

ECSEL JU

Photo Thermo Acoustic Imaging

E. van Zwet[1], W. Koek[2], M. Plissi[2], E. Nieuwkoop[3], J. Winters[1], M. Eschen[2], M.J. van der Lans[1], H. Sadeghian[1]

[1]TNO Optomechatronics Department
[2]TNO Optics Department
[3]TNO Radartechnology Department

TNO innovation for life

INTRODUCTION

Photo Thermo Acoustic Imaging (PTAI) is a pump-probe technique where a short light pulse is used to generate a high frequency acoustic wave in a material. A second light pulse is used to measure the changes at the surface due to the acoustic wave that is reflected at sub-surface objects.

Acoustic waves can travel trough optically opaque materials, allowing to image objects buried under opaque (e.g. metals) layers. By measuring the time of arrival of the acoustic waves, the depth of features can be measured, enabling 3D sub-surface metrology.

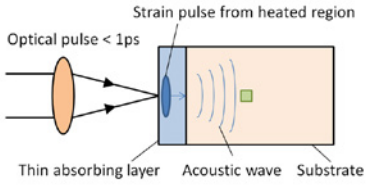

A short optical pulse heats an absorbing layer and generates an acoustic wave inside the underlying material.

APPLICATIONS

Possible applications of PTAI are:

- Measurement of sub-surface defects
- Measurement of alignment markers under metal layers
- Depth profiling of mechanical properties of coatings

Design PTAI test setup

A test setup has been designed based on a common path Sagnac interferometer. With target specifications of 1 pm surface displacement sensitivity at measurement frequencies up to 250 kHz.

The common path design significantly reduces the sensitivity to external disturbances, removing the need to use a lock in amplifier.

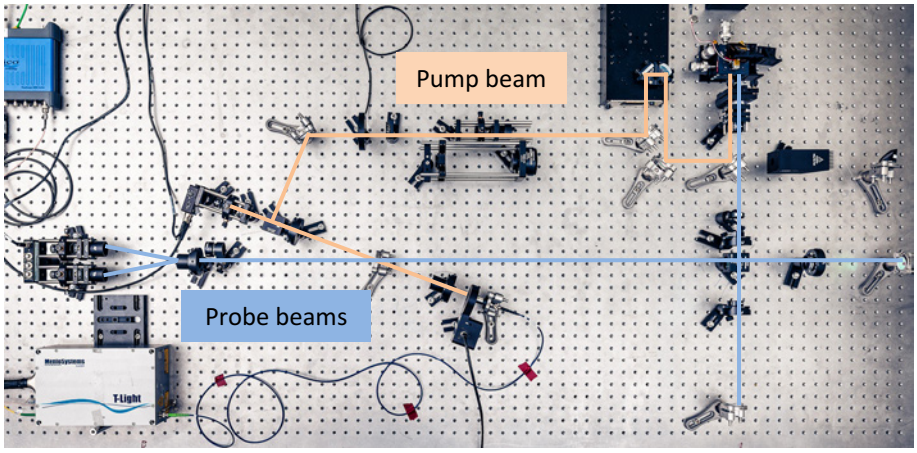

Common path Sagnac interferometer setup for Photo Thermo Acoustic Imaging

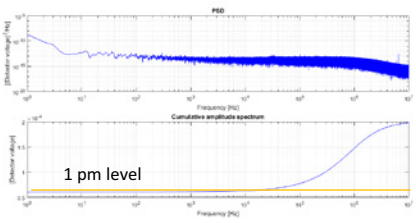

Measured background noise level of the Sagnac interferometer without optical pumping.

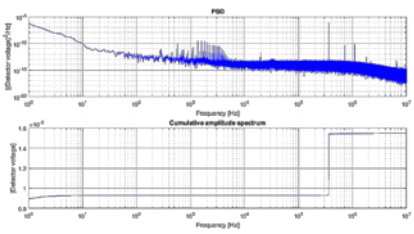

Spectrum showing the measurement of a surface displacement of a piezo of +/- 60 pm in 300 ps @ 360 kHz.

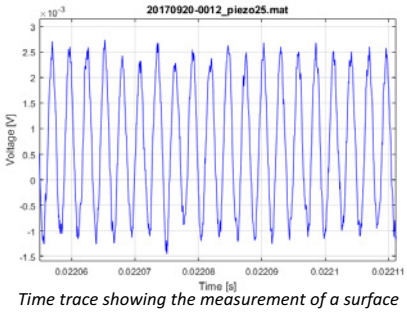

Time trace showing the measurement of a surface displacement of a piezo of +/- 60 pm in 300 ps @ 360 kHz.

EXPERIMENTAL RESULTS

The qualification of the setup shows a perfectly flat noise spectrum up to 10 kHz measurement frequency, enabling measurements up to 100 kHz.

A piezo vibrating at 360 kHz has been used to measure the surface displacements of +/- 60 pm, in the time of 300 ps between the 2 probe pulses.

CONCLUSIONS

A PTAI test setup has been realized that enables to perform optical pump probe measurements with a surface displacement sensitivity down to 1 pm. This enables the verification of the simulation models and the measurement of client samples

This research was supported by TNO's Early Research Program 3D Nanomanufacturing Instruments

Dynamics of AFM in tapping mode

Aliasghar Keyvani [1,2], Hamed Sadeghian[1], Hans Goosen[2], Jan-Willem van Wingerden[3], Fred van Keulen[2]

1 TNO Optomechatronics, Stieltjesweg1 Delft, the Netherlands.
2 Precision and Microsystems Engineering, Delft University of Technology, Mekelweg2, Delft, the Netherlands.
3 Delft Center for Systems and Control, Delft University of Technology, Mekelweg2, Delft, the Netherlands.

TNO innovation for life

This research investigates the **transient behavior of the closed loop Tapping Mode (TM) AFM.** This study is essentially important because of the following reasons:

- Capturing high quality, stable and repeatable images.
- Increasing the imaging speed with model based control designs.
- Prevention of damaging the surface structures.

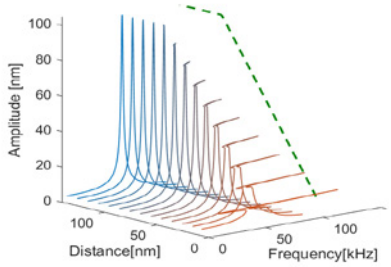

1 | steady-state behavior of cantilever in frequency domain

Preliminaries

So far many studies investigate the dynamics of the TM-AFM in steady state conditions. These studies attribute the amplitude reduction mechanism of the AFM cantilever to the shift in resonance frequency as shown in the Fig.1. However, not all aspects of the AFM can be described with these models. Namely, the Tip-Sample Interaction force, optimum imaging parameters, Image quality, and overall bandwidth of the system.

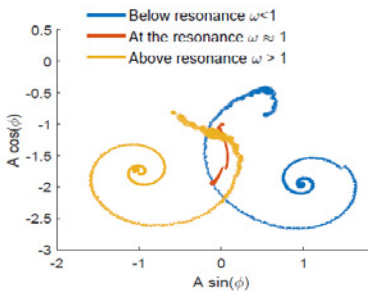

2 | Transient behavior of cantilever in phasor space (experimental)

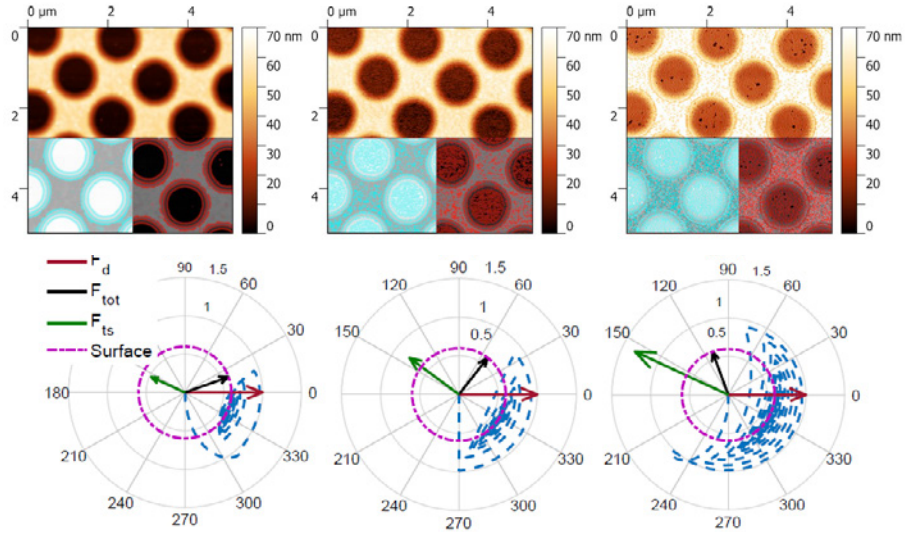

3 | Relationship between image quality and transient behavior of the AFM cantilever.

The question is: how does the curves in Fig.1 evolve transiently when the tip-sample distance suddenly changes? Only by answering this question one can design model based controllers for TM-AFM. Fig.2 shows the measured transient motion trajectory of the amplitude-phase pair of an AFM cantilever. In fact, depending on the excitation frequency, the cantilever follows a clockwise or a counterclockwise path, which significantly affects the imaging performance of the AFM, as seen in Fig.3.

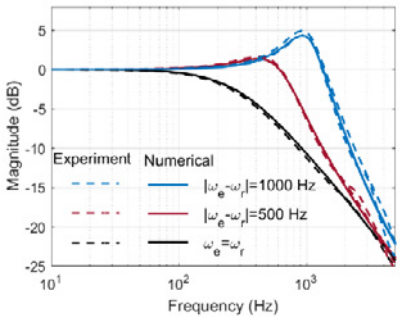

2 | comparison of the measurements and the proposed model for transient behavior of AFM cantilever.

We derive a modulated model, which fully agrees with the existing theories in steady state regime, and accurately explains the experimental results.

The model

The presented model is defined on an imaginary (slow) time scale, in which the position and the velocity of the motion of the cantilever are unknown in any instance of the time. Yet, the amplitude, phase in Cartesian coordinates and the rates of amplitude and phase constitute the state space. The model in intrinsically linear forms a robust basis for real-time estimation of the periodic average of the Tip-sample interaction force.

$$\begin{Bmatrix} \dot{q}_1 \\ \dot{q}_2 \\ \dot{q}_3 \\ \dot{q}_4 \end{Bmatrix} = \begin{bmatrix} -\xi & \omega & -1 & 0 \\ -\omega & -\xi & 0 & -1 \\ 1 & 0 & 0 & \omega \\ 0 & 1 & -\omega & 0 \end{bmatrix} \begin{Bmatrix} q_1 \\ q_2 \\ q_3 \\ q_4 \end{Bmatrix} + \begin{Bmatrix} F_d + \Re(F_{ts}^{(1)}) \\ \Im(F_{ts}^{(1)}) \\ 0 \\ 0 \end{Bmatrix}$$

CONCLUSION

In this research we present a theoretical model for the transient behavior of the TM AFM. The model perfectly matches the experimental results and previously reported theoretical solutions. The presented model explains the important factors behind capturing high quality, repeatable images (e.g. excitation frequency) and enables the model based control design for TM-AFM.

This project was funded by TNO's Early Research Program on 3D Nanomanufacturing.

The tip-sample interaction force in Tapping Mode Atomic Force Microscopy

M.S. Tamer[1,2], H. Sadeghian[2], J.F.L. Goosen[1], F. van Keulen[1]

[1]Delft University of Technology, Department of Precision and Microsystems Engineering
[2]Netherlands Organization for Applied Scientific Research TNO, Department Of Optomechatronics

TNO innovation for life

Introduction

AFM utilizes a sharp tip attached to a cantilever for imaging the sample surface and measuring physical properties of the sample. The sharpness of the tip enables imaging sample surface with very high resolution. On the other hand, the tip-sample interaction force in the order of nano-Newton can cause huge stress in the order of giga-pascal which can easily damage the surface or the tip itself.

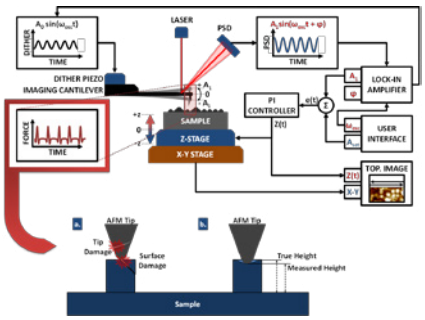

Theoretical and experimental analysis

The AFM is proposed as a non-destructive imaging and inspection tool for semiconductor industry and biological applications. Thus, we have to know the Tip-Sample Interaction (TSI) accurately. The TSI forces in TM-AFM is studied theoretically using numerical solutions.

Tip-Sample Interaction Force in Time Domain (Theoretical)

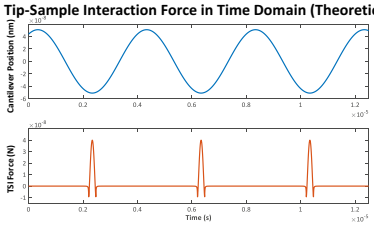

Tip-Sample Interaction Force in Time Domain (Experimental)

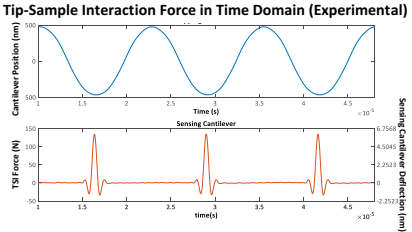

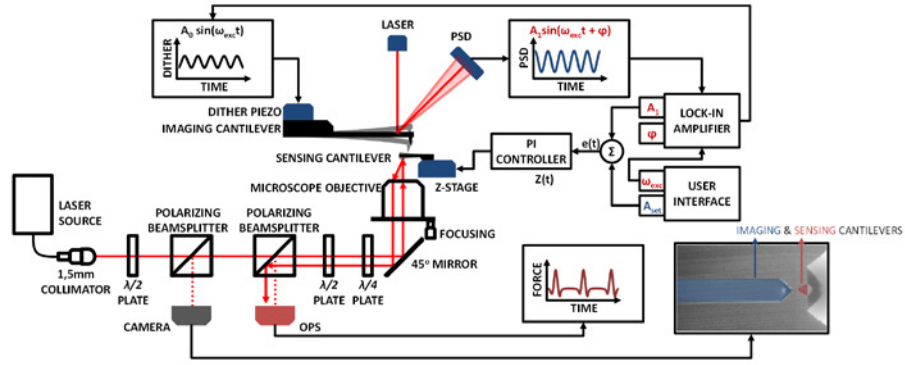

An experimental method for measuring the TSI is designed and the experimental results are compared with the theoretical foundations.

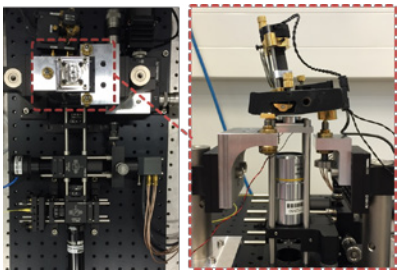

The maximum repulsive TSI force depends on different parameters like excitation frequency and amplitude setpoint. The trend in the maximum repulsive force with respect to these parameters is investigated.

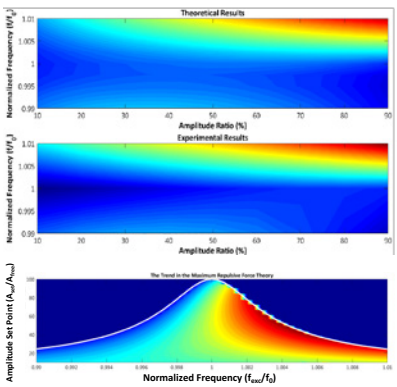

Using the experimental results verified with the theoretical calculations, we created the map of the maximum repulsive TSI. Using this map, we created a new method for surface imaging and modification simultaneously.

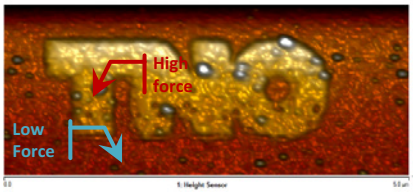

Using the TSI map we created, we also investigated the effect of maximum repulsive TSI force on measured the surface topography

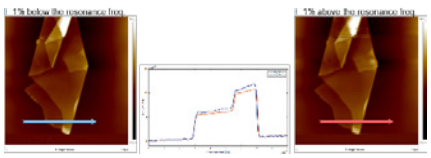

CONCLUSION

We had investigated the tip sample interaction force using experimental and theoretical methods and the effects of excitation frequency and amplitude set point. Using this information we can tune the tip sample interaction forces to increase the measurement accuracy or nano patterning.

This research was supported by TNO's Early Research Program 3D Nanomanufacturing Instruments

Versatility of the TNO Subsurface probe microscopy technique

A. Mohtashami[1], M.H. van Es[1], R. Thijssen[1], D. Piras[1], P. van Neer[2], M.J. van der Lans[1], and H. Sadeghian[1]

[1]TNO Department Of Optomechatronics
[2]TNO Department Of Acoustics and Sonar

TNO innovation for life

INTRODUCTION

Nondestructive subsurface imaging of nanostructures is considered an effective method for inspection and metrology in semiconductor nanomanufacturing processes. Examples are mapping through the layers in semiconductor structures, characterizing nanolayers in EUV lithography masks, and wafer overlay and alignment. The ability to manufacture, measure and align the nanostructures on top of each other directly impacts chip's performance and yield. Here we demonstrate the versatile capabilities of our subsurface probe microscopy technique for imaging buried features in materials of different properties.

RIGID STRUCTURES IN RIGID MATRICES: ($E_{str} \geq E_{mat}$)

- With the TNO subsurface method, we are able to image rigid nanostructures (aluminum) that are buried under a layer of another rigid material like SiO_2.
- The features can be imaged through few hundred nanometers thick layer of rigid material with stiffness equal or higher than the buried features.

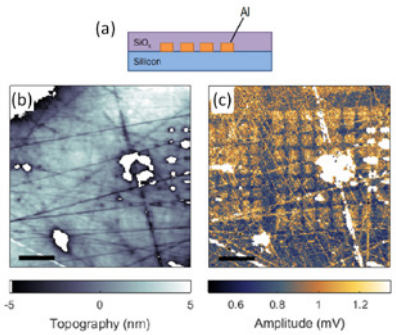

Fig. 1: (a) Rigid-Rigid sample 1 ($E_{str} \geq E_{mat}$): Aluminum nanostructures buried under a layer of SiO_2. (b) Topography and (c) subsurface amplitude images.

RIGID STRUCTURES IN RIGID MATRICES: ($E_{str} < E_{mat}$)

- Subsurface imaging is possible even for rigid nanostructures (50nm Au/Pd lines) that are buried within highly stiff materials like SiN.

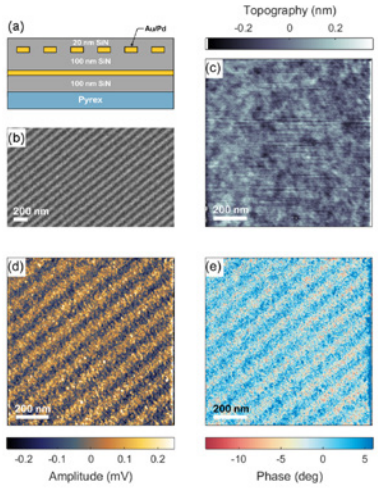

Fig. 2: (a) Rigid-Rigid sample 2 ($E_{str} < E_{mat}$): Au/Pd lines (15nm x 50nm) buried within a layer of SiN. (b) SEM image, (c) topography, (d) subsurface amplitude and (e) phase images of the periodic nanostructures.

RIGID STRUCTURES IN SOFT MATRICES:

- Subsurface imaging is also possible in soft matrices like photoresists.
- Features of the size of 100 nm can be detected through layers of few 100 nm of photoresist.

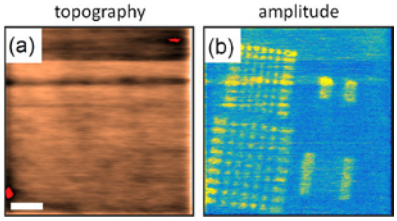

Fig. 3: (a) Topography and (b) subsurface amplitude images of the buried aluminum nanostructures under 300nm thick layer of photoresist. The scale bar corresponds to 2µm in length.

MULTILAYERS:

- Imaging through several layers of different materials is highly desirable in semiconductor processes.
- Here is an example of subsurface nanoimaging of aluminum nanostructures buried under 300nm layer of photoresist and 50nm layer of Titanium.

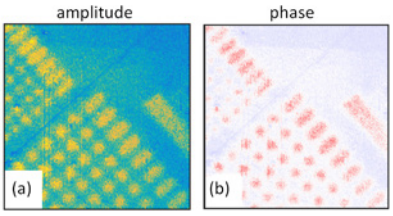

Fig. 4: (a) Subsurface amplitude and (b) subsurface phase images of the buried aluminum nanostructures under 300nm photoresist and 50nm Titanium. The buried nanostructures are 100nm thick and 300nm (left) to 400nm (bottom) in size

CONCLUSION

We have demonstrated subsurface nanoimaging for different material types and configurations. Developing a versatile subsurface imaging technique is critical to many applications such as defect inspection and overlay and alignment control in semiconductor industries.

Acknowledgement

We would like to thank H. van den Berg and A. Storm from TNO and G. Pandraud from Else Kooi Laboratory for fabricating the samples.

This research was supported by TNO's Early Research Program 3D Nanomanufacturing Instruments

Defect metrology of Self-Assembled monolayers for selective ALD and ALE

H. Sadeghian[1], M. van Es[1], R. Thijssen[1], S. Sayan[2] , G. van denberghe[3]
[1]TNO
[2]Intel
[3]IMEC

TNO innovation for life

Introduction

Self Assembled monolayer (SAM), is used as mask for selective atomic layer deposition and selective atomic layer etching

Quality of SAM is critical for

- Surface coverage
- Adherence to the substrate
- Sensitive to pinholes: these transfer to ALD, causing defect in final product
- Unwanted etching or unwanted deposition

Metrology challenges

- Ebeam inspection disturbs the molecules
- The sample/wafer must be metal coated for defect metrology with ebeam

AFM

- Has sufficient resolution
- Interaction forces must be very low to avoid disturbing the molecules
- Postprocessing and analyzing the raw data

Goal

To develop a metrology solution for defectivity of SAM based on high throughput low force AFM.

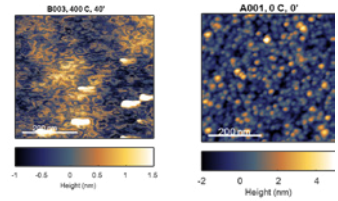

Examples of measured SAM molecules

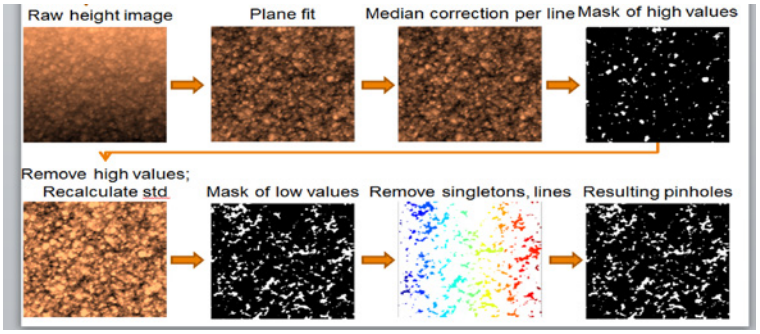

Developed data process to get the defect metrology parameters from raw images of low Force AFM

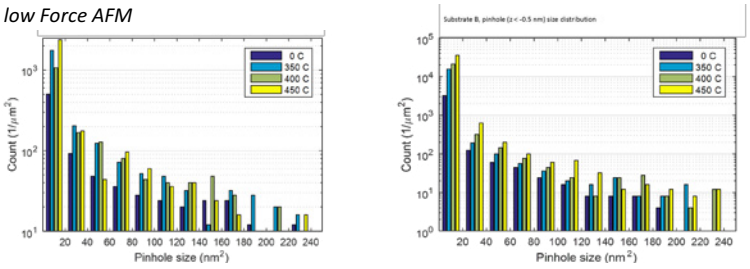

Defect size distribution: Biggest increase in smallest pinhole size for both substrate types

Automated measurements

Stronger adhesion implies that coverage will be higher for same heating temperature. We performed experiments at different temperature for two different substrates: Samples A and B each heated to 350^{o}, 400^{o} nad 450^{o} C. One of each substrate was left unprocessed for comparison

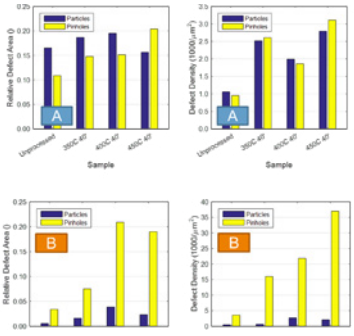

Relative defect area and defect density for both substrates, separated out to particles and pinholes. Clearly substrate B is cleaner (less particles) while having more, smaller pinholes.

Experiment conclusion

- B has higher pinhole defect density
- B has stronger temperature dependence
- particle area much larger on A substrate

CONCLUSION

Surface coverage by SAM reduces on the samples that have been processed at the highest temperatures, Based on:

- Observation of substrate B images
- Analysis of pinhole count and number as a function of processing temperature
- AFM is a suitable tool for self-assembled monolayer defect inspection

Contrast mechanism in TNO Scanning Subsurface Ultrasonic Force Microscopy

M.H. van Es[1], R. Thijssen[1], A. Mohtashami[1], M.J. van der Lans[1], H. Sadeghian[1]

1 TNO Optomechatronics

TNO innovation for life

TNO SubSurface Probe Microscopy

Scanning Subsurface Ultrasonic Force Microscopy (SSURFM) relies on high frequency ultrasound in combination with Atomic Force Microscopy to detect viscoelastic properties of buried materials with high spatial resolution. The key ingredient is a very high frequency ultrasound wave which is amplitude modulated at the sensing cantilevers resonance frequency.

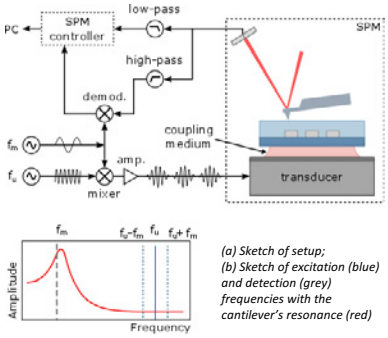

(a) Sketch of setup; (b) Sketch of excitation (blue) and detection (grey) frequencies with the cantilever's resonance (red)

TNO SSPM Method

Other subsurface methods have been published in scientific journals, notably CR-AFM and UFM. SSURFM combines the best of UFM and CR-AFM by exciting in an amplitude modulation scheme with a signal at a high carrier frequency f_c which is modulated at the contact resonance f_m:

- high dynamic stiffness of the sensing cantilever at high frequencies causing large indentations
- high sensitivity at contact resonance
- contrast both due to dynamic stiffening and resonance shift.

We carefully characterized contrast as a function of experimental parameters to optimize the technique for applications in semiconductor industry.

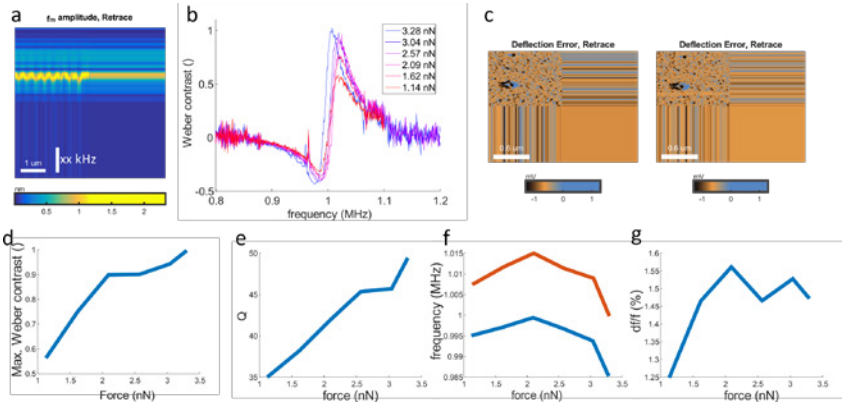

Systematic investigation of contrast mechanism

Expected contrast and SNR as function of

- force;
- center frequency;
- modulation frequency and
- amplitude

for various subsurface techniques based on viscoelastic or scattering contrast

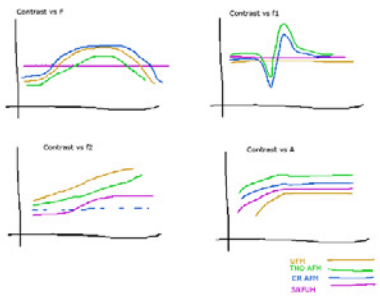

Fig 2: Schematic overview of expected dependencies in a systematic characterization of contrast for SSURFM and various other proposed schemes

CONCLUSION

- Observed contrast is consistent with visco-elastic contrast mechanism.
- Clear handles on parameters to optimize detection of subsurface features.
- Detailed understanding paves the way to quantitative measurements of subsurface material properties

Systematic measurement results

- Contrast vs modulation frequency as expected for viscoelasticity (fig a, b)
- Contrast in frequency vs force as expected for viscoelasticity (fig g)
- Contrast in ampltiude vs force increases because of increase in Q factor with force (fig d, e)
- Significant change in contact resonance due to change in surface roughness with prolonged scanning (here from high force to low force over time) (fig c, f)

TNO SSPM Images

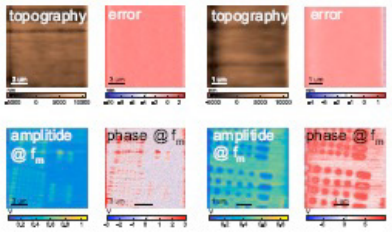

Fig. 3: Example subsurface images of custom created patterns in silicon under 300nm resist. Note the flatness of the topography and error signals which do not reveal the subsurface structure at all. Also note the contrast inversion between both measurements - f_m was chosen above respectively below the contact resonance in these measurements.

This research was supported by TNO's Early Research Program 3D Nanomanufacturing Instruments

Using heat transfer to measure distances at the sub-micrometer scale

R.J.F. Bijster[1,2], H. Sadeghian[2], F. van Keulen[1]

1 Department of Precision and Microsystems Engineering, Delft University of Technology, Delft, The Netherlands
2 Nano-Opto-Mechatronic-Instruments group (NOMI), Department of Optomechatronics, TNO, Delft, The Netherlands

TNO innovation for life + TU Delft

INTRODUCTION

By understanding the fundamental physics of heat transfer at the submicrometer scale, new applications become available. We work on understanding and controlling the radiative heat flow for contactless metrology at this length scale.

THREE APPLICATIONS

Accurate measurements of the sub-micrometer heat flow allows for three applications: distance sensing, contactless scanning probe microscopy (SPM) and local surface modification by localized heating.

DISTANCE SENSING

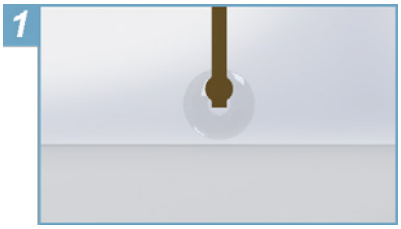

CONTACTLESS SPM

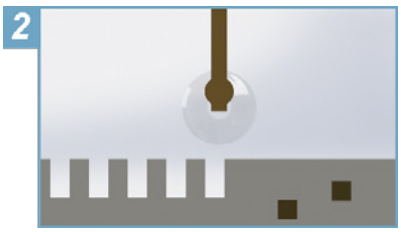

SURFACE MODIFICATION

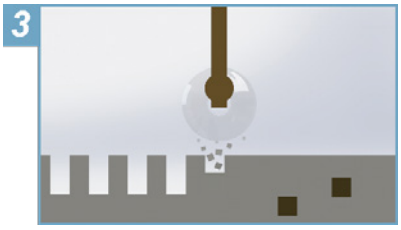

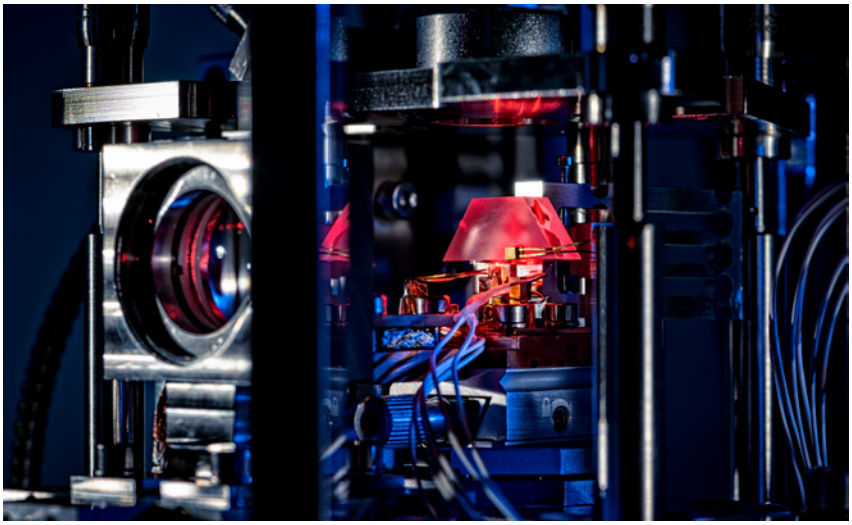

INSTRUMENT ARCHITECTURE

At the heart of the calorimeter is a microscopic bilayer cantilever. When heat is exchanged at the tip, the resulting thermal gradient along the cantilever length causes it to bend. This curving is counteracted by precise modulation of the incident laser power. This restores the thermal balance. A measurement of the required change in optical power allows for a 2 nW accuracy and 20 pW resolution in the flux measurement.

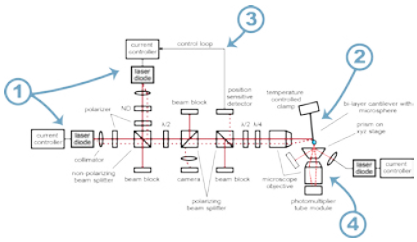

1. Laser diodes illuminate the cantilever probe. 2. Heat transfer between probe and sample induces a temperature change in the bilayer cantilever. This causes it to bend. 3. The optical power of the laser diode is tuned to compensate the change in temperature and null the deflection. The change in power is a measure for the heat transfer. 4. A total internal reflection microscope provides a reference measurement for the distance between probe and sample.

ANALYSIS OF RESOLUTION AND SHAPE OPTIMIZATION

The absolute flux and flux patterns are calculated using a fluctuating-surface-current formulation of radiative heat transfer (Phys. Rev. B., 88(5):054305, 2013) that is paired with a boundary element method.

Scan me to see an example of probe optimization.

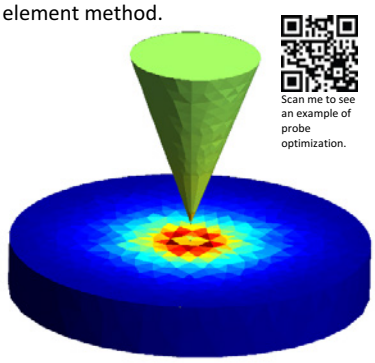

We use these simulations to estimate the lateral resolution and optimize tip geometry for the specific application.

CONCLUSION

Heat transfer at the sub-micrometer scale is a viable technique for distance measurement and contactless scanning probe microscopy. Sub-nm resolutions are possible for distances smaller than 100 nm.

This research was supported by TNO's Early Research Program 3D Nanomanufacturing Instruments

Torsional subsurface imaging using atomic probe microscopy

V. Navarro[1], M.H. van Es[1], M.J. van der Lans[1], H. Sadeghian[1]

1 **Department Of Optomechatronics**

TNO innovation for life

INTRODUCTION

- Torsional subsurface probe microscopy (TSPM) is a non invasive technique that allows the detection of features below the surface of a sample, enhancing the contrast at the edges.
- Excitation of a sample parallel to its surface, at the cantilever's contact torsional resonant frequency, f0CT, induces the torsional oscillation of the cantilever in contact with the sample.
- Example of application, torsional APM allows the detection of in-plane defects such as delamination, edge dislocations or stacking faults, essential to detect in the semicon industry where high epitaxial surface quality is essential in order to prevent adverse effects on device characteristics.

TECHNIQUE

Amplitude and phase (demodulated at f0CT) contain information of subsurface features with enhancement of boundaries between different phases of the material or defects below the surface.

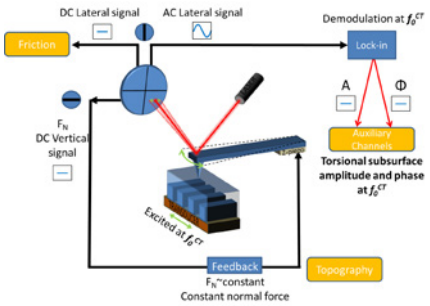

Subsurface, no friction:
→Tip pivots

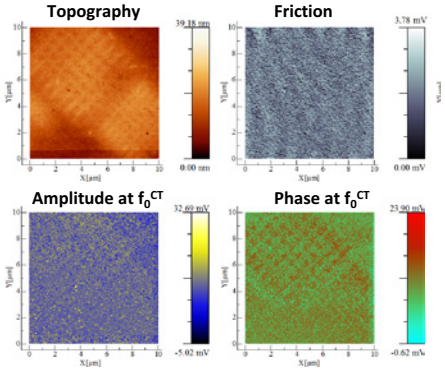

Subsurface and friction:
→Tip slides

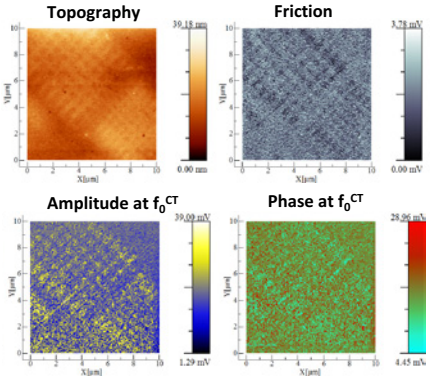

RESULTS

A stress field below the surface is induced due to the force applied by the tip.

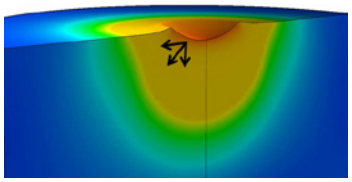

A stress field below the surface is induced due to the force applied by the tip.

1. Subsurface shear elasticity → conservative
2. Friction → Dissipation of energy

Subsurface torsional amplitude shows buried features not visible in topography

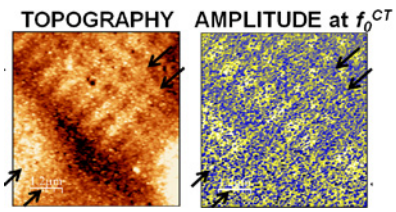

CONCLUSION

TSPM is a promising non-invasive technique to obtain enhancement of boundaries or in plane-defects buried below a surface.
Torsional signal gives information of dissipation at the surface (friction) and the shear elastic properties below the surface (torsional subsurface).

This research was supported by TNO's Early Research Program 3D Nanomanufacturing Instruments

Simulation tools to improve understanding and to optimize sub-surface SPM imaging

L. Fillinger[1], D. Piras[2], M.H. van Es[2], A. Mohtashami[2], V. Navarro[2], P. van Neer[1], M.J. van der Lans[2], and H. Sadeghian[2]
1 TNO, Acoustics and Sonar, The Hague
2 TNO, Optomechatronics, Delft (Stieltjesweg)

TNO innovation for life

SUBSURFACE ULTRASONIC RESONANCE FORCE MICROSCOPY (SSURFM)

In Atomic Force Microscopy (AFM), a cantilever with a sharp tip is brought near a sample's surface, and scanned along it while vibrating the cantilever and/or the sample and monitoring the inclination of the cantilever with a laser. It was initially developed to measure topography.

AFM is also sensitive to physical properties of the samples' surface and subsurface, which enables imaging of sub-surface features, as shown in Figure 1.

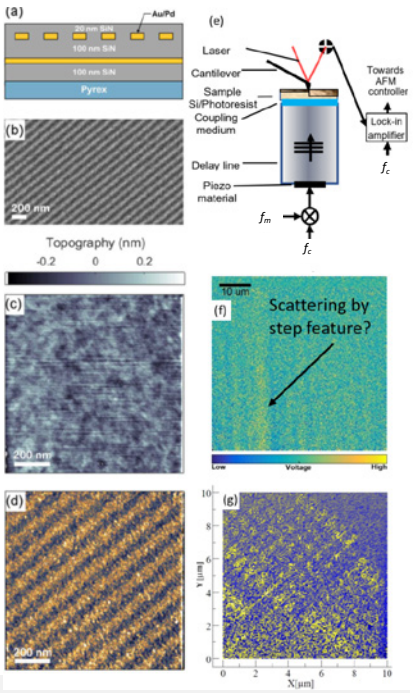

Figure 1: Experimental subsurface ultrasonic resonance force microscopy (SSURFM) imaging with MHz ultrasound (a-d), GHz ultrasound (e-f) and in torsion with MHz ultrasound (g). (a) Sketch of a Rigid-Rigid sample: Au/Pd lines (15x50nm^2) buried within a layer of SiN. (b) SEM image (c) topography (d) subsurface amplitude. (e) Schematic of the setup for the measurement of a sample with a step feature (370 nm high silicon step under 1.6μm of photoresist) and (f) subsurface image demodulated from 1 GHz ultrasound. (g) Example of demodulated subsurface image measured with a torsional cantilever.

FREQUENCY MIXING

- Sample excited with high frequency amplitude modulated ultrasonic signal
  - Carrier f_m at frequency of transducer
  - Modulation near the contact resonance frequency f_c of the cantilever in contact with the sample.
- Frequency mixing
  - Due to nonlinearity of the interaction between the tip and the sample (Force-Distance (FD) curve)
  - Results in excitation of the cantilever vibration at f_c (downmixing)
  - Downmixing more efficient when the modulation frequency corresponds to the contact resonance.
- Ultrasound wavelength λ and subsurface feature size L
  - MHz → $\lambda \gg L$
  → subsurface affects local elasticity
  - GHz → $\lambda \sim L$
  → subsurface affects local elasticity and sound propagation.

PROBLEM AND APPROACH

Development of modelling tools to:
- **improve physical understanding;**
- **support experiment optimization**

(choice of cantilever and excitation parameters).

MODELLING

A. Sample with subsurface feature
- Bottom ultrasonic excitation using piezoelectric transducer
- Propagation within sample, including interaction with feature

B. Tip-sample interaction (contact)
- Nonlinear relation between force and indentation
- Localized stress field at contact, typical size 2-3 times the contact radii
- Feature affects contact stiffness within stress-localization volume

C. Cantilever's dynamics
- Vibrated from "clamped-end"
- Tip at "free-end", in contact

A and B are modelled using finite elements in Comsol; C is modelled in matlab, solving a Euler-Bernoulli beam subject to a nonlinear tip-sample interaction using the successive approximation method.

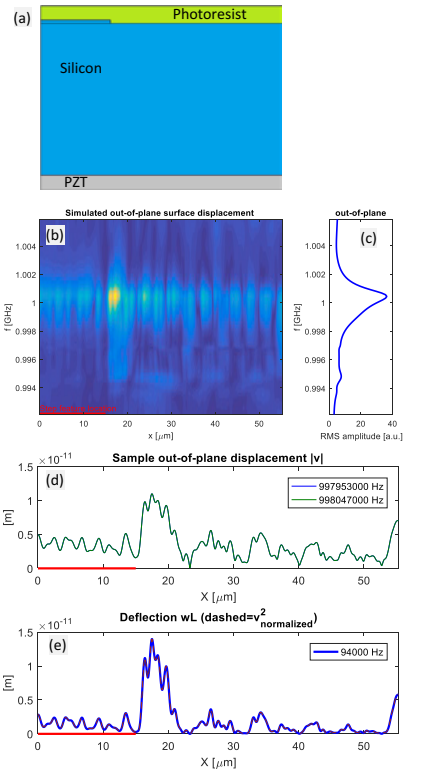

Figure 2: Simulation of the measurement from Figure 1(f). (a) Sketch of comsol model of the transducer and sample with step feature, and (b-c) simulated surface displacement distribution. (d) Surface distribution of ultrasonic displacement (from Comsol) used as input of the cantilever dynamic simulation (Matlab). Resulting demodulated signal (e).

CONCLUSION AND PERSPECTIVES

- **Various modelling components have been developed.**
- They enable modelling of MHz and GHz AFM experiments.
- **Good agreement between experiment and simulation is observed.**
- **The tools can be used for optimization** of the modeled aspects, such as the cantilever (stiffness, resonance frequency, tip radius…) and to the excitation (static load, frequency content, transducer material and position…) in relation to a particular sample (matrix material, feature depth, size…).

This research was supported by TNO's Early Research Program 3D Nanomanufacturing Instruments

Deterministic chaos limiting the speed of AFM

Aliasghar Keyvani [1,2], Farbod Alijani[2], Hamed Sadeghian[1], Klara Maturova[1], Hans Goosen[2], Fred van Keulen[2]

1 TNO Optomechatronics, Stieltjesweg1 Delft, the Netherlands.
2 Precision and Microsystems Engineering, Delft University of Technology, Mekelweg2, Delft, the Netherlands.

TNO innovation for life

It is known that the imaging speed of the AFM is limited. However, an understanding of the nature of this upper bound, -which is critical for resolving it- is still incomplete. In this research we investigate the non-linear dynamics of the closed loop TM-AFM and conclude that a deterministic chaotic attractor is limiting the bandwidth of the closed loop system.

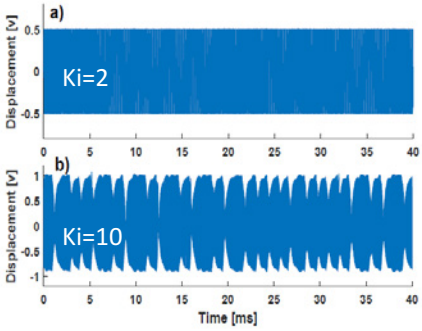

1 | Measured cantilever motion in TM-AFM, for a) low and, b) high control gains

Experimental observations

Increasing the scanning speed of the AFM demands increasing the bandwidth of the Z control unit, so that the cantilever can follow the surface without flying away or crashing into the sample. This can be done via increasing the controller gains. However, at a certain point, the whole system start to vaguely fluctuate. The amplitude suddenly quenches and builds up with an aperiodic scheme, as shown in Fig.1.

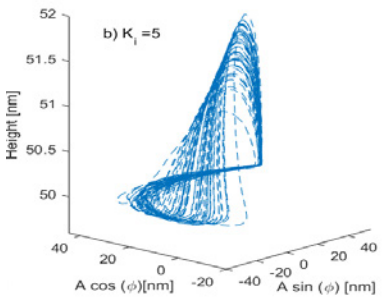

2 | chaotic attractor geometry of the cantilever (experimental)

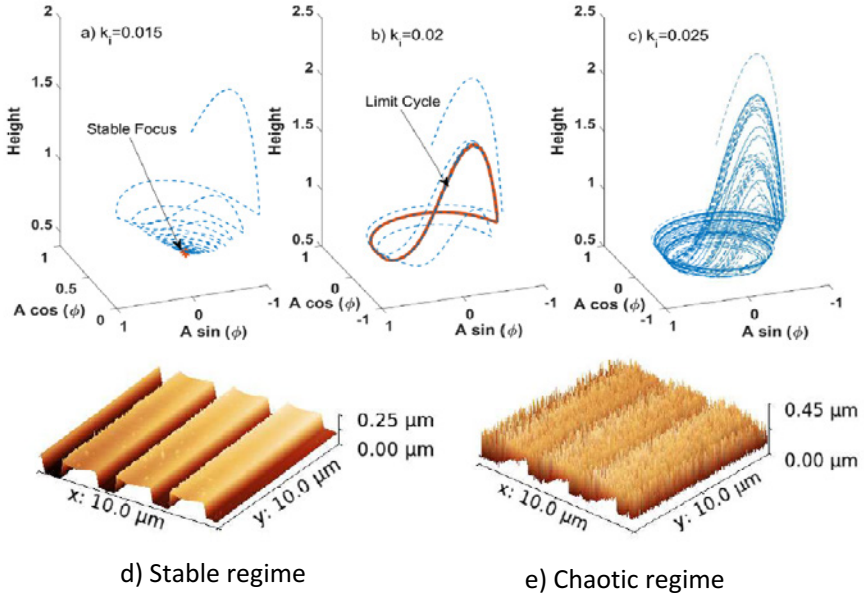

d) Stable regime e) Chaotic regime

3 | Relationship between image quality and transient behavior of the AFM cantilever.

Strange attractors

To investigate the nature of this aperiodic motion, we developed a modulated model for the closed loop TM-AFM system. After validation of the model with experimental results, we calculated the bifurcation diagrams, Poincare' sections and Lyapunov exponents of the system. As it can be seen in Fig.3, The integral gain of the controller determines the behavior of the closed system. For low control gains (low speed AFM) any perturbation to the system damps out and the states of the system settle down to a stable focus point. Increasing the control gain, a stable periodic limit cycle emerges that any perturbation from that limit cycle eventually damps. However, passing a certain integral gain, the system exhibits a strange attractor. (Figs. 2, 3.c, 3.e)

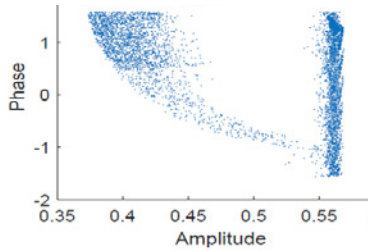

4 | A Poincare section of the strange attractor of TM-AFM.

Formal proof of chaos

Fig.4 and Fig.5 show a Poincare' section, and the Lyapunov exponents of the strange attractor of the TM-AFM, for high control gains. Presence of complex cluster of points in the Poincare section, and one having one Lyapunov exponent above zero formally proof that the observed phenomenon is deterministic chaos.

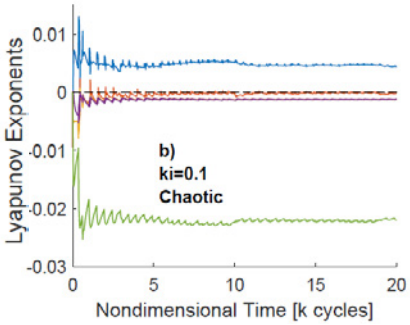

CONCLUSION

Experimental and numerical results unanimously show that there exists an upper bound for the imaging speed of the AFM which is strictly posed with deterministic chaos. This makes it impossible to further increase the speed of AFM without fundamental changes in its architecture.

This project was funded by TNO's Early Research Program on 3D Nanomanufacturing.

DEVELOPMENT OF A SAMPLE CLAMP FOR GHZ SUBSURFACE PROBE MICRO-SCOPY

P.L.M.J. van Neer[1], M.C.J.M. van Riel[2], M.H. van Es[2], P.S. Shoeibi Omrani, K. Hatakeyama[2], A. Mohtasami[2], B.A.J. Quesson[1], M.J. van der Lans[2], H. Sadeghian[2]

[1]Department of Acoustics and Sonar
[2]Department of Optomechatronics
[3]Department of Heat Transfer and Fluid Dynamics

TNO innovation for life

Introduction

Surface Probe Microscopy (SPM):

- Used to characterize surface topology at nano-scale

Subsurface Probe Microscopy (SSPM):

- Combines SPM + MHz/GHz acoustic excitation
- Used to probe subsurface
- Application: Semiconductor metrology

SSPM + GHz excitation:

- Image contrast: acoustic impedance
- Minimal force applied on cantilever: damage minimized
- Inspection depth > 700 nm

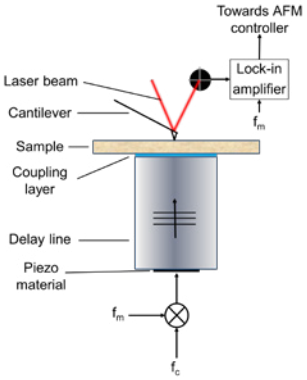

Problem

Coupling layer required to couple sound from transducer into sample

Geometry coupling layer strongly affects sample surface displacement

- amplitude,
- frequency dependency,
- time dependency,
- (x,y)-dependency.

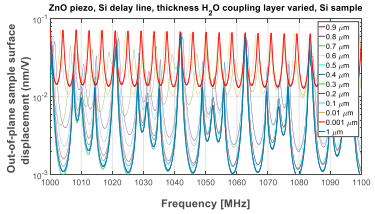

Out-of-plane sample surface displacement per Volt versus the frequency for different coupling layer thicknesses.

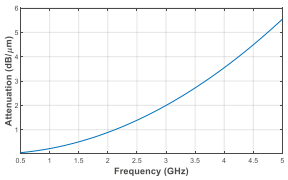

Attenuation versus frequency for a coupling layer consisting of water

Goal

A clamp is required to control coupling layer geometry.

- Static maximum z-thickness 1 µm
- Required z-stability 2 nm

Coupling layer

Coupling layer is chosen to be water

- Low viscosity
- Low sound attenuation
- Non-toxic
- Acceptable evaporation rate
- Easily cleanable

Coupling layer stabilization

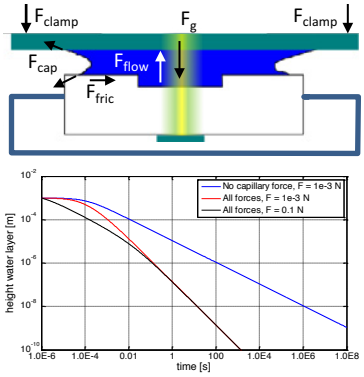

Coupling layer < 1um after 0.1 – 100s depends on:

- forces acting on sample
- droplet volume

Clamp design

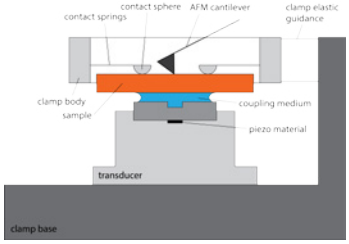

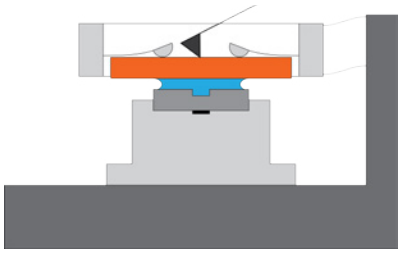

Preliminary clamp tests

Initial experiments with clamp, transducer, coupling layer, example sample performed

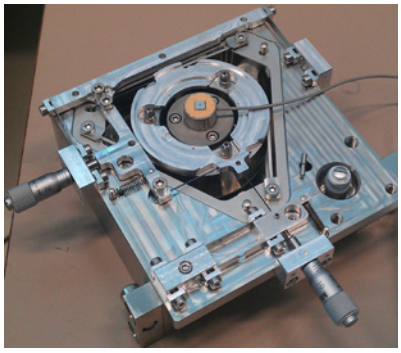

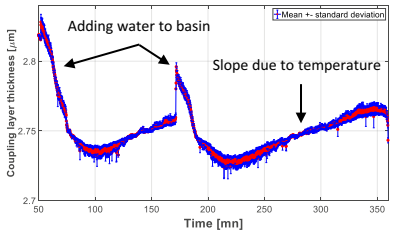

- Coupling layer thickness @ 2.75 µm
  Probable cause: surfaces not clean
- Random measurement error:
  < 10 nm (6σ)
- Coupling layer stable for ~3 hours
  Limited by evaporation

CONCLUSION

- Clamp design was realized to control coupling layer
- Promising preliminary performance

This research was supported by TNO's Early Research Program 3D Nanomanufacturing Instruments

Pulsed Excitation in Subsurface Ultrasonic Resonance Force Microscopy

K. Hatakeyama[1], M.H. van Es[1], P.L.M.J. van Neer[2], H. Sadeghian[1]

[1]Department Of Optomechatronics
[2]Department Of Acoustics and Sonar

TNO innovation for life

INTRODUCTION

Scanning Subsurface Ultrasonic Force Microscopy[1] (SSURFM) relies on high frequency ultrasound in combination with Atomic Force Microscopy to detect visco-elastic properties of buried materials with high spatial resolution. The key ingredient is a very high frequency ultrasound wave which is amplitude modulated at the sensing cantilevers resonance frequency.

[1] M.H. van Es, A. Mohtashami, R.M.T. Thijssen, D. Piras, P.L.M.J. van Neer, H. Sadeghian, *Mapping buried nanostructures using subsurface ultrasonic resonance force microscopy*, Ultramicroscopy, Volume 184, Part A, 2018, Pages 209-216, doi:10.1016/j.ultramic.2017.09.005

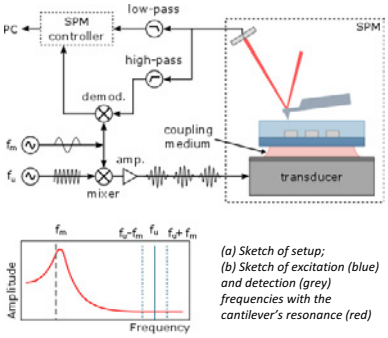

(a) Sketch of setup; (b) Sketch of excitation (blue) and detection (grey) frequencies with the cantilever's resonance (red)

AMPLITUDE MODULATION

In standard SSURFM, the amplitude is modulated with a sine function. How is the cantilever motion – and ultimately the sensitivity to subsurface features – dependent on the type of modulation function? Here we consider sine, square, ramp and triangle as exemplary different modulation functions and examine their influence on the cantilever response.**However, signal generation also includes nonlinearities!**

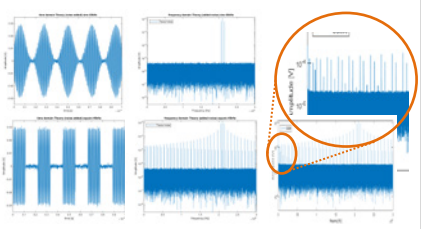

Theoretical time trace and frequency spectrum for sinusoidal modulation (a) and square modulation (b). (b) Also shows the measured spectrum from our signal generator for this case. Note the appearance of new peaks at the modulation frequency due to non linear behaviour of the device.

Energy by linear excitation in contact is estimated by alpha. Phase difference was took into account for the proper estimation of Energy by nonlinear excitation in contact.

$$E_{c,nonlinear} = \sqrt{(E_{lin+nonlin} - E_{lin}\cos(\theta))^2 + (0 - E_{lin}\cos(\theta))^2}$$

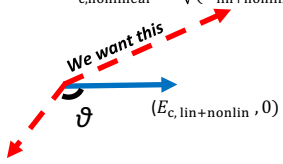

$$E_{c,lin+nonlin} = \sum_{f=f_{start}}^{f_{end}} V_{OBD,c}$$

E = energy in cantilever motion
θ = phase of cantilever motion
[]$_c$= measured in contact
[]$_a$= measured without tip-sample contact
[]$_{lin}$= 'linear' contribution, i.e. due to signal generator non linearity
[]$_{nonlin}$= 'nonlinear' contribution due to tip-sample interaction
H = transfer function

$$E_{c,lin} = \alpha \sum_{f=f_{start}}^{f_{end}} V_{OBD,a}$$

$$\alpha = \frac{H_{OBD,c}(f_m)}{H_{OBD,a}(f_m)}$$

$$\theta = \theta_{lin+nonlin} - \theta_{lin}$$

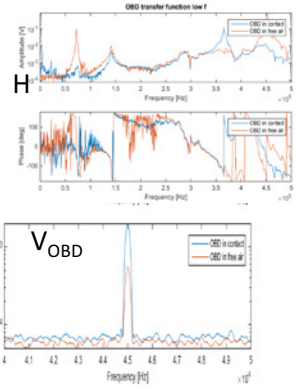

ISOLATE EFFECTS OF SIGNAL GENERATION AND TIP-SAMPLE INTERACTION

To properly evaluate the effect of the various modulation functions we need to isolate the effect of the non-linearities in the signal generation and in the tip-sample interaction. By carefully considering the response amplitude and phase with the tip-sample interaction either present or not, we can recover the effect due to tip-sample interaction which contains the subsurface information.

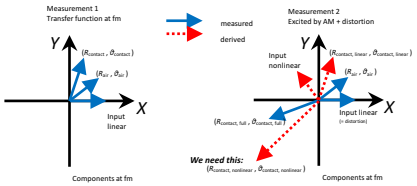

Sketch of signal components with their real and imaginary parts (X resp Y) for the cases of tip sample interaction present (right) or not (left).

COMPLEX EXCITATION SPECTRUM

The frequency components that look like they are mirrored from DC, are not aliased but are real. The reason is as follows:
Square modulation function has number of frequency components:

$$A_{square}(t) = \frac{4}{\pi}\sum_{k=1}^{\infty}\frac{\sin(2\pi(2k-1)f_m t)}{2k-1} = \frac{4}{\pi}\{\sin(2\pi f_m t) + \frac{1}{3}\sin(6\pi f_m t) + \frac{1}{5}\sin(10\pi f_m t) + \ldots\}$$

AM signal with this square envelope is:

$$S_{AM,\,square}(t) = (1 + A_{square}(t))\sin(2\pi f_c t)$$

This signal has AM side bands at frequency:

$$2\pi\{f_c \pm (2k-1)f_m\}$$

This frequency can be negative when:

$$f_c < (2k-1)f_m$$

However, cos(-a) = cos(a).

RESULTS

Energy in tip motion due to downmixing in the nonlinear tip sample interaction depends on the modulation envelope. A possible reason is the difference in time spent at large indentation. It is expected that this effect will influence achievable contrast in SSURFM imaging.

This analysis has been performed off-resonance but should be repeated on-resonance which is the typical scenario for SSURFM. This will complicate the analysis due to the phase response at resonance.

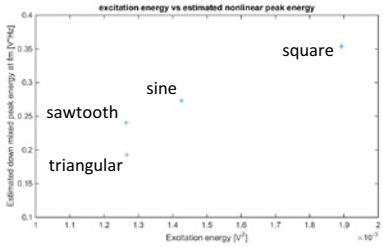

Down mixed peak energy as function of excitation energy. One can see that different modulation envelope functions give different results, what likely influences the contrast in SSURFM

CONCLUSION

Variations in the modulation envelope functions have shown variations in the effeciency of downmixing due to nonlinear tip-sample interaction. This is likely to influence contrast in SSURFM imaging.

This research has been supported by TNO's Early Research Program 3D Nanomanufacturing Instruments

Characterizing electron beam induced damage in metrology and inspection of advance devices

Abbas Mohtashami [1], Violeta Navarro [1], Hamed Sadeghian [1], Ilan Englard [2], Dror Shemesh [2], Nitin Singh Malik [2]

[1] **Netherlands Organization for Scientific Applied Research, TNO, Delft, the Netherlands;**
[2] **Process Diagnostics and Control, Applied Materials, Israel**

ECSEL Joint Undertaking
Electronic Components and Systems for European Leadership

TNO innovation for life

Introduction

The semiconductor manufacturing technologies require usage of low dielectric (low-k) materials together with novel metrology tools. The electron beam (e-beam) has emerged as a complementary metrology and inspection tool. However, the e-beam can cause damages to the materials under inspection due to its relatively high energy. Here, we present scanning probe microscopy techniques with the capability of measuring the e-beam induced damages on various materials. These techniques can be considered as a complementary approach to e-beam to ensure minimizing damage to the features.

Inspection of the e-beam damage

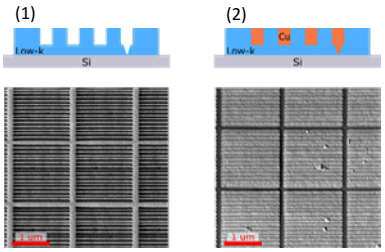

Two types of samples

We investigate the e-beam induced damages on two sets of samples (300 mm wafers):

1- Patterned low-k material on Si wafer.
2- Patterned low-k material on Si wafer filled with copper (Cu).

Systematic damage is induced by scanning the e-beam over square areas of the size 2×2 µm². The exposure energy and the dose (number of frames) are varied at each location.

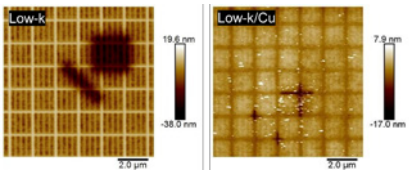

Measured e-beam damage formation

E-beam damage: low-k sample

- the e-beam damage is uniform.
- At fixed energy, damage increases linearly with dose.
- At fixed dose, damage is higher at certain energy windows (7kV)

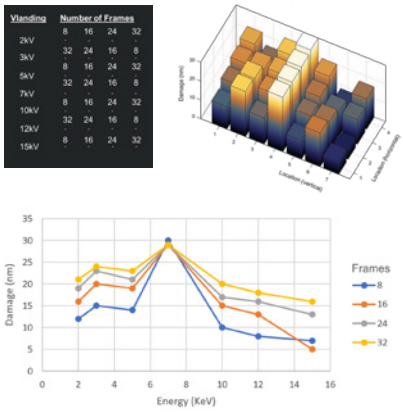

e-beam damage on low-k sample

E-beam damage: low-k/Cu sample

- Overall damage is much less than in the low-k sample.
- The e-beam damage is more pronounced on the low-k material, away from the copper. Detectable damage on the low-k/Cu lines only at the e-beam energy of 7kV
- Overall height drop we assign to the damage of the underlying low-k material beneath the low-k/Cu lines.

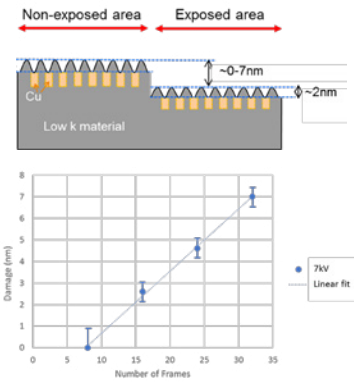

e-beam damage on low-k/Cu sample

TNO resonance-shift method

- We have developed a new scanning probe microscopy technique at TNO.
- The method is based on detecting the mechanical resonance shift of the probe that is in contact with the sample.
- This technique can provide information on the material changes of the sample.
- The e-beam exposure can slightly modify the visco-elastic properties of the materials on the sample.
- This visco-elasticity change can be detected by our technique as it modifies the resonance characteristics of the probe.

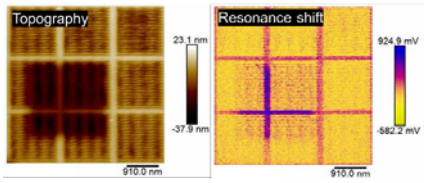

TNO resonance-shift method, detection of visco-elasticity change

CONCLUSION

The scanning probe microscopy can

- Measure the e-beam induced damages
- Detect visco-elasticity change of materials caused by e-beam
- Be used as a complimentary technique to the e-beam to ensure minimum damage to the features.

Acknowledgement

This project has received funding from the Electronic Component Systems for European Leadership Joint Undertaking under grant agreement No 692527. This Joint Undertaking receives support from the European Union's Horizon 2020 research and innovation programme and Netherlands, Belgium, France, Hungary, Ireland, Denmark, Israel.

Wafer-Scale Fabrication of Electrostatically Actuated AFM Probes

Edin Sarajlic[1], M.H. van Es[2], M.J. van der Lans[2], R. Vermeer[3]

1 SmartTip BV, Enschede, The Netherlands
2 TNO, Delft, The Netherlands
3 University of Twente, Enschede, The Netherlands

AFM probes with an integrated electrostatic micro-actuator have potential for various applications, including friction control, subsurface imaging and high-speed scanning.

By replacing the external piezoelectric drive in an AFM system with an integrated electrostatic micro-actuator, vertical displacement of the scanning tip can be more accurately controlled at high driving frequencies giving a cleaner excitation without parasitic resonances. We present wafer-scale fabrication methods for a monolithic integration of an electrostatic micro-actuator on an AFM cantilever.

MEMBRANE AFM PROBE

The membrane AFM probe consist of an electrostatic membrane actuator, which is monolithically integrated at the end of the cantilever. Vertical displacement of the tip can be generated and controlled by applying the driving voltage at the membrane actuator. The tip-sample interaction can be resolved by deflection of the cantilever.

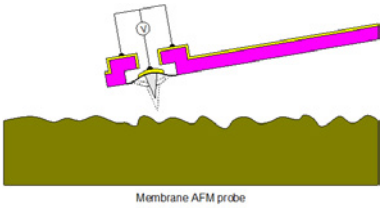

Membrane AFM probe

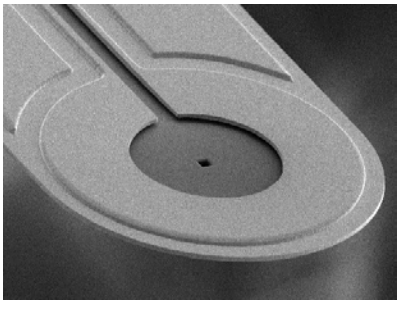
A SEM micrograph of the successfully fabricated membrane AFM.

The process of wafer-scale fabrication of the novel electrostatically actuated AFM probe using standard surface and bulk micromachining techniques.

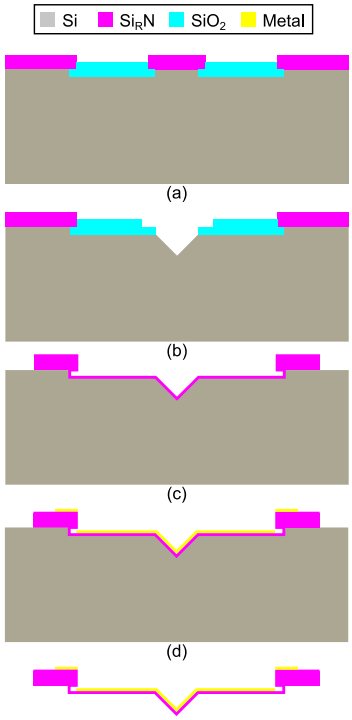

DOUBLE-CANTILEVER AFM PROBE

The double-cantilever probe has a small, soft cantilever integrated at the end of a long, stiff cantilever. An integrated electrostatic gap-closing allows deflection of the small cantilever and consequently vertical displacement of the probe tip.

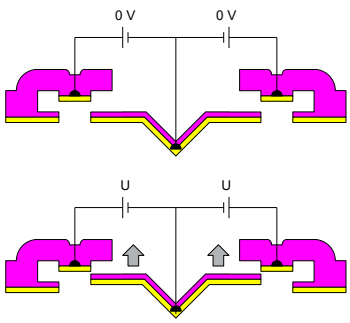

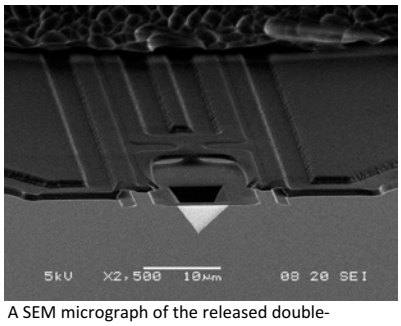

A SEM micrograph of the released double-cantilever probe.

The probe is fabricated in an wafer-scale fabrication process using standard surface micromachining.

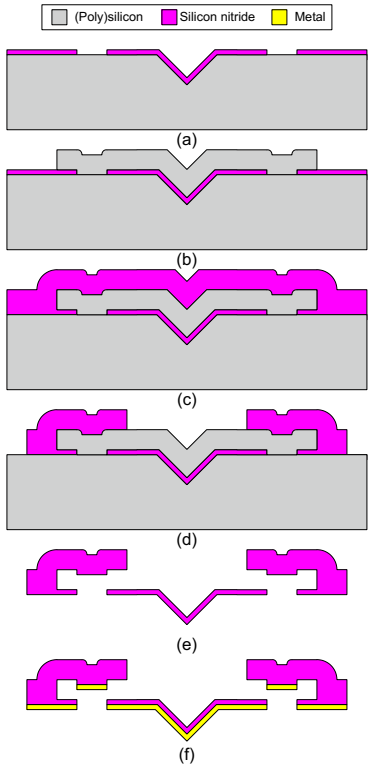

CONCLUSION

Wafer-scale fabrication of the AFM probes with an integrated electrostatic micro-actuator is demonstrated using solely standard surface and bulk micromachining processes.

This project has received funding from the Electronic Component Systems for European Leadership Joint Undertaking under grant agreement No 737479. This Joint Undertaking receives support from the European Union's Horizon 2020 research and innovation programme and Netherlands, France, Belgium, Germany, Czech Republic, Austria, Hungary, Israel

Frequency Modulation Subsurface Ultrasonic Force Microscopy

Maarten. H. van Es[1], Hamed Sadeghian[1]

[1] *NOMI, Optomechatronics, TNO, Stieltjesweg 1, 2628CK, Delft, The Netherlands*

TNO innovation for life

INTRODUCTION

Scanning Subsurface Ultrasonic Force Microscopy[1] (SSURFM) relies on a change in the sensing cantilever's resonance frequency to detect subsurface structures through their mechanical properties. It gains sensitivity both from exploiting the cantilevers large dynamical stiffness at high frequency and from using the sensitivity of the shifting contact resonance frequency.

[1] M.H. van Es, A. Mohtashami, R.M.T. Thijssen, D. Piras, P.L.M.J. van Neer, H. Sadeghian, *Mapping buried nanostructures using subsurface ultrasonic resonance force microscopy*, Ultramicroscopy, Volume 184, Part A, 2018, Pages 209-216, doi 10.1016/j.ultramic.2017.09.005

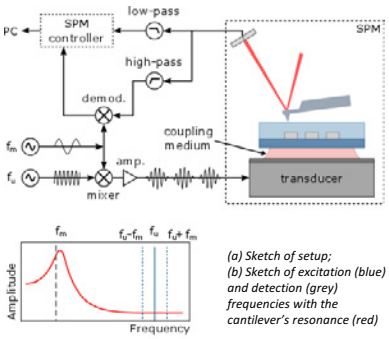

(a) Sketch of setup; (b) Sketch of excitation (blue) and detection (grey) frequencies with the cantilever's resonance (red)

WHY FREQUENCY MODULATION SSURFM

In Amplitude Modulation SSURFM, the cantilevers amplitude is monitored at a fixed frequency. In Frequency Modulation SSURFM (FM-SSURFM) the frequency is tracked instead. Advantages include

- quantitative analysis
- robust against large variations
- Maximum sensitivity by always being at the optimal frequency

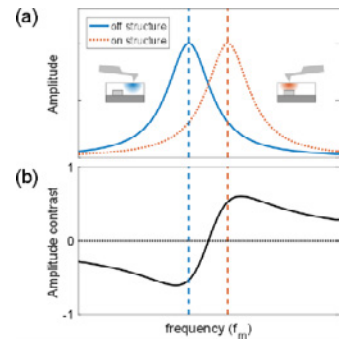

(a) Shift in contact resonance frequency from on to off a subsurface structure; (b) Frequency dependent amplitude contrast associated with the shift in contact resonance when measuring at a single fixed frequency

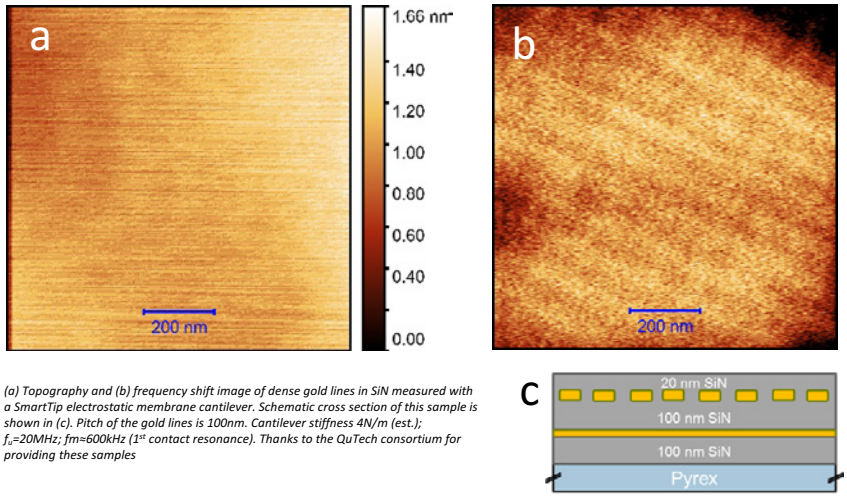

(a) Topography and (b) frequency shift image of dense gold lines in SiN measured with a SmartTip electrostatic membrane cantilever. Schematic cross section of this sample is shown in (c). Pitch of the gold lines is 100nm. Cantilever stiffness 4N/m (est.); f_o=20MHz; fm≈600kHz (1st contact resonance). Thanks to the QuTech consortium for providing these samples

IMPLEMENTATION

Dual Frequency Resonance Tracking is a FM technique which relies on keeping the amplitude at two frequencies – below and above the resonance – equal through a feedback loop which adjusts the central frequency based on the measured amplitudes.

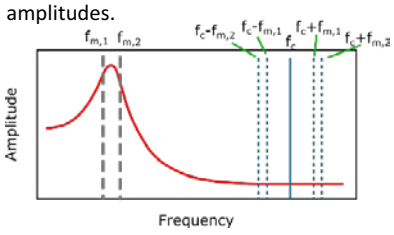

Sketch of excitation (blue) and detection (grey) frequencies in FM-SSURFM with the cantilever's resonance (red). $f_{m,1}$ and $f_{m,2}$ are the two modution frequencies which are adjusted based on their amplitude difference

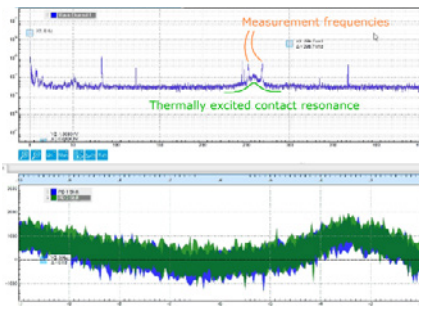

FM-SSURFM in action. (Top) Spectrum of cantilever motion showing the thermal contact resonance with both excited sidepeaks. (Bottom) Frequency shift over time, in this case due to thermal drift in the cantilever bending.

EXPERIMENTAL RESULTS

In the bottom figure in the middle column we show the signal spectrum of a working FM-SSURFM setup. For this measurement, the setup was tuned to clearly show the thermally excited contact resonance by using a soft cantilever (0.03N/m). Temperature fluctuations caused slow but large changes in contact resonance frequency through bending of the cantilever allowing a basic test of functionality of the method.

For optimal performance, FM-SSURFM needs a clean cantilever excitation spectrum. We therefore subsequently implemented FM-SSURFM with an electrostatically driven tip (see poster "Electrostatically driven cantilever tip for SSURFM"). With this equipment it was easy to setup the technique for subsurface imaging culminating in the frequency shift subsurface image above.

CONCLUSION

We implemented FM-SSURFM on our commercial AFM system with some modifications to ensure a clean frequency response of the cantilever. FM-SSURFM is a robust, quantitative tool for subsurface imaging.

This project has received funding from the Electronic Component Systems for European Leadership Joint Undertaking under grant agreement No 737479. This Joint Undertaking receives support from the European Union's Horizon 2020 research and innovation programme and Netherlands, France, Belgium, Germany, Czech Republic, Austria, Hungary, Israel

ECSEL JU

Virtual standards for nanoscale calibration of scanning probe microscopes

Motivation

Conventional calibration methods and standards for AFM have limitations and disadvantages for highly accurate applications in production environments. We will describe the development of robust virtual standards as a replacement for delicate physical standards to calibrate the lateral scale and height axis of an atomic force microscope (AFM) in harsh environments.

Richard Koops*, Arthur van de Nes

VSL Dutch Metrology Institute, Thijsseweg 11, 2629 JA Delft
www.vsl.nl

* corresponding author: rkoops@vsl.nl

Conventional AFM calibration

Except for metrology AFMs that contain internal calibrated references, AFMs need to be calibrated when accurate measurement results are required. The conventional approach to calibrate the measurement space of an AFM is based on delicate physical nano-structured standards.

The calibration of the height information along the z-axis of the AFM requires several step height standards but the result suffers from crosstalk between the axes. The lateral scale is usually calibrated using 1D or 2D calibration grids where the pitch of the structures has been accurately calibrated by diffraction measurements. However, for small AFM scanning areas, only a limited amount of information of the standard can be captured while imperfections become visible that deteriorate the accuracy of the AFM calibration.

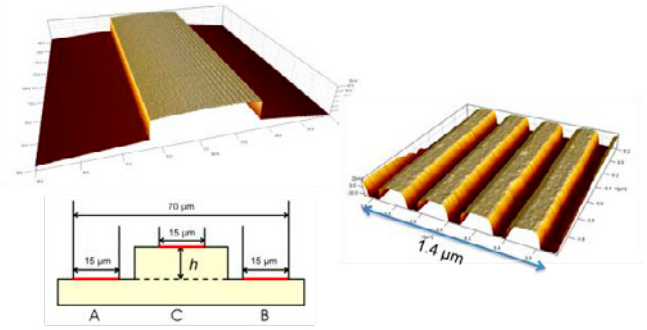

ISO 5436 step height standard

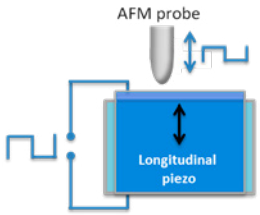

Virtual standards

Instead of using delicate physical standards, their functionality can be mimicked by piezo-based virtual standards. The calibration of the AFM z-axis is hereby realized by a highly linear piezo and the calibration of the lateral axes is realized by a, equally linear, shear piezo. The linearity of the piezo response has been established by a dedicated interferometer that can detect displacements at the picometer level.

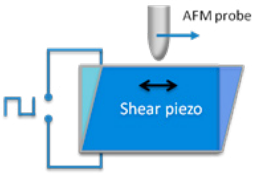

Results

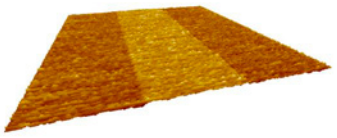

Generated 0.1 nm step height to calibrate the AFM height axis at the sub-nm level.

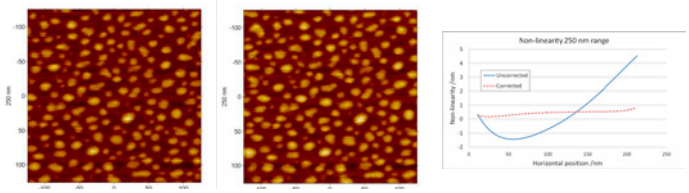

Calibration of a 250 nm lateral range is performed by cross correlation of two images that are displaced by a well-known distance. Sub-image correlation reveals the piezo non-linearity for one of the AFM lateral axis.

The virtual standard that we have developed overcomes the main disadvantages of physical standards:

- In contrast to physical standards, any surface texture will do so we don't need accurate and difficult to manufacture nanostructures.
- Changes in the surface texture due to contamination or damage are not relevant making the method very robust and suitable for use in a production environment.
- The method is especially useful for calibrating small lateral or height ranges where conventional physical standards fail.
- The measurement uncertainty of the virtual standards is at the sub-nanometer level.

Acknowledgements

This project has received funding from the Dutch Ministry of Economic Affairs and the European Union's Seventh Framework Programme for research, technological development and demonstration for the aim4np[1)] project under Grant agreement No. 309558.

1) aim4np = automated in-line metrology for nanoscale production, www.aim4np.eu

An approach towards 3D sensitive AFM cantilevers

Motivation

The AFM tapping mode is a highly sensitive local probing technique that is very useful to study and measure surface properties down to the atomic scale. The tapping mode is mostly implemented using the resonance of the first bending mode of the cantilever and therefore provides sensitivity mainly along the direction of this oscillation. In order to be able to not only measure the magnitude of the interaction but the entire interaction vector, sensitivity in additional directions is required. Here we present our efforts to micro engineer an AFM cantilever to create an additional vibration mode and enhance the cantilever response. In combination with the fundamental bending and torsion modes, the cantilever can simultaneously vibrate in three orthogonal modes to enable 3D sensitivity or the probe.

Richard Koops

VSL Dutch Metrology Institute, Thijsseweg 11, 2629 JA Delft
www.vsl.nl

* corresponding author: rkoops@vsl.nl

Actuation of multi-vibration modes

Traditionally, the probe vibration for the AFM tapping mode is realized by actuating a piezo attached to the cantilever. This method has some drawbacks when we want to create three vibration modes simultaneously. Photo-thermal actuation provides full control over the selection of excitation modes and their individual amplitudes. We use a 405 nm (purple) diode laser for thermal excitation and a 635 nm (red) for measuring the cantilever response.

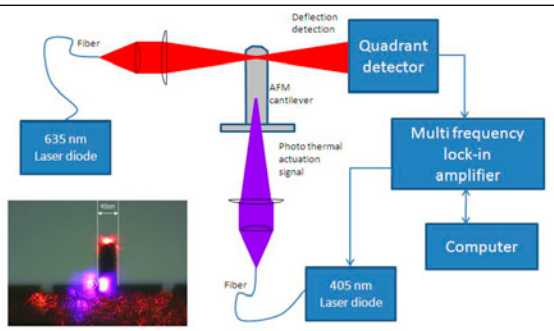

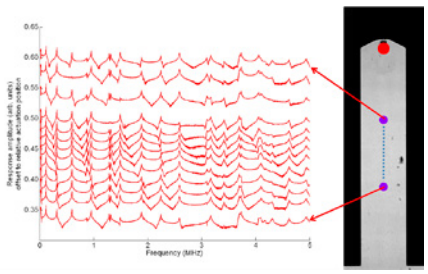

Controlled mode excitation

To illustrate the control potential of photo thermal excitation the cantilever response as a function of the excitation position along the cantilever was measured. The amplitude of the various modes can even be influenced depending on the mode structure and the position of the excitation spot.

By adding the three modulation signals for the desired modes, these modes are simultaneously exited.

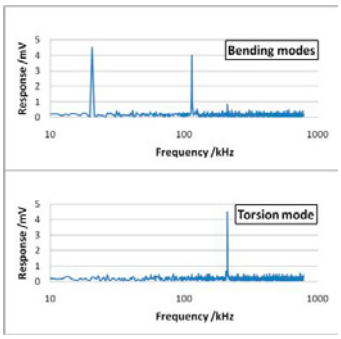

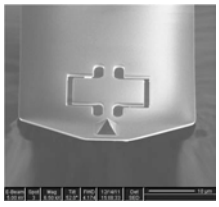

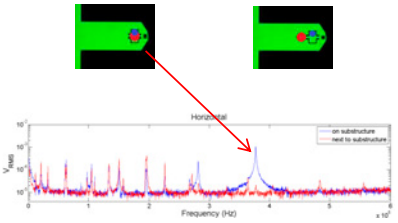

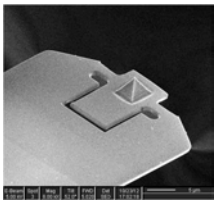

Cantilever engineering

Next to the bending and torsion modes of a standard AFM cantilever, an engineered mode was designed with a resonance around 4 MHz. This mode is indeed observed when we directly excite the engineered microstructure. The final design includes the probe area.

Acknowledgments

This project has received funding from the Dutch Ministry of Economic Affairs and was performed within the EMPIR programme. Additionally, we want to thank Hozanna Miro and Paul Alkemade from the Delft University of Technology for their contribution on the FIB micro machining of the cantilevers.

EMPIR
EURAMET
The EMPIR initiative is co-funded by the European Union's Horizon 2020 research and innovation programme and the EMPIR Participating States

3DNano

Rijksoverheid

Conductive Single Crystal Diamond Probes for 3D-AFM with TNO and 3DAM

J. I. Kilpatrick[1,2], P. De Wolf[3], N. O'Hara[2], C. McManamon[2], H. Cavazos[2], G. L. W. Cross[2,4,5]

1 Conway Institute of Biomedical and Biomolecular Research, University College Dublin, Ireland
2 Adama Innovations, CRANN, Trinity College Dublin, Ireland
3 Bruker Nano Surfaces, 112 Robin Hill Road, Santa Barbara, CA-93117, USA
4 School of Physics, Trinity College Dublin, Ireland
5 Advanced Materials and BioEngineering Research Centre (AMBER), CRANN Institute, Trinity College Dublin, Ireland

ECSEL Joint Undertaking

TNO innovation for life

INTRODUCTION

Sharp single crystal diamond probes are formed at wafer scale using a mask and plasma etch process. The diamond probes are made electrically conductive by heavily doping with boron during the CVD process. By adjusting the processing conditions the tip shape and sharpness can be controlled at the nanometer scale. These single crystal diamond probes have demonstrated high performance electrical data from the atomic to the whole device scale.

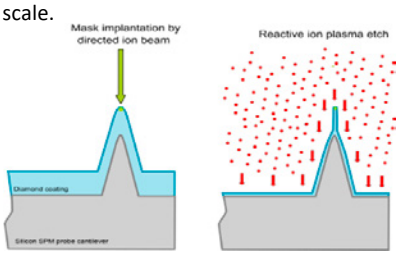

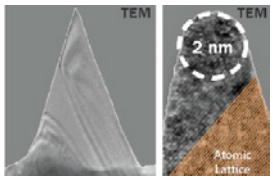

Single crystal conductive diamond tip with a Super Sharp tip radius of 2nm

SCANNING CAPACITANCE MICROSCOPY

Scanning Capacitance Microscopy (SCM) of a pnp transistor (top surface) with 250nm effective gate length. Probe: 10nm radius, 1.5N/m. AC voltage is set to a low value (200mV). The different transistor regions (p-doped source & drain, and medium doped n-type channel) are well resolved. Data: Bruker Nano.

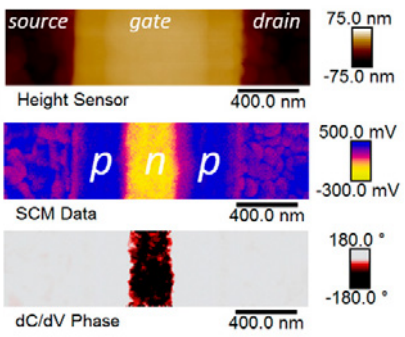

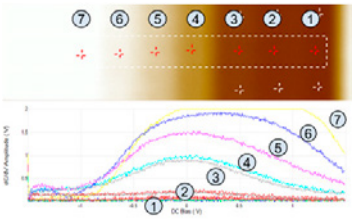

SCM image (6 x 2µm) and dC/dV-V spectra of Si sample with a staircase carrier profile. All dopant steps are clearly resolved with good signal/noise ratio illustrating the high sensitivity and dynamic range of the conductive diamond probes (10^{15} to above 10^{20} atoms/cm^3). Data: Bruker Nano.

SCANNING SPREADING RESISTANCE

Scanning Spreading Resistance Microscopy (SSRM) image of Si sample with a staircase carrier profile. Probe: 10nm radius, 40N/m. All dopant steps are clearly resolved with good signal/noise ratio illustrating the high sensitivity and dynamic range of the conductive diamond probes (10^{15} to above 10^{20} atoms/cm^3). The probes easily resist the high loads required for stable SSRM imaging of Si surfaces in air (penetrating through the native oxide & establishing a β-tin phase transformation of the Si with low contact resistance). Data: Bruker Nano.

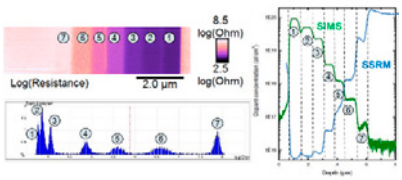

Doped sample measured with standard doped diamond probes (40 N/m) (Left). Same measurement with Adama 10 N/m probe (Right). Vertical Scale = 100 uA. The single crystal diamond probe used has a lower spring constant and so exerts a lower pressure on the sample enhancing lateral resolution. Data: CSI Instruments.

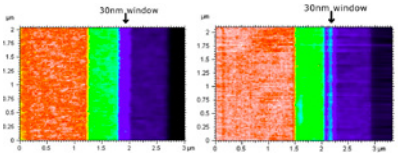

FinFET METROLOGY

Capillary adhesion and Van der Waals interactions must be overcome in narrow trenches by using the higher bending modulus offered by single crystal diamond. Ultimately there will be a resolution trade-off between sidewall interactions and probe diameter.

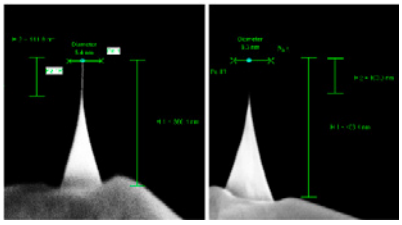

Examples of single crystal diamond probe tips for FinFET metrology. (Left) 20:1 aspect ratio probe with 5.4 nm diameter. (Right) 25:1 aspect ratio probe with a 3.5 nm diameter. These probes are highly doped with boron to allow electrical measurements and/or controlling tip-sample electrostatics.

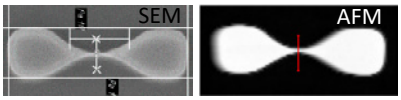

A 10 nm width FinFET measured using SEM (left) and AFM using high aspect ratio diamond probes (right). Sample: LETI

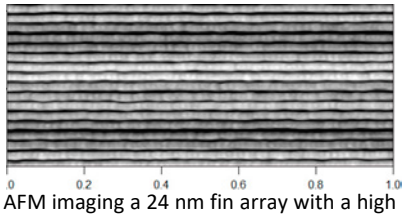

AFM imaging a 24 nm fin array with a high aspect ratio diamond probe (Lateral scale = 1um). Sample: IMEC

CONCLUSION

These sharp conducting diamond probes can be used for a wide range of electrical modes, with large dynamic range, excellent sensitivity, and resolution down to a few nm.

High aspect ratio diamond probes enable FinFET characterization at the 10 nm node and beyond.

CONTACT MECHANICS MODELING OF TIP-SAMPLE INTERACTION IN SUBSURFACE PROBE MICROSCOPY

D. Piras, J. de Vreugd, M.J. van der Lans, H. Sadeghian

Department of Optomechatronics

TNO innovation for life

INTRODUCTION

Study of the tip-sample interaction stiffness in AFM:

- contact stiffness
- Effect of features buried deep in the substrate
- Hertzian contact theory

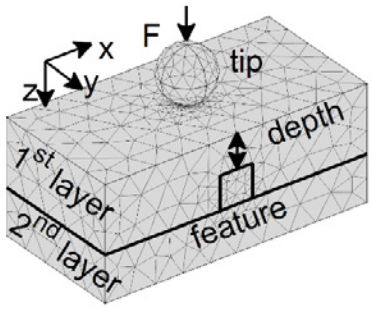

Fig. 1: FEM model for tip-sample interaction studies

METHODS

1) Estimate indentation δ via:

a) Use FEM contact;

b) Use FEM Hertz theory:

- contact radius
- contact pressure

2) From δ estimate the reduced and effective Young's moduli:

$$\langle M \rangle_{1st\ layer} = \sqrt{\left(\frac{3F}{2\delta}\right)^3 / 6FR_{tip}}$$

$$1/\langle E \rangle^* = 1/M_{tip} + 1/\langle M \rangle_{1st\ layer}$$

3) Estimate the contact stiffness

$$k^* = \sqrt[3]{6FR_{tip}\langle E \rangle^{*2}}$$

4) Scan the position of the feature below contact area

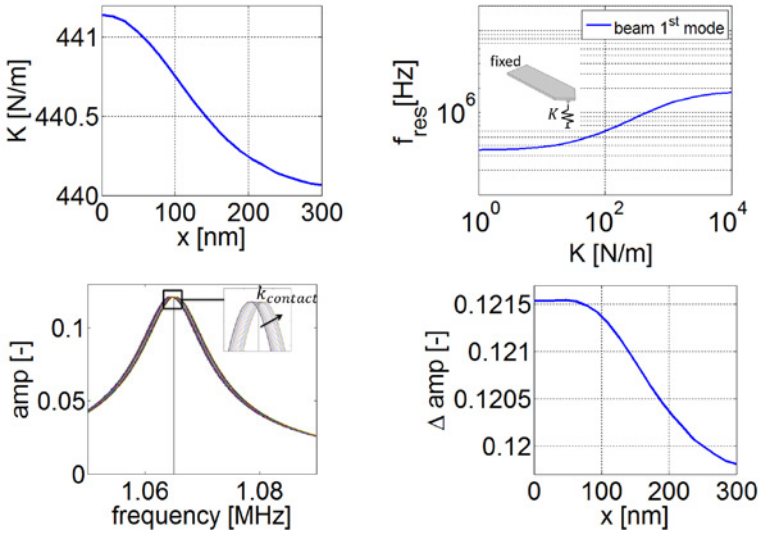

Fig. 2: Contact stiffness is used as boundary in the frequency analysis of the cantilever to extract the contact resonance shift

RESULTS

Fig 2: FEM modelling of the frequency behavior of the cantilever with compliant boundary at the tip

- from contact stiffness to contact resonance frequency

Fig 3: Comparison of contact (COMSOL and ANSYS) and pressure (COMSOL) model approaches

- computation time severely reduced
- the stiffness variation from on-feature to off-feature is remarkably the same
- COMSOL-pressure slightly overestimates the contact stiffness (1.9% vs ANSYS-contact, 1.3% vs COMSOL-contact)
- test multiple material, tip sizes, applied force and depth combination

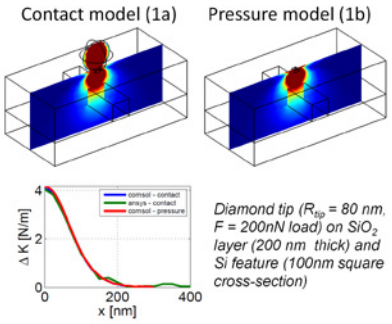

Fig. 3: comparison of contact and pressure model approaches

CONCLUSION

Faster computation: use outlined procedure for time dependent analysis

Frequency analysis: estimate the contact resonance shift

This research was supported by TNO's Early Research Program 3D Nanomanufacturing Instruments

Deep subsurface imaging with subsurface probe microscopy @ GHZ

P.L.M.J. van Neer[1], M.H. van Es[2], D. Piras[2], V. Navarro[2], A. Mohtashami[2], M. Lans[2], H. Sadeghian[2]

[1]Department Of Acoustics and Sonar
[2]Department Of Optomechatronics

TNO innovation for life

INTRODUCTION

Atomic Force Microscopy (AFM):
- Used to characterize surface topology at nano-scale

Subsurface Probe Microscopy (SSPM):
- Combines AFM + MHz/GHz excitation
- Used to probe subsurface

AFM + MHz excitation:
- Image contrast depends on visco-elasticity (princess-on-pea)
- Significant force applied on cantilever: danger of damage
- Inspection depth < 500 nm

AFM + GHz excitation:
- Image contrast depends on acoustic impedance
- Minimal force applied on cantilever: damage minimized
- Inspection depth >> 1000 nm

This work details the initial simulation and experimental GHz SPM work carried out at TNO

METHOD

SSPM hardware:

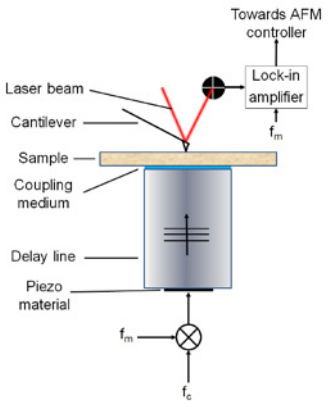

SSPM imaging method:
- Low force (~1-10 nN)
- Ultrasound excitation frequency (f_c) around 1 GHz modulated at contact resonance frequency (f_m) of cantilever
- Cantilever excited at contact resonance (f_m).

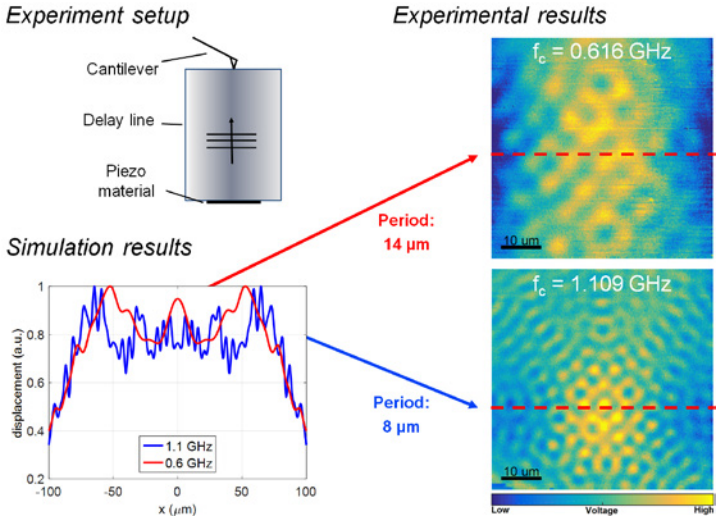

Experiment conclusion:
Comparable standing wave pattern produced in experiments as in simulations.

RESULTS: EDGE DIFFRACTION

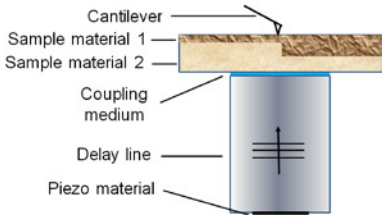

Experimental setup

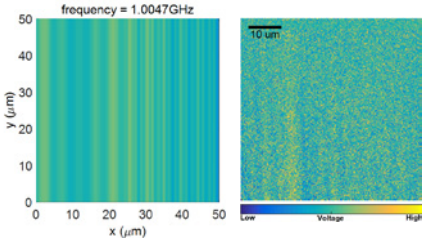

Simulation results *experimental results*

Experiment conclusion:
Comparable diffraction patterns detected in experiments as those produced in simulations

RESULTS: SCATTERING

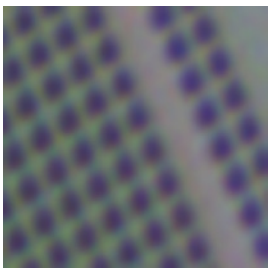

Sample schematic

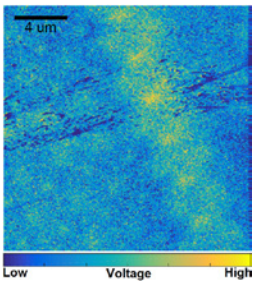

SSPM image

Experiment conclusion:
Clear evidence of scattering in SPM image

CONCLUSION

This work presents the first successful experimental and simulation results obtained at TNO using GHz Subsurface Probe Microscopy (SPM).

This research was supported by TNO's Early Research Program 3D Nanomanufacturing Instruments

Nano-precision multi-agent Maglev positioning platform

Teun van den Dool[1], Lukas Kramer[1], Rik Kruidhof[1], Aukje Kastelein[1], Bert Dekker[1], Marla van Koppen[2] , Johan Lugtenburg[3] , Evert Nieuwkoop[4]

[1] Department of Optomechatronics, TNO, Delft
[2] Department of Instrument Manufacturing, TNO, Delft
[3] Department of Optics, TNO, Delft
[4] Department of Radar technology, TNO, Delft

TNO innovation for life

INTRODUCTION

This project is aiming to realize miniature self-contained carriers that can independently perform positioning and scanning tasks on nano-scale.

Such carriers can support agents for performing tasks such as inspection, deposition, repair, and cleaning. All at the nano-scale. The carriers can make large movements in X- and Y-direction and have a smaller range in Z, and rotations. This is sufficient to cover relevant surfaces in, for instance, semicon industry, such as wafers and reticles.

TERGET SPECIFICATIONS:

Scanning area X,Y: >300x300 mm
Vertical range Z: +/-100 um
Position accuracy: 10 nm
Position resolution: <1 nm
Acceleration: >10 m/s2
Carrier size: from current 50x50 mm to 10x10 mm in future.
Number of carriers: up to at least 50

HOW

After trading several solutions, magnetic levitation has been chosen as the most flexible solution to provide centimeter range scanning at sub-nanometer resolution. In a first demonstrator a moving coil system has been implemented with coarse position sensing based on Hall sensing. The control will be on-board in future but has been implemented on a generalized purpose computer for the first experiments.

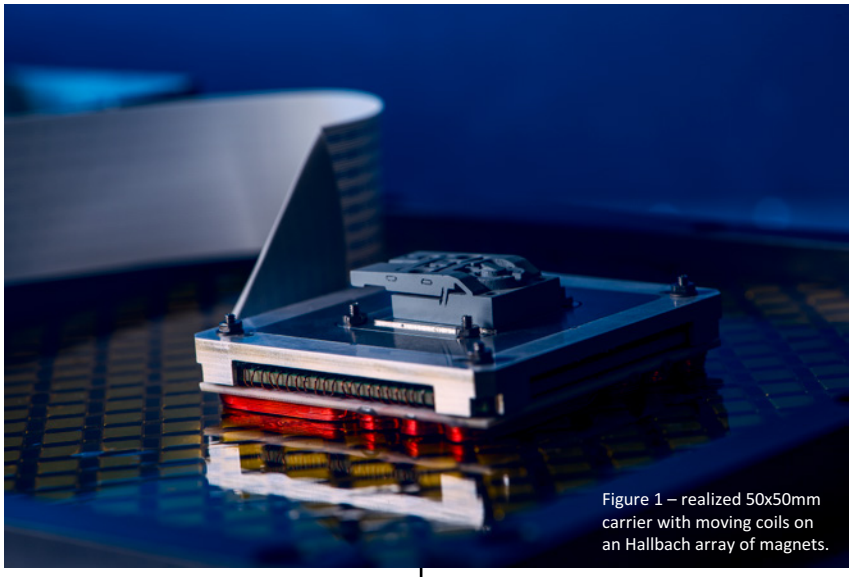

Figure 1 – realized 50x50mm carrier with moving coils on an Hallbach array of magnets.

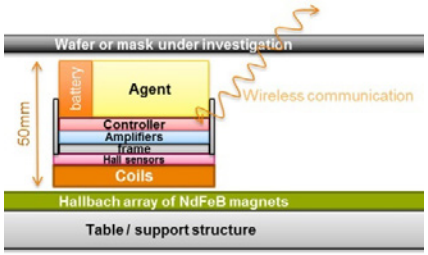

Figure 2 – vertical stack of a single carrier.

RESULTS AND NET STEPS

The Hall sensor X,Y-position readout is being tested (see figure4). Its resolution is as expected in the order of 100nm. The position control is being implemented. Next steps involve implementing miniaturized on-board sub-nanometer encoders, on-board control electronics, and wireless communication and power transfer.

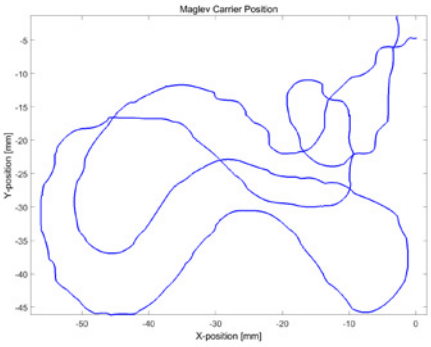

Figure 4 – Measured (coarse) X.Y-position with Hall sensors.

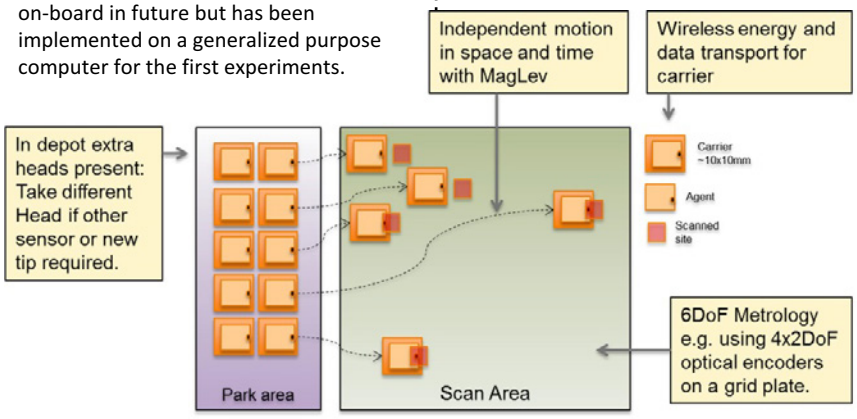

Figure 3 – Example use-case of the positioning platforms.

CONCLUSION

The demonstrator for the MagLev multi-agent positioning system has been build successfully and the performance is currently being assessed.

This research was supported by TNO's Early Research Program 3D Nanomanufacturing Instruments

Opto-mechanical platform for optical near-field imaging instruments

R.J.F. Bijster[1,3], R.W Herfst[1], J.P.F. Spierdijk[1], A. Dekker[1], W.A. Klop[1], G.F.IJ. Kramer[1], L.K. Cheng[2], R.A.J. Hagen[2] and H. Sadeghian[1]

1 Department of Optomechatronics, TNO, Delft, The Netherlands
2 Department of Optics, TNO, Delft, The Netherlands
3 Department of Precision and Microsystems Engineering, Delft University of Technology, Delft, The Netherlands

TNO innovation for life

High resolution optical imaging is within reach by probing the optical near-field that exists tens of nanometers away from the sample. This field carries the high frequency information that cannot be imaged with far-field optics.

The meta-instrument concept takes these new techniques from the laboratory to industrial application by providing a high speed, high precision positioning platform.

THREE TIER ARCHITECURE

To achieve a large stroke, and achieve nanometer positioning precision at a large bandwidth of more than 500 kHz, the platform is designed as a three-tier architecture. A large stroke of several millimeters is achieved using a linear stepping motor. Large height variations of several micrometers are covered using a piezo-electric stage at 10 kHz bandwidth. The last 167 nm are bridged by a micro-electro-mechanical system (MEMS) at 550 kHz bandwidth.

LARGE STROKE ACTUATOR

A large stroke is achieved by clamping a carbon rod in a V-groove. The impulse action ('hammer' motion) of the piezo stage forces a vibration through the rod. If local friction is over come in the clamp, the stage moves back or forth. Repeatable 0.32 µm steps can be made at velocities up to 3.2 mm/s. This allows the instrument to quickly engage the sample surface.

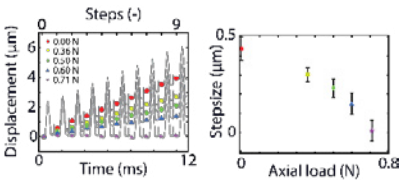

FIBER INTERFEROMETERS

Sub-nanometer precision tracking of the motion of the stages is achieved by using three fiber-interferometers. The three interferometers are located at the corners of the instrument and allow tracking of the piston motion, tip- and tilt.

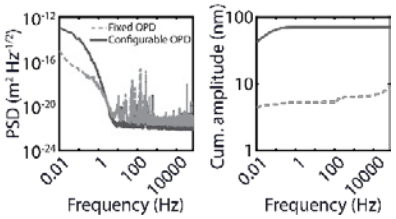

PIEZO STAGES

Three piezo stages allow a micrometer stroke at a bandwidth of 10 kHz. Located close to the fiber interferometers, they allow control over the piston motion and tip-, and tilt angles.

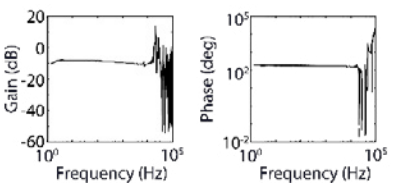

MEMS STAGE

The MEMS stage moves the 'lens' at a high bandwidth of 550 kHz and sub-nanometer precision. A parallel plate actuator allows motion over 167 nm distance. To maximize the bandwidth and minimize the 'flapping mode', the placement of the leaf springs is optimized and the moving electrode is made of SiC. Shown in the figures below are (1) the lens, (2) electrodes, (3) electrodes, (4) SiC body, (5) 500 nm gap, and (6) leaf springs.

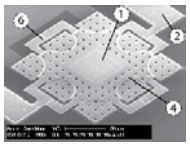

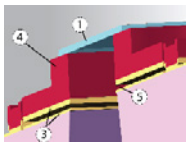

FUTURE

A new design further shrinks the size and has increased stability. The distance between sample and lens will be measured using the local heat-flow.

CONCLUSION

Taking new optical near-field imaging lenses from 'lab to fab', requires a high speed, high precision position platform. The meta-instument offers that capability.

This research was supported by TNO's Early Research Program 3D Nanomanufacturing Instruments

Control of a 6-DoF Large Dynamic Range Atomic Force Microscope

Stefan Kuiper, Gert Witvoet, Joost Peters, Max Baeten, Ramon Rijnbeek, Thomas Liebig, Geerten Kramer, Ton Overtoom, Tom Duivenvoorde, Erik Fritz, Rob Willekers

TNO, P.O. Box 155, 2600 AD, Delft, The Netherlands
stefan.kuiper@tno.nl

TNO innovation for life

In the field of semiconductor- and nano-manufacturing there is a strong need for metrological tools that allow for accurate measurements of both local nanometer scale dimensional properties of individual features, as well as global dimensional properties of feature grids. The Large Dynamic Range Atomic Force Microscope (LDR-AFM) enables measurement with sub-nanometer uncertainty over several millimeters range.

Application: overlay improvement

To assess overlay within semiconductor devices, an inter-layer marker to product feature measurement is proposed (Figure1). This enables mixed-machine overlay improvement.

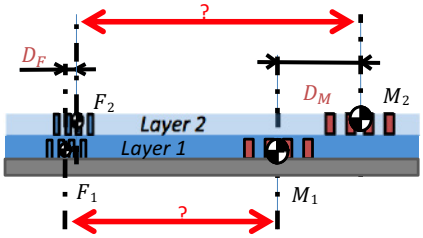

Figure 1: Conceptual drawing of two layers within a semiconductor device, with product features (F_i) and marker features (M_i) in each layer. The intra-layer overlay is assessed via marker features distances (D_M), while the relative position of the product features (D_F) is actually determining the functionality of the semiconductor device. The idea of the LDR-AFM metrology concept is to measure the unknown inter-layer marker to product feature distance marked by the red (?).

Large Dynamic Range 6DOF AFM

To show the feasibility of this metrology concept, a demonstrator system is developed.

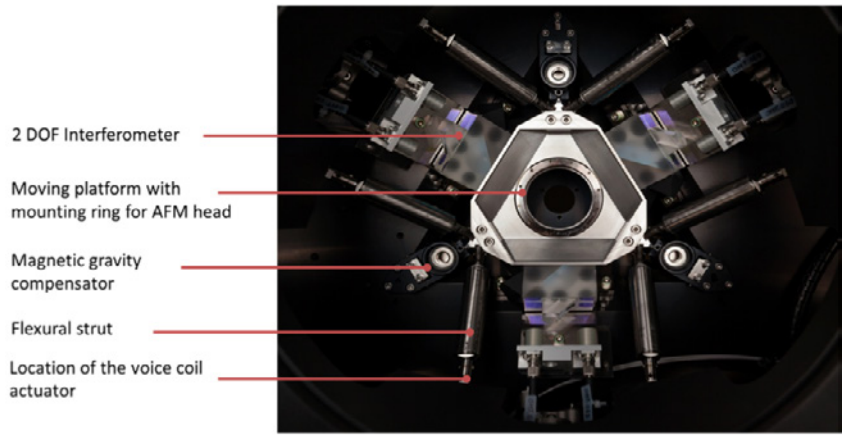

Figure 2: Hexapod stage in the large dynamic range AFM. Using six voice coil actuators and three 2-DOF interferometers, the position of the AFM head located in the center of the hexapod is controlled with sub-nanometer accuracy in a 4x8x8 mm hexagonal area.

A 6 degrees of freedom (DOF) hexapod positioning stage (Figure 2) enables highly accurate positioning of the probe with respect to the sample substrate. In the hexapod stage, an AFM head (Figure 3) is mounted that scans the product and marker features.

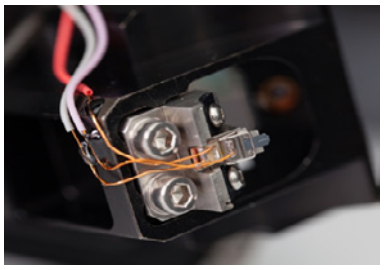

Figure 3: AFM head in the LDR-AFM .

MIMO Stage Control Design

The 6 DOF hexapod is controlled using decentralized feedback control. Decoupling based on geometric sensor transformation and a rigid body model is derived to allow for effective feedback design resulting in accurate positioning of the AFM head. Figure 4 shows the feedback design for the hexapod stage.

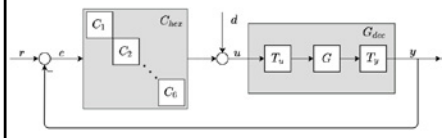

Figure 4: Feedback design for the hexapod stage control.

Performance

To evaluate the performance of the closed-loop controlled hexapod, the power spectral density (PSD) of the positioning error is evaluated (Figure 5). The feedback control design is aimed at optimizing the PSD of the closed-loop error, i.e. achieve a flat as possible error spectrum.

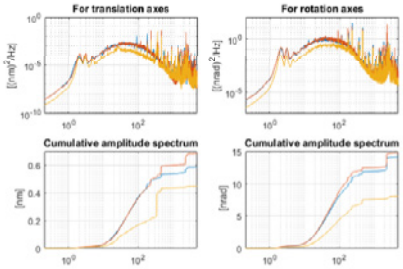

Figure 5: PSD of closed-loop error.

Accuracy in the imaging direction (z) is **<0.45 nm RMS** over the full range, and in x-y direction **<0.7 nm RMS**. Rotational errors are in the order of nrad, sufficiently minimizing induced Abbe errors.

CONCLUSION

The LDR-AFM is a metrology tool enabling **large dynamic-range** measurements. Developments in the control design have reduced the positioning error to **sub-nanometers**. Further work includes enhancing control design for AFM operation and performing end-to-end test to verify measurement repeatibility.

High-throughput parallel Atomic Force Microscopy

Rodolf Herfst[1], Hamed Sadeghian[1], Tom Bijnagte[1], Bert Dekker[1], Tom Duivenvoorde[1] Marla van Koppen[2], Max Baeten[1], Teun van Kuppeveld[1], J. Winters[1], Bert Dekker[1], Alexander Eigenraam[1], Klara Maturova[1], Daniele Piras[a], Francois Bouquet[1], Ramon Rijnbeek[2], Nicole Nulkes[1]

1 Department of Optomechatronics
2 Department of Instrument manufacturing

ECSEL Joint Undertaking
Electronic Components and Systems for European Leadership

TNO innovation for life

Introduction

As the semiconductor industry is fast approaching the 10 nm node, demands on metrology tools are becoming ever more stringent. New methods for accurate assessment are required. Parallel High speed scanning probe microscopy (SPM) is a promising candidate for very high throughput and various measurement possibilities.

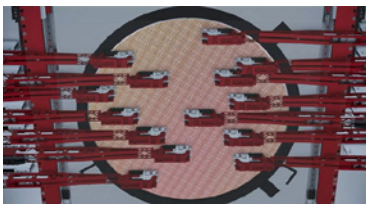

Wafer stage in the middle, with on two sides up to 50 postioning arms for miniaturized AFM's

High Throughput concept

High throughput is achieved through:

- High-speed scanning
- Simultaneous scanning with miniaturized AFM's
- Overhead reduction (e.g. loading, navigation, approach)

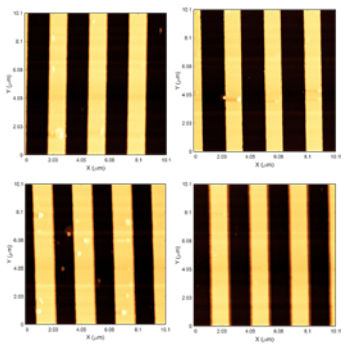

Simultaneous imaging of 4 AFM's, 10x10 µm images (3 µm pitch)

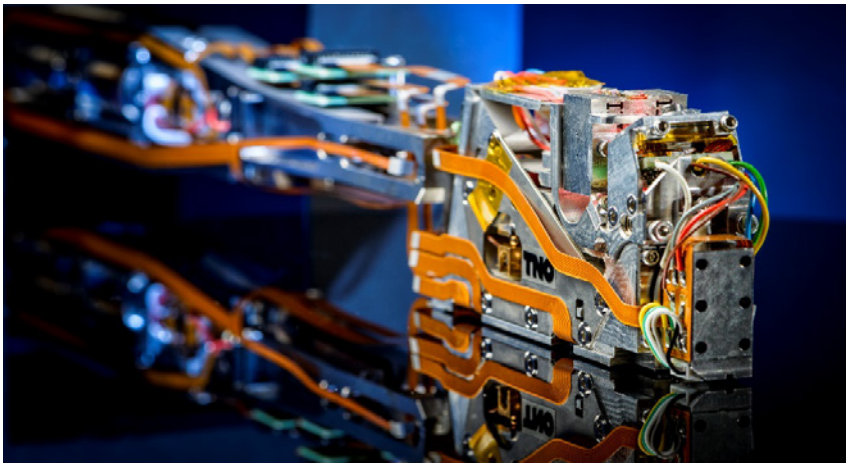

Miniaturized AFM (70x19x45 mm³) positioned by a positioning arm on the wafer

Application area's

- Automated defect review (material characterization)
- Roughness measurement
- Patterned resist wafer
- Patterned wafers after etch
- Mask metrology
- Sub-surface defects & features
- DSA metrology

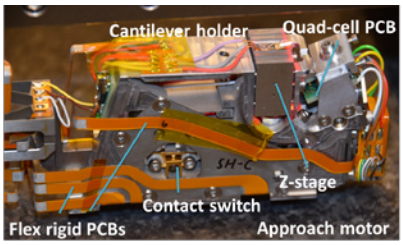

Miniaturized AFM (70x19x45 mm³)

Proven specifications

- Resolution x,y 5nm on 10x10 µm scan, 0,5nm on 1x1µm scan, z 0,5nm
- Drift 12nm/frame
- Scanning speed up to 13 lines/s
- Scan 450, 300, 100 mm wafer
- Each site circa 10 × 10 µm
- 4 sites in parallel

Target specifications

- Resolution, z 0,1nm
- 40 sites in parallel
- Each site circa 20 × 20 µm
- Throughput based upon measurements requirements.
- Positioning accuracy: 200 nm

CONCLUSION

First simultaneous AFM measurements using four scanheads, with high-speed actuators and control realized

For a demonstration of the system see https://www.youtube.com/watch?v=lOWFk8XtKFM

Acknowledgement

This project has received funding from the Electronic Component Systems for European Leadership Joint Undertaking under grant agreement No 325613. This Joint Undertaking receives support from the European Union's Horizon 2020 research and innovation programme and Netherlands, Belgium, France, Hungary, Ireland, Denmark, Israel.

Automatic cantilever alignment and exchange for high throughput atomic force microscopy

Tom Bijnagte[1], Bert Dekker[1] , Rodolf Herfst[1], Ramon Rijnbeek[2], Geerten Kramer[1], Evert Nieuwkoop[3], Wimar Klop[1], Ferry Corbet[2], Tom Duivenvoorde[1], Ben van Essen[1], Martijn van Riel[1], Marla van Koppen[2], Lukas Kramer[1], Teun van Kuppeveld[1], Nicole Nulkes[1], Hamed Sadeghian[1]

1 Department Of Optomechatronics

2 Department Of Instrument Manufacturing

3 Department Of Radar technology

ECSEL Joint Undertaking

TNO innovation for life

An automated cantilever exchange and optical alignment instrument is developed. Experimental proof of principle is demonstrated by exchanging various types of AFM cantilevers in 6 seconds with an accuracy better than 2 µm. The exchange and alignment unit is miniaturized to allow for integration in a parallel AFM.

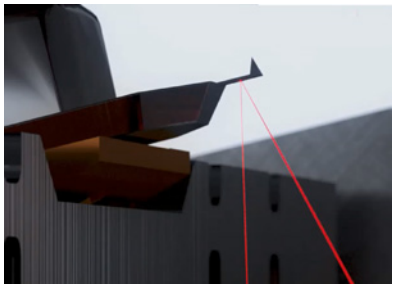

Beam reflected at cantilever

Reliability of the cantilever exchange

The reliability of the cantilever exchange and alignment unit has been evaluated. Ten thousand continuous exchange and alignment cycles were performed without failure. The automated exchange and alignment of the AFM cantilever overcomes a large hurdle toward bringing AFM into high-volume manufacturing and industrial applications.

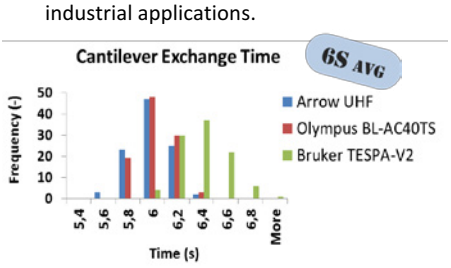

Cantilever exchange time

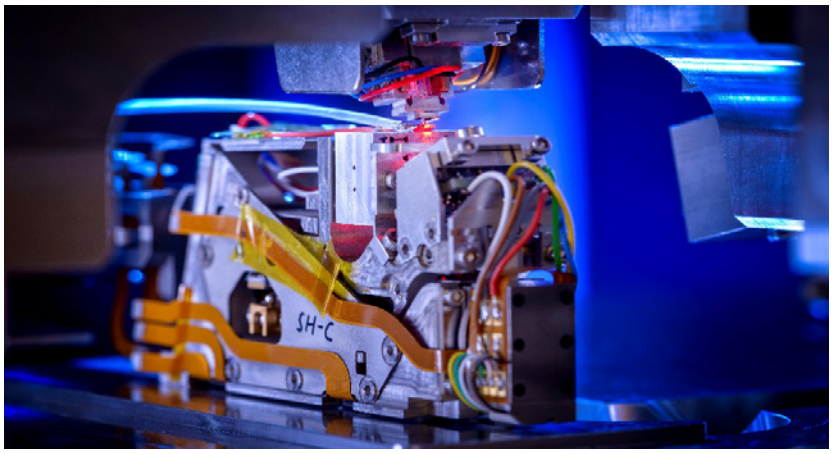

Contactless chip take-over, fly-over height is 10um

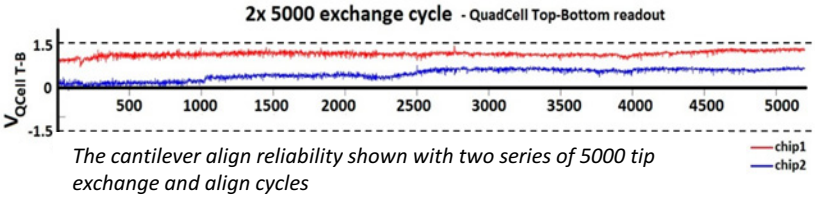

The cantilever align reliability shown with two series of 5000 tip exchange and align cycles

Image performance after exchange

The imaging performance was verified after 1 and 150 automatic cantilever exchanges.

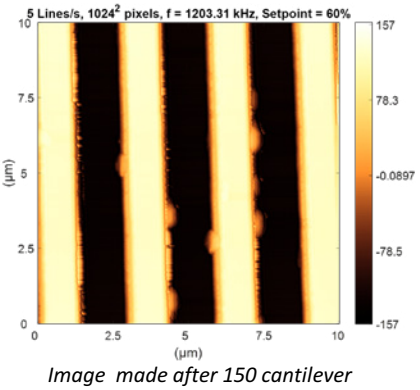

Image made after 150 cantilever exchanges

Application area's

- High Throughput Parallel AFM system of TNO
- Inline metrolgy in semiconductor manufacturing processes

Proven Specifications

- Exchange time is 6 ±0.8s
- Cantilever placement accuracy, width cantilever ±0,25µm, length cantilever ±2,3µm,
- Align reliability: 10,000 cycles image
- Exchanged and aligned tips, Arrow UHF, Olympus BL-AC41, Bruker Tespa-V2

CONCLUSION

The cantilever exchange and alignment functionality are successfully demonstrated. This automated and miniaturized cantilever exchange and alignment can be integrated in high throughput parallel atomic force microscopy

Acknowledgement

This project has received funding from the Electronic Component Systems for European Leadership Joint Undertaking under grant agreement No 692527. This Joint Undertaking receives support from the European Union's Horizon 2020 research and innovation programme and Netherlands, Belgium, France, Hungary, Ireland, Denmark, Israel.

High Throughput 2D arrays of miniaturized AFM

T. vd Dool[1], A. Kastelijn[1], G. Kramer[1], T. v Kuppeveld[1], L. Schriek[2], B. v Essen[1], B. Dekker[1], P. Toet[2] , E. Nieuwkoop[4], R. Kruidhof[1], R. Rijnbeek[3] M. Koppen[3], J. Lugtenburg[2]

1 Department of Optomechatronics, TNO, Delft
2 Department of Optics, TNO, Delft
3 Department of Instrument Manufacturing, TNO, Delft
4 Department of Radar technology, TNO, Delft

TNO innovation for life

The goal of this project is to develop further miniaturized, arm-less AFM scanning system, to reach higher speed and higher precision.

HIGH THROUGHPUT AND ACCURATE AFM

In order to achieve the required higher throughput and accuracy the following improvements are proposed:

1. Miniaturized mechanics to improve dynamic behavior and increase parallelism.
2. Fiber interferometer to measure both cantilever deflection and cantilever z-displacement.
3. Dedicated high speed electronics and control to maximize potential of mechanics.

SYSTEM CONCEPT

The proposed system concept, shown in figure 1, is to use pick & place robots to position a multitude of scanning heads anywhere on a grid plate to achieve a highly flexible and parallelized system.

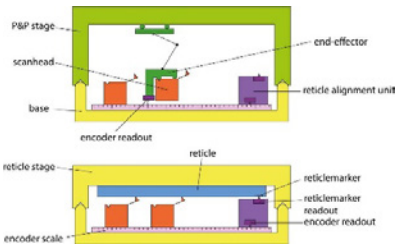

Figure 1 – Proposed system concept.

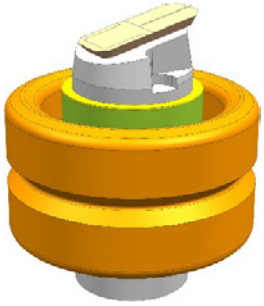

Figure 2 – Z-scanner design (with cantilever).

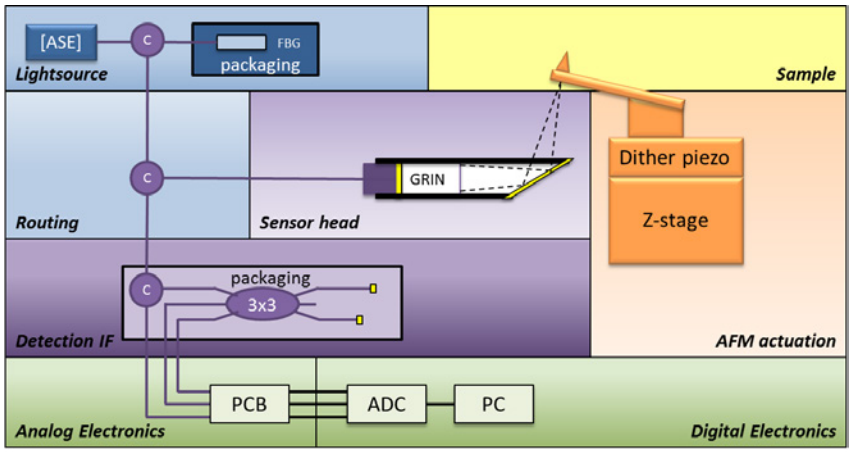

Figure 4 – Fiber Interferometer for readout of the cantilever and the displacement.

MINIATURIZED MECHANICS

The heart of the improved mechanical design is the miniaturized z-scanner shown in Figure 2. The rotational symmetry brings mechanical integrity. The form factor was chosen in such a way that a stationary ring was created, shown in Figure 3, which reduces dynamic cross-talk between the scanner and the supporting structure.

FIBER INTERFEROMETER

The challenge in developing the fiber interferometer, shown in figure 4, is combining the large working range needed for the z-stage (2 µm) with the large bandwidth required for the readout of the cantilever (10 MHz) and still achieve the low noise required for mask profilometry measurements.

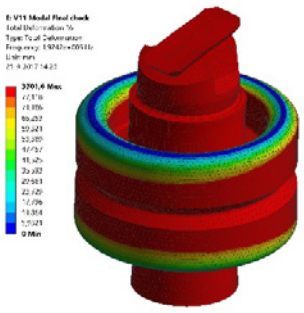

Figure 3 – Modal analysis showing stationary ring.

The fiber interferometer that will be used in the scan head has been qualified in a separate setup. The tests show that we can achieve the performance necessary for the mask profilometry application.

SCAN HEAD INTEGRATION

The miniaturized scan head was fully designed and build. At the time of this publication it is being integrated with the sensor for final qualification of the system. A CAD rendering is shown in figure 5 below.

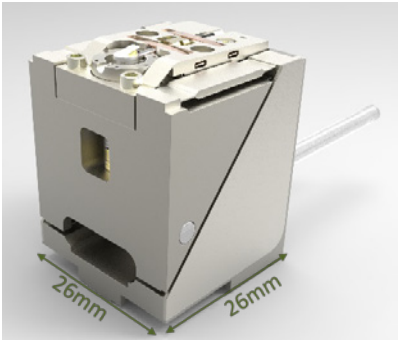

Figure 5 – Miniaturized AFM scanhead.

CONCLUSION

A highly miniaturized, arm-less AFM scanner has been designed and its main components have been shown to perform as required. The next step is full integration and verification.

ECSEL JU

This project has received funding from the Electronic Component Systems for European Leadership Joint Undertaking under grant agreement No 621280. This Joint Undertaking receives support from the European Union's Horizon 2020 research and innovation programme and Netherlands, France, Belgium, Germany, Czech Republic, Austria, Hungary, Israel.

Smart integrated tips for massively parallel high-throughput atomic force microscopy

Federico Galeotti[1], Francesco Pagliano[2], Žarko Zobenica[1], Frank van Otten[1], Rob van der Heijden[1], Hamed Sadeghian[3], and Andrea Fiore[1]

1 Department of Applied Physics and Institute for Photonic Integration, Eindhoven University of Technology, The Netherlands

2 nanoPHAB, Eindhoven, The Netherlands

3 Nano-Optomechatronics Instruments, TNO Delft, The Netherlands

A concept for an all-integrated Atomic Force Microscope is proposed, that would enable massive parallelization for high-throughput nanometrology and nanomechanical sensing.

Nanoelectronics industry metrology requirements NOT met by current solutions:

- Optical systems: feature size
- Electron microscopy: beam size, depth of field, speed
- Atomic Force Microscopy (AFM): speed, low throughput

Proposed solution:
All-integrated AFM concept with massively parallel operation for increased throughput.

DEVICE CONCEPT

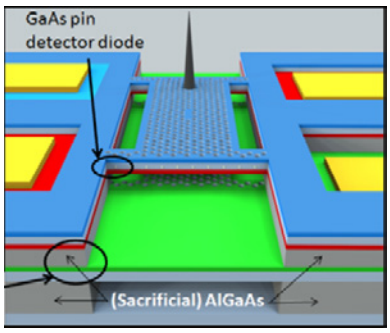

Nano-Opto-Electro-Mechanical System*:

- Semiconductor (III-V) layer stack
- Wafer-scale nano-processing
- Double membrane electro-mechanically tunable Photonic Crystal cavity
- Built-in resonantly enhanced photodiode self sensing detector
- Tip actuation for AFM function:
- Footprint ≈ 15 x 15 μm²
- Target demonstrator: 5 x 5

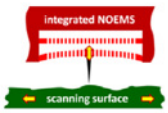

*Midolo et al., Appl. Phys. Lett. **98**, 211120 (2011)

DOUBLE MEMBRANE PHOTONIC CRYSTAL CAVITY CHARACTERIZATION

(Zobenica et al, [2017])

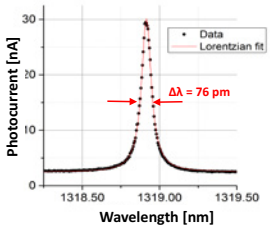

photocurrent spectrum from tunable laser

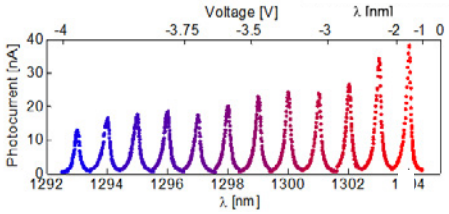

photocurrent spectra for different tuning voltages

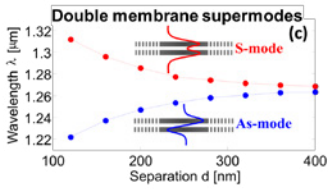

Calculated tuning curves

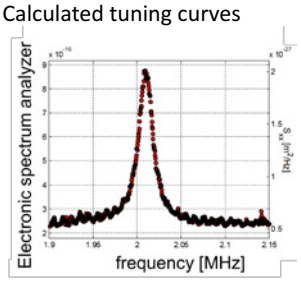

Thermal Brownian motion from photocurrent noise spectrum
Expected displacement resolution:
≈ 10's fm/Hz$^{1/2}$

TIP MANUFACTURING & TESTING

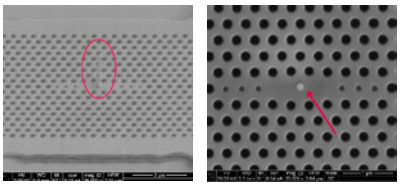

Electron beam induced deposition

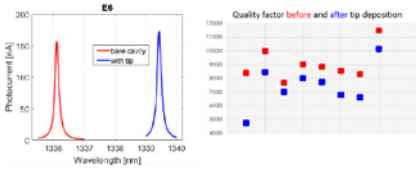

Wavelenght shift

Influence resonance width

From simulations:

- Tip can be placed at center of L3 cavity, which is optimum for mechanical transduction

Experimentally confirmed:

- Expected shift of cavity resonances because of dielectric
- Modest influence on quality factor

PRELIMINARY TEST RESULTS

Test setup with simultaneous use of bent lensed fiber as mechanical actuator / test surface / optical excitation under optical microscope

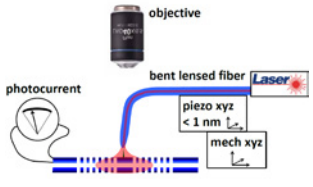

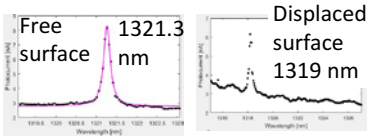

Photocurrent spectra

CONCLUSION

Double membrane Photonic Crystal feasibilty as sensitive displacement sensor with tip actuator demonstrated. Further work for waveguide coupling and AFM operation.

NEARFIELD INSTRUMENTS: DELIVERING ATOM-SCALE METROLOGY AT INDUSTRY-LEVEL THROUGHPUT

Hamed Sadeghian[1,2], Roland van Vliet[2]

1 TNO
2 Nearfield Instruments B.V.

TNO innovation for life

NEARFIELD INSTRUMENTS

INTRODUCTION

The semiconductor industry struggles to meet sub-10 nm node manufacturing metrology needs:
3D complex structures, ultra-sensitive materials, mechanical, electrical, magnetic, thermal properties.

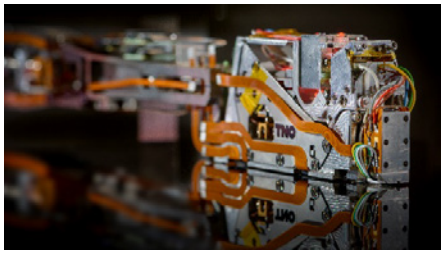

OFFERING

Based on TNO technology, Nearfield Instruments develops a revolutionary multiple parallel atomic force microscopy system enabling atom-scale resolution metrology at industry-level throughput, based on three pillars:

- **unrivaled measurement speed**
- **parallelization capability**
- **advanced measurement modes**

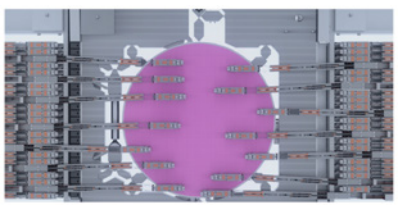

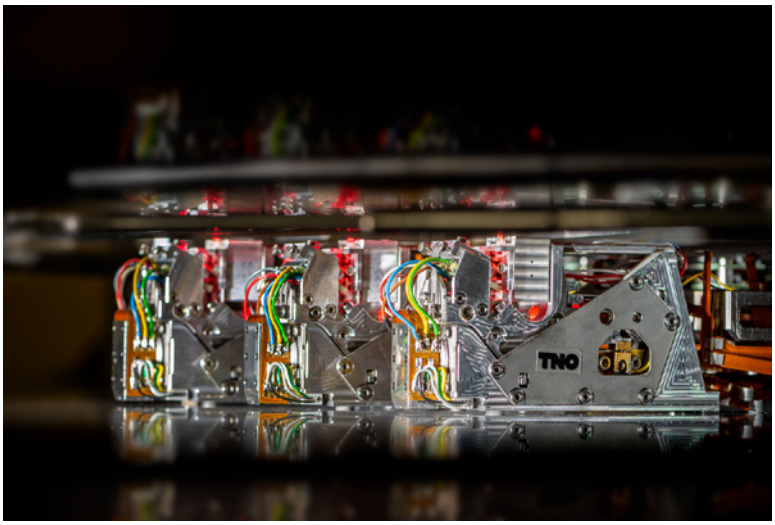

SYSTEM STRENGTHS

- Up to **750x throughput** of current AFM systems
- Up to **30 parallel, independent** AFM measurement heads
- True **die-to-die comparison** and **simultaneous multiple parameter measurement** capability
- Fully **automated tip exchange** and alignment
- Advanced, **non-damage** measurements modes

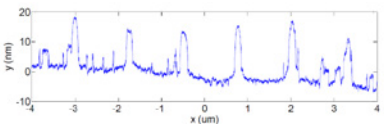

Profile measurement at the edge after CMP

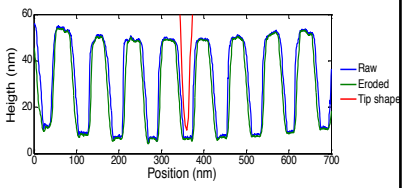

3D profile measurement of EUV contact holes

COMPANY STATUS

- Series A **venture-backed start-up**
- 4-arm demonstrator system available
- Working together with potential customers on application development
- Development on-going on alpha-demo system
- Actively seeking partnerships in application development and funding
- Several job positions available in field of system engineering, mechanical and electronics design

Application

- CD Metrology; Height, SWA, line width
- CMP process profilometry
- Defect review
- Height mapping

Monitoring mechanical properties of cell cultures at the nanoscale

Hector Tejeda[1,2], Evita van de Steeg[3], Marco van der Lans[1], Maurits van der Heiden[1]

1 TNO, Opto-mechatronics , the Netherlands
2 TU Delft, Bionanoscience department, the Netherlands
3 TNO, Microbiology & Systems Biology, the Netherlands

TNO innovation for life

BACKGROUND

The behavior and mechanical properties of cells are affected by health condition, disease state (e.g. cancer), toxic response and/or experienced physical forces in the environment. Changes in nano-mechanical properties of the cells may be used as an (online) read-out parameter to monitor these reactions.

Revealing the mechanical properties of cells at the nanoscale allows the understanding of cellular processes, like:

- Organ behavior & functionality[1]
- Cell Development[2]
- Response under stress[3]

OBJECTIVE

Analysis and characterization of cellular and epithelial functionalities by monitoring biomedical processes using AFM technologies. Intermediate step: check if the mechanical properties of cells stay constant over time during AFM sampling?

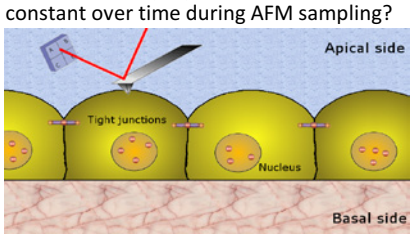

Fig. 1. Schematic repr. of Caco2 culture after 24h of incubation.

Methods

Cell Culture

Human intestinal cells (Caco2) were cultured on polystyrene TC glass in DMEM to form a monolayer.

AFM – Bruker Icon Dimension. Mode: Force-volume spectroscopy. Parameters: force 1.5 nN, ramp size 4-6 µm, ramp rate 1 Hz. MLCT-C tips (0.01 N/m, pyramidal). Measurements done at room temperature in PBS (Fig. 1). Multiple cells are measured every 20 min for 2 hr.

Data analysis

The approach sections of F-D curves are used for analysis (Fig. 2). The contact point, indentation depth and the E-modulus (Hertz Model) are obtained using MATLAB. Fig. 3 shows a histogram of E-modulus distribution from a Caco2 cell. Fig. 4 shows the topology and E-modulus of the sample over time.

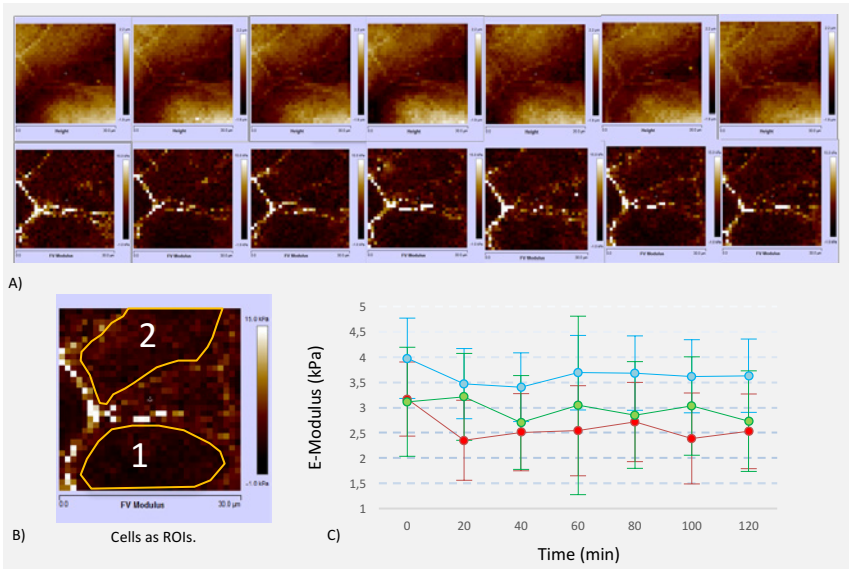

Fig. 4. A) Height and E-Modulus maps from a Caco2 cell monolayer. Images taken 20 min after each other. B) Single cells from the monolayer were identified manually. C) Graph shows the changes in the Young's Modulus over time for the recorded area (BLUE), cell #1 (RED), cell #2 (GREEN). Statistics, P-ANOVA: 0.83

Results

- Small tip indentation forces lead to adequate reproducibility of the data.
- Cell borders are stiffer than the inner part of the membrane due to cytoskeletal components.
- The average value of Young's modulus keeps constant over time.

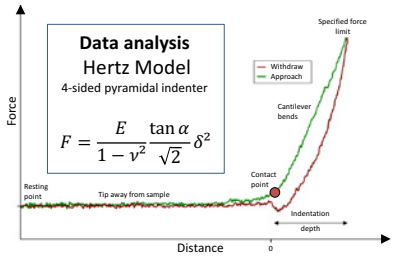

Fig. 2. F-D curve of Caco2 cells. Inset, model for data analysis.

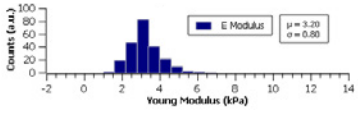

Fig. 3. Histogram of E-modulus of a single Caco2 cell.

CONCLUSION

- No relevant changes in the mechanical properties of Caco2 monolayers over AFM sampling were observed
- Small indentation forces caused cell membrane topology to readjust after tip interaction
- No cell disruption was observed.
- The established conditions allow monitoring the nanomechanical properties of *in-vitro* tissue using relevant time scales

Outlook

Next steps in this study will be;

- Probe the mechanical properties of Caco2 monolayers during development.
- Correlate mechanical properties to cellular responses upon exposure to (toxic) drugs.

References

1. Lecuit & Lenne, Nat Rev Mol Cell Bio 8, 2007.
2. Miller & Davidson. Nat Rev Genet., 14(10):733, 2013.
3. Butcher, Alliston, & Weaver. Nat. Rev. Cancer, 9(2), 2009.

This research has been supported by TNO's Early Research Program 3D Nanomanufacturing Instruments

VIRUSCAN: Identification and characterization of viruses from their nano-mechanical properties

Maurits van der Heiden[1], Jasper Winters[1], Javier Tamayo[2], Marco van der Lans[1]
[1] TNO, opto-mechatronics , the Netherlands
[2] Agencia Consejo Superior de Investigaciones Científicas (CSIC)

TNO innovation for life

Background

The nano-mechanical physical properties of viruses are highly conserved during the virus evolution. Obtaining the viral mass by mass-spectroscopy is well known. Addressing the stiffness of viruses opens a new route to assess the infectiveness of viral traces in human samples, which is a difficult objective to tackle with present technologies.

VIRUSCAN aims to detect individual virus in human samples and identify the viruses from their mass and stiffness and assess their infectiveness.

Approach

- Integral approach for detection and identification of viruses.
- Concept is based on mass and stiffness measurement of individual viral particles.
- Comparing measurements with reference database for identification and classification.
- Prototype to be developed will be developed based on 5 main modules:

Sample preparation:

- Microfluidics with Deterministic Lateral Displacement (DLD).
- Sample isolation and purification.

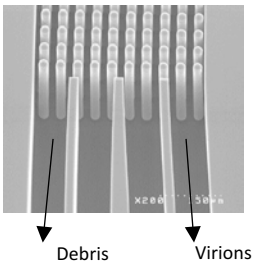

Array of micropillars of the DLD (CEA) for isolation and purification.

ViruScan

Sample delivery:

- Nano-electrospray with aerolens for buffer fluid removal, focusing and soft landing of viruses on the detector.

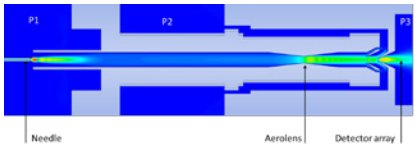

CFX velocity simulation of focusing with an aerolens (Fasmatech).

Particle detection:

- Nano-disk resonators for detection of viral particles.
- Viral particles cause shifts in mechanical vibration modes.
- Shift in vibration modes are measured optically (frequency shifts).

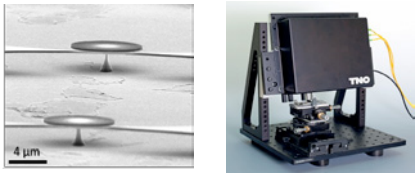

Left: Disk resonator (UPD). Right: TNO Fresco setup for readout of the disk resonator array.

Sample identification:

- Mass and stiffness of viruses are extracted from measured frequency shifts.
- Comparison with reference database for identification and maturation.

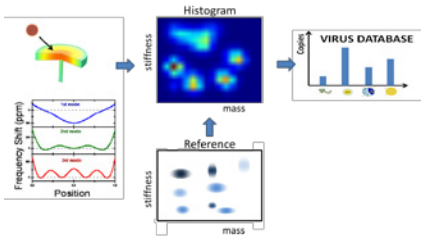

Flowchart describing the process from detection (top left) to identification (top right)

Reference database:

- Database for virus identification.
- Data obtained from AFM and MS measurements.

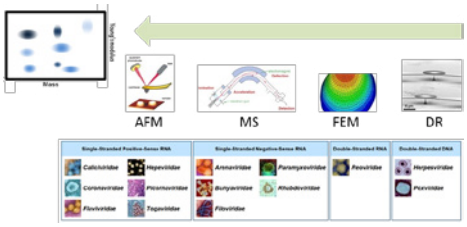

Flowchart describing the process of the reference database development (HPI and RUG).

Current status

- Program started end 2017.
- Requirements defined and main risk analysis performed.
- First TRL2 proof concept to be evaluated end 2018.
- TRL4 demonstrator planned for 2021.

Outlook

VIRUSCAN aims to identify viruses and nanoparticles. For the proof of concept a short list of particles and viruses is selected:

Virus	Shape	Size [mm]	Mass [MDa]
Nanoparticles	Spherical	± 30-250	± 10 - 10.000
Tobacco Mosaic Virus (TMV)	Rod-like	300x18	± 40
Hong Kong virus (HK97)	Icosahedral	60	± 50-60
Mouse CytoMegaloVirus (MCMV)	Spherical	150-200	1.000 – 3.000
Ebola-like particles virus	Helix	± 1000x80	3.000 – 10.000

Partners

IMN Instituto de Micro y Nanotecnología IMN-CNM
HPI
Servicio Madrileño de Salud SERMAS
rijksuniversiteit groningen
FasmaTECH
leti ceatech
PARIS DIDEROT
TNO innovation for life

This project is financially supported by H2020-FETPROACT-2016-731868
European Commission
Horizon 2020 European Union funding for Research & Innovation

AFTERWORD

Nano-Optomechatronical Instrumentation (NOMI) is a key technology. NOMI Innovation program is at the forefront of research and development in Nanometrology and nanomanufacturing of future nanodevices. We are establishing a NOMI Innovation program together with our key partners. The following mission and vision have been established for this long term Joint Development program:

– We see a future where humanity will solve many of future's challenges in data, energy and life sciences by a continuous miniaturization in device fabrication down to an atomic scale
– The NOMI-ecosystem develops the technologies that enable exploration and exploitation of the atom-scale world level leading to the real-world applications
– The NOMI-ecosystem research to create the instruments to image, measure and fabricate devices at the level of individual atoms at an humanly acceptable and economically attractive level

In the following years, NOMI will continue developments in its 4 core technology roadmaps:

1- 3D Nanomanufacturing
2- Nanotomography and nanometrology
3- Nanomotion control and dynamics
4- Bio-NOMI

We have strived to put together a challenging and inspirational event, aiming to share our view on the major developments in the nano-instrumentation field. We hope you have enjoyed the event and hope to see you again next year.

Hamed Sadeghian

COLOPHON

Text: TNO
Layout: grafisch ontwerp PI&Q, Zeist

TNO.NL